4-8-2013

Topics In Physics Beyond The Standard Model

Karoline Koepp
The Florida State University

THE FLORIDA STATE UNIVERSITY

COLLEGE OF ARTS AND SCIENCES

TOPICS IN PHYSICS BEYOND THE STANDARD MODEL

By

KAROLINE KÖPP

A Dissertation submitted to the
Department of Physics
in partial fulfillment of the
requirements for the degree of
Doctor of Philosophy

Degree Awarded:
Spring Semester, 2013

Karoline Köpp defended this dissertation on March 6, 2013.

The members of the supervisory committee were:

Takemichi Okui
Professor Directing Thesis

Ettore Aldrovandi
University Representative

Laura Reina
Committee Member

Todd Adams
Committee Member

Christopher Gerardy
Committee Member

The Graduate School has verified and approved the above-named committee members, and certifies that the dissertation has been approved in accordance with the university requirements.

To Dominik.

ACKNOWLEDGMENTS

Many readers will likely end their reading of this thesis after the preface. While this should call for particular care and effort in writing this section, I have joined the tradition of delaying it to the very last moment. So I apologize to anybody who I might fail to acknowledge and blame it on sleep deprivation.

Working on my Ph.D. thesis has been a rollercoaster of fun, frustration, concentration and challenge. And now, it is (almost) done.

This work would not have been possible without my advisor Takemichi Okui. His guidance and insights and many long discussion sessions were indispensable along the way. His determination to cut to the core questions of a problem have hopefully permanently influenced my own approach to do research. I am thankful to the members of my committee Laura Reina, Todd Adams, Christopher Gerardy and Ettore Aldrovandi for their input and encouragement.

Thanks to the PhD students and Postdocs at FSU for many discussions about physics and beyond and for providing a friendly and helpful environment. And to Kathy for always having a friendly word and for her untiring support in navigating the university bureaucracy. I want to thank Seth, Joe, Chris, Prerit, Nathalie and Nobuo for their friendship and for providing many fun distractions from work. I would not want to imagine these past three years without them and deeply appreciate all the help I received from them along the way, ranging from reviving my computer to emergency ice cream. My gratitude also goes to the friends I met at TASI. Also, I thank Beate for her loyal friendship and for making me look forward to Mondays.

The support of my parents is deeply appreciated. They always were on my side, even from a continent away. Thanks also to Fidi, Basti and Tine for their encouragement and patience.

I feel blessed beyond words for Tom's unwaivering support and love throughout every minute of every day and thank him in particular for his help in finishing and proofreading this dissertation.

TABLE OF CONTENTS

LIST OF TABLES

LIST OF FIGURES

ABSTRACT

In this work, topics in physics beyond the standard model of high energy phyics relevant to the experimental studies at the Large Hadron Collider (LHC) at CERN are discussed. We introduce an effective theory to describe the dynamics of heavy Majorana particles, whose existence is predicted in many extensions of the standard model. Further, it is demonstrated how by combining the two independent concepts of a weakly interacting massive particle accounting for the dark matter observed in our universe and gauge coupling unification, strong phenomenological trends can be inferred. The scenario we present predicts new colored states within LHC reach that can be either collider stable or decay promptly to final states including a Higgs particle. In both cases, interesting LHC signatures are expected. The LHC discovery of the long predicted Higgs boson as well as new lower bounds on supersymmetric particle masses provide motivation to re-evaluate the issue of fine-tuning in supersymmetric theories. We provide an overview of the current state of this ongoing discussion. In the last part of this work we introduce an alternative approach termed stable near-criticality, in which the standard limits on superparticle masses stemming from fine-tuning considerations are relaxed. This approach requires specific and robust correlations among soft mass terms. We discuss how reduced fine-tuning can be achieved even if the gauge and Yukawa couplings are considered variable parameters. Finally, we illustrate our findings with a possible model implementation and demonstrate the validity of our approach by analysing a representative benchmark point.

CHAPTER 1

INTRODUCTION

The standard model of particle physics (SM) is considered to be among the greatest scientific achievements of the 20th century. It combines the unified theory of electromagnetic and weak interactions, originally proposed by Glashow, Salam and Weinberg [4, 5] with the theory of Quantum Chromodynamics (QCD) [6–9] describing the strong interactions. In the SM, the electroweak symmetry is broken spontaneously via the Higgs mechanism [10–15], allowing for weak boson and matter field masses. The standard model has earned its status through a series of astonishing experimental successes.

It gained universal acceptance after the first measurements of the weak current [16–18] and the discovery of the $W^{\pm}$ and Z bosons [19–22] and has since passed a number of increasingly rigorous experimental tests. Data from e^{+}-e^{-} collisions collected by the CERN LEP experiment [23] allowed to verify SM predictions of electroweak sector observables with accuracies reaching the permille level. Examples include the $g-2$ muon anomalous magnetic moment [24] and higher order corrections to the ρ parameter [25–28]. With the discoveries of the last missing fermions, the top quark at the Tevatron [29, 30] and the τ neutrino by the DONUT experiment [31] at Fermilab, the entire predicted SM fermion content has been accounted for.

The past decade of experimental activities has been largely focused on the search for the final missing ingredient of the standard model, the Higgs boson. With the beginning of its operation in 2010, the Large Hadron Collider (LHC) at CERN has marked the beginning of a new era in particle physics. The LHC has been designed for the double purpose of searching for the Higgs particle as the last building block of the SM, as well as putting scenarios for physics beyond the standard model to the test. It has already fulfilled part of its mission: On July 4, 2012, the CMS and ATLAS collaborations confirmed the discovery of a new particle [32,33] that, according to the data analyzed so far, appears to be the Higgs boson.

Despite its successes, the SM does not provide a complete picture of the fundamental particles and interactions. For instance, the standard model lacks an explanation for the experimentally confirmed neutrino masses and neutrino flavor oscillations and fails to explain why the existing number of particles in our universe is not balanced by an equal number of antiparticles.

The probably most obvious shortcoming of the standard model, however, is the fact that it does not account for a share of roughly 80% of the observed matter content in the universe, the so-called dark matter (DM). The existence of dark matter is well-established experimentally in several independent ways, including the observation of galactic rotation curves [34] and the cosmic microwave background [35]. According to the evidence gathered so far, dark matter is most readily explained by one or several species of new particles that are electrically neutral, do not participate in strong interactions and propagate through the universe at non-relativistic velocities.

The SM model also suffers from problems of theoretical nature, namely the infamous hierarchy problem [36,37]. The hierarchy problem can be stated as follows. While defining the SM at the weak scale with a negative Higgs mass term of the order of $m_H^2 \simeq -(100\,\mathrm{GeV})^2$ is by itself unproblematic, as soon as the SM is embedded into a theory involving higher energy scales, the Higgs mass term receives quantum corrections δm_H^2 that are quadratically divergent. If the cut-off scale of the theory is raised up to the Planck scale, these corrections become huge, typically of the order of $\delta m_H^2 \simeq 10^{35}\mathrm{GeV}^2$. In order obtain a physical mass term of order $m_H^2 \simeq -(100\,\mathrm{GeV})^2$ and ensure electroweak symmetry breaking with a vacuum expectation value (VEV) of the correct size, the bare Higgs mass term has to cancel the quantum corrections to an accuracy of about $1 : 10^{31}$. Such an extremely fine-tuned cancellation among two independent terms is deeply unsettling. To illustrate the extent of fine-tuning in the SM, the hierarchy problem is sometimes compared to a scenario in which understanding of the dynamics of galaxies would require detailed knowledge about effects at the subatomic level.

The hierarchy problem belongs to the category of so-called naturalness problems, which arise whenever a parameter of a physical model is determined to take a value much smaller than what would generically be expected. Instances of known naturalness problems include the cosmological constant problem and the unexplained small value of the strong CP angle θ_{CP}.

These open problems of the standard model are an invitation to theorists to speculate about the nature of physics beyond the standard model (BSM) and to substantiate these speculations by deriving experimentally testable predictions. The LHC is designed to have high sensitivity to a wide range of possible new physics signatures and thus to hopefully gather information about the nature of fundamental interactions and particles beyond the standard model. To accomplish this goal, the LHC experimental program requires reliable and precise predictions from the theory side.

An indispensable tool to perform the necessary calculations, which often involve several disparate scales, are effective field theories (EFTs). EFTs provide tools to systematically organize the operators of a theory and to identify the dominant effects and the symmetry structure at any given energy scale. In the context of beyond the standard model physics, effective field theories are of particular significance as their predictive power extends to cases in which the full theory at high energy scales is unknown.

In analogy to heavy quark effective theory (HQET), which has been very successfully applied to describe the dynamics of heavy mesons, in this work we detail how to derive an effective theory for hypothetical heavy Majorana fermions. Majorana fermions differ from Dirac fermions in that they are their own antiparticles. They are predicted in many

extensions of the SM. A widely known example is the gluino in supersymmetric extensions of the SM. If heavy Majorana particles exist, are long-lived and carry color charge, they will form heavy stable bound states called R-hadrons, whose dynamics can be described by an effective field theory for heavy Majorana fermions analogous to the description of heavy B mesons by HQET. R-hadrons can lead to spectacular signatures at the LHC. A specific example for BSM scenarios potentially featuring R-hadrons are simple models built on the assumptions of gauge coupling unification and that a weakly interacting massive particle (WIMP) constitutes dark matter [38].

In addition to the analysis of the Higgs signal, a primary objective of the LHC is the search for supersymmetry. Because it solves the hierarchy problem, contains a dark matter candidate and exhibits unification of the gauge couplings, supersymmetry is widely considered to be the most compelling scenario of physics beyond the standard model. Supersymmetry is a space-time symmetry introducing a superpartner field for every standard model field. The superpartners carry the same gauge quantum numbers as their respective SM counterparts but differ by $\frac{1}{2}$ in spin. The solution to the hierarchy problem in supersymmetry is based on chiral symmetry preventing large quantum corrections to the Higgs mass term. While in the SM chiral symmetry protects fermion masses only, in supersymmetry the protection mechanism is at work for the entire supermultiplet containing both the scalar and the fermionic Higgs field.

Since no superpartner has been experimentally observed to date, however, supersymmetry cannot be an exact symmetry. The scale of supersymmetry breaking determines the size of the superpartner masses. The naturalness problem of electroweak symmetry breaking (EWSB) is re-introduced, albeit to a much less severe extent than in the hierarchy problem of the SM, if the scale of supersymmetry breaking Λ_{SB} exceeds the scale of electroweak symmetry breaking Λ_{EWSB}. The LHC has already delivered significant lower bounds on masses of superparticles. The discovery of the Higgs with $m_h \sim 125\,\mathrm{GeV}$ also poses a challenge to supersymmetric models which generally favor lighter Higgs mass values. At a first glance, these combined limits appear to indicate that supersymmetry, if realized in nature, does not resolve the naturalness problem associated with electroweak symmetry breaking. Closer inspection is needed to clarify whether that assertion actually holds true. There are two major approaches to identify models that are compatible with the recent LHC results and yet remain natural, i.e. are minimally fine-tuned. One approach is based on the search for non-standard spectra for which the LHC exclusion bounds do not apply. The other utilizes the effect that in certain models with highly correlated superpartner mass terms, a hierarchy $\Lambda_{\mathrm{EWSB}} \ll \Lambda_{\mathrm{SB}}$ can be a built-in stable feature and not the result of a fine-tuned cancellation. Further investigation of both approaches is needed in order to design tailored searches and to settle the question whether LHC bounds have the power to exclude natural EWSB in supersymmetry.

The structure of this work is as follows: In chapter 2, a short introduction to effective field theories is given. In chapter 3, our work Ref. [39] developing an effective field theory for heavy Majorana particles is presented. We carefully compare our result to the well-known heavy quark effective theory (HQET). Chapter 4 begins with two short sections introducing the concepts of dark matter, in particular weakly interacting massive particles or WIMPs as dark matter candidates, and grand unification. In the remainder of that chapter we present

strong phenomenological trends that can be inferred from combining these two concepts based on our work in Ref. [38]. Specifically, we demonstrate that with limited assumptions new colored states are expected and discuss their resulting experimental signatures. In chapter 5, we introduce supersymmetry with particular focus on assessing the current state of naturalness in supersymmetric models. In chapter 6, we work out a comprehensive strategy to circumvent the standard naturalness constraints [40]. The strategy is illustrated with an explicit model and we analyze the fine-tuning at a representative benchmark point. We conclude in chapter 7.

CHAPTER 2

EFFECTIVE FIELD THEORIES

2.1 Effective field theories are everywhere

Physical phenomena take place at a wide range of scales. The age of the universe, about 10^{18} s, differs by over 40 orders of magnitude from the W and Z lifetimes of about $10^{-24}s$, and at almost every scale in-between interesting physics phenomena take place. It is not obvious a priori why the multitude of effects taking place at different scales should not be all non-trivially interdependent, in which making predictions for any physical observable would be daunting task. Even more worrisome is the well-known fact the SM cannot be valid above the Planck scale $M_{\rm Pl} \sim 10^{18}\,{\rm GeV}$. The consequences of the physical effects taking place at this scale are beyond the scope of our current, very limited understanding of a quantum theory of gravity. However, all physical observables are subject to radiative corrections and require the evaluation of integrals containing momenta above the Planck scale.

In the light of these considerations, it would appear hopeless to even attempt to make a detailed prediction about any observable, such as for instance the splittings of the hydrogen energy levels. In practice however, experiments confirm theory predictions of hydrogen energy levels to a high degree of precision. This agreement between prediction and data might be surprising considering that these calculations have been performed without the knowledge of the physics at higher energy scales, like e.g. the fact that the proton is composed of quarks. The hydrogen spectrum is just one of many examples that it is possible to focus on a given set of phenomena taking place at a certain scale and decouple it from the details of other effects occurring at very different scales. Effective field theory (EFT) provides a framework to accomplish this decoupling in a systematic way.

In the relativistic regime relevant for particle physics applications, the only relevant scale parameter is distance. In the usual high-energy convention of $c = \hbar = 1$, distance carries units of $[\text{mass}]^{-1}$. Phenomena taking place at long distances and low energy effects are called infrared (IR) effects, while phenomena occurring in the short distance, high energy limit are called the ultraviolet (UV) physics. In the following we will use $M_{\rm UV}$ to denote the UV scale. From the point of view of long distance scales, effects of short distance physics appear local i.e. contracted to a point in coordinate space and thus acting just like local operator insertions. Therefore, the short distance physics can simply be mimicked by adding new local operators into the lagrangian. The effect of those new operators amounts

to either (i) changing the operator coefficients (couplings) in the renormalizable lagrangian or to (ii) adding higher dimensional operators suppressed by the UV scale $M_{\rm UV}$.

As far as renormalizable operators are concerned, changes of their coefficients is inconsequential since their values are determined by measurement. To be clear, it is not that unknown effects of short distance physics are parametrically small or negligible in any way, there is just no way to independently determine the size of contributions from the UV physics to low energy observables such as e.g. the electron mass. The UV effects are absorbed into the couplings whose physical sizes are measured by experiments.

In contrast, non-renormalizable operators induced by UV physics are parametrically suppressed by $M_{\rm UV}$. After performing a systematic expansion in $1/M_{\rm UV}$, for a fixed precision goal, all operators above a certain order in the expansion can be safely cut off in the lagrangian. In that manner, a predictive theory with a finite number of operators is obtained.

Historically, renormalizability has been considered to be the sine qua non for valid physical theories, particularly after Veltman and 't Hooft proved renormalizability of spontaneously broken gauge theories [41], an achievement awarded with the Nobel prize in 1999. Yet in the modern view, effective field theory and theories containing non-renormalizable terms are not regarded as incomplete or inferior anymore. As a matter of fact, every theory is ultimately an effective theory since physics above the Planck scale is unknown and there is good reason to expect further new physics phenomena already at energy scales considerably below $M_{\rm Pl}$. The inherent breakdown of EFTs at some high scale is not regarded to be a consistency problem, but rather is an advantage insofar as the theory comes with a built-in disclaimer about its validity regime. Effective field theory allows to investigate crucial questions about physics without committing to any specific guess about what happens at arbitrarily high energies. Effective theories fall into two categories:

(I) The UV physics might be unknown or not calculable perturbatively. In that case, even without information about UV effects, effective field theory still allows to perform sensible calculations and to organize the unknown UV effects into a finite number of higher-dimensional operators. Measuring the coefficients of these non-renormalizable terms allows to estimate the scale where the EFT breaks down.

(II) In case the UV physics is known, it is in principle possible to perform calculations in the full theory. However this can turn out to be a complicated or even impossible endeavour if disparate scales giving rise to large logarithms that can make the perturbation series non-converging. Effective field theory can greatly simplify the task at hand. More importantly, the EFT picture is often clearer and makes approximate symmetries that are obscured in the full theory manifest. By concentrating only on the physics relevant for a given problem, effective field theory can provide a better understanding and enhanced predictive power.

The standard model belongs to category (I), as does any higher dimensional gauge theory without UV fixed points. Examples for effective theories of type (II) are e.g. four-Fermi-theory, chiral perturbation theory, heavy quark effective theory and soft collinear effective theory.

Table 2.1: Operator classification in effective field theories.

$\dim(\mathcal{O}_i)$	scaling dim. γ_i	Behavior for $E \to 0$	Terminology
$< D$	> 0	increases	relevant (super-renormalizable)
$= D$	$= 0$	remains constant	marginal (renormalizable)
$> D$	< 0	decreases	irrelevant (non-renormalizable)

2.2 Basics of effective field theory

In this section, the general procedure to formulate and analyze effective field theories is outlined. The aim is to introduce the basic concepts and vocabulary. Much more exhaustive discussions, examples and details of the versatile EFT techniques can be found e.g. in the reviews [42–48].

2.2.1 Relevant, marginal and irrelevant operators

According to the arguments presented in the previous section, at low energies all effects of UV physics can be absorbed into local operators. In particular all physical effects of heavy degrees of freedom are suppressed by their mass scale $M_{\rm UV}$. The EFT lagrangian thus only contains light fields ϕ with masses much smaller than $M_{\rm UV}$ and has the general form

$$\mathcal{L}_{\rm EFT} = \sum_i C_i \mathcal{O}_i(\phi)\,. \tag{2.1}$$

The coefficients C_i can be written as

$$C_i = c_i M_{\rm UV}^{\gamma_i} \tag{2.2}$$

where coefficients c_i have mass dimension zero and are expected to be of order one by the hypothesis of (Dirac) naturalness. The exponents $\gamma_i = D - \dim(\mathcal{O}_i)$ are the so-called naïve scaling dimensions. At low energies $E \ll M_{\rm UV}$, the operators in the effective lagrangian scale as $c_i(E/M_{\rm UV})^{\gamma_i}$. This means that depending on the value of γ_i the operators behave differently in the low energy limit. Operators that grow, remain constant, or fall in the limit $E \to 0$ are called relevant, marginal and irrelevant, respectively. The nomenclature is summarized in Table 2.1.

Relevant operators rarely matter because they are usually forbidden by symmetries as they are in conflict with the concept of naturalness. Consider as an example a scalar mass term $m^2\phi^2$ with $\dim(\mathcal{O}) = 2$. From loop corrections, m^2 will receive contributions proportional to Λ^2, where $\Lambda \lesssim M_{\rm UV}$ is the cut-off scale of the effective theory. The mass of the field ϕ however has to be much smaller than Λ, or else by definition ϕ would not be part of the effective theory. Therefore, the existence of the scalar mass term would require an unnatural cancellation between the unrelated bare mass term and the loop-correction. In the SM with a light scalar Higgs field H, this tension is known as the hierarchy problem and is the reason for the SM not being considered a natural effective field theory.

In the absence of problematic relevant terms, renormalizable theories only consist of marginal operators. Moreover, in a general theory, non-renormalizable operators are increasingly suppressed when approaching the low-energy limit. Therefore, *every* theory appears renormalizable in the IR limit, without the need to postulate renormalizablity as validity criterion.

Irrelevant operators, if measurable, are despite their name actually the most interesting objects of the EFT lagrangian. Their coefficients contain information about the underlying physics at the scale M_{UV}. The importance of irrelevant operators is exemplified by the historic case of how measurements of the magnitude and energy dependence of low-energy processes singled out $M_{\mathrm{UV}} \sim 100\,\mathrm{GeV}$ as the appropriate cut-off scale of Fermi theory of weak interactions. That scale was subsequently found to be precisely the mass scale of the weak W and Z bosons. The discovery of these bosons completed the picture of the standard model gauge interactions. Another instructive example is provided by the case of small but non-vanishing neutrino masses. No renormalizable mass terms for neutrinos can be added to the standard model lagrangian without requiring new field content. However in the effective field theory picture, the standard model is expected to contain the irrelevant operator

$$\frac{1}{M_{\mathrm{UV}}}(l^T \mathcal{C} H)(lH), \tag{2.3}$$

where l and H denote the SM left-handed lepton and Higgs field respectively, $\mathcal{C}$ is the charge conjugation matrix satisfying $\mathcal{C}^{-1}\gamma^\mu\mathcal{C} = -\gamma^{\mu T}$ and the $SU(2)_L$ indices of the fields which are grouped together in brackets are contracted antisymmetrically. The operator defined in (2.3) is suppressed by a high scale M_{UV} denoting the scale of new physics beyond the standard model. Once the Higgs field ϕ_h acquires a vacuum expectation value $v \sim 246\,\mathrm{GeV}$, this operator leads to a neutrino mass of $m_\nu \sim v^2/M_{\mathrm{UV}}$. Thus, in the effective theory picture, the standard model predicts small but non-zero neutrino masses.

2.2.2 Matching of effective field theories

Let us now consider an example of a full theory containing a heavy particle Φ with mass m_H and light particles ϕ with masses much smaller than m_H. Suppose the processes of interest take place at energies much below the creation threshold of the heavy particle. The goal is to formulate a local effective theory with only light fields ϕ that correctly reproduces the full theory as long as only external momenta p^μ with $p^2 \ll m_H^2$ are considered. The procedure of constructing the correct EFT lagrangian is known as *matching*:

- Operators including only light fields remain unchanged in the EFT. Thus, $\mathcal{L}_{\mathrm{EFT}}$ contains all the operators that can be obtained from the full theory lagrangian by setting the heavy field to zero. The coefficients of these operators in the effective field theory need not equal the ones in the full theory.

- To account for the effects of the heavy fields, appropriate local operators need to be added. To obtain these operators, amputated Greens functions are calculated order by order in the full and the effective theory. Subsequently, the difference is added back into the effective field theory

$$\delta\mathcal{L}_{\mathrm{EFT}} = \text{full theory result} - \text{effective theory result} \tag{2.4}$$

This way, an effective field theory which correctly reproduces the full theory at low energies is engineered.

The matching procedure will only produce local operators, since the EFT lagrangian contains the same light degrees of freedom as the full theory. Also, since higher n-point functions generate higher dimensional operators, for any fixed value of desired accuracy and maximal energy of the experiment $E \ll m_H$, only a finite set of n-point functions needs to be calculated.

Beyond tree level, the matching procedure becomes more complicated, because the theory needs to be regulated. More detailed discussions on that topic can be found e.g in [42,44]. The method of choice in most cases is the mass-independent dimensional regularization scheme, since powers of $1/m_H$ only appear in the operator coefficients and power-counting cannot be obstructed by introducing a dimensionfull regulator. Of course, using different regularization schemes in constructing the EFT lagrangian will produce the same physical result, even if the counter-term will differ.

Note that the UV divergencies of the full and the effective theory do not cancel in the matching procedure, which after all is tailored to make the EFT mimic the full theory in the IR limit and not in the UV limit. The mismatch is obvious from the fact that the EFT contains non-renormalizable operators leading to new UV divergencies at each order in perturbation theory which are not present in the full theory.

In the case of many heavy fields, the effective field theory approach can be iterated: Each particle mass can be considered the boundary between two effective theories. For energies above the particle mass the field is included as dynamic degree of freedom, while at lower energies its effects are encoded in higher dimensional operators containing only light fields. Between the thresholds, renormalization group running is used to evolve the operator coefficients. Eliminating the heavy particles successively leads to a descending sequence of effective theories, with a decreasing number of fields and an increasing number of suppressed non-renormalizable operators.

2.3 Example: heavy quark effective theory

In the remainder of this chapter we discuss heavy quark effective theory (HQET) [49–52] to give a concrete example of the usefulness of effective field theories. This section also provides the foundation to our work constructing a similar effective theory for hypothetical heavy Majorana particles in Ref. [39]. In addition to the original HQET publications, many review articles exist [45, 53–56] that provide details and information beyond the scope of the short discussion in this section.

HQET falls into the category of effective field theories where the full UV theory, in this case QCD, is known. The effective picture not only simplifies calculations but more importantly reveals symmetry structures that are obscured in the full QCD point of view. There are two reasons for a heavy quark being a simpler object than a light one. Firstly, because of asymptotic freedom, α_s is weak when the relevant distance scale is small. A bound system of two quarks which are both heavy enough to have very short Compton wavelengths can be calculated using perturbation theory just like calculating spectra in atomic physics. Secondly, and more importantly, in colored systems with one heavy quark

and any number of light degrees of freedom, a form of decoupling takes place: As with increasing mass m the relevant length scale of the heavy quark becomes very small, the details of its structure cannot be probed anymore by the surrounding cloud[1] of light quarks and gluons, whose size is determined by the confinement scale Λ_{QCD}. While the color flux extends out to long distances such that the color charge of the heavy quark remains visible to the cloud, relativistic effects such as color magnetism are suppressed in the heavy m limit. In this limit, the spin of the heavy quark and the spin of the cloud are separately conserved quantities, and the non-perturbative effects taking place within the light subsystem become independent of the heavy quark's spin.

2.3.1 The HQET lagrangian

Heavy quark effective theory formalizes and sharpens this physical argument by making use of the hierarchy $m \gg \Lambda_{\mathrm{QCD}}$ between the mass m of a heavy quark such as the bottom quark b and the QCD scale Λ_{QCD}. HQET is obtained from the QCD lagrangian by taking the limit $m \to \infty$ while the heavy quark's 4-velocity v^μ is held fixed. This limit is appropriate for the description of states with one heavy particle ψ with mass m and an arbitrary number of light particles, such as e.g. a meson $Q\bar{q}$ with one heavy quark and a light antiquark. Because the light degrees of freedom only carry momentum of the order of Λ_{QCD}, the heavy particle momentum can be expanded as

$$p^\mu = mv^\mu + k^\mu \tag{2.5}$$

where v is a timelike 4-velocity satisfying $v^0 > 0$, $v \cdot v = 1$ and $k \sim \Lambda_{\mathrm{QCD}} \ll mv$. Neglecting all interactions with the light degrees of freedom, the state is simply described by the solution to the free Dirac equation $(\mathrm{i}\partial\!\!\!/ - m)\psi = 0$:

$$\psi(x) = e^{-\mathrm{i}mv\cdot x} u_v \tag{2.6}$$

The rapidly varying part of the heavy quark field's space-time dependence has been factored out such that u_v is just a constant spinor obeying the constraint $v\!\!\!/ u_v = 1$. Interactions lead to fluctuations around this constant solution, and the constant spinor u_v has to be replaced by a x-dependent spinor with both $v\!\!\!/ = \pm 1$ components. The following ansatz

$$\psi(x) = e^{-\mathrm{i}mv\cdot x} \left[h_v(x) + H_v(x)\right] \tag{2.7}$$

is made, where $h_v(x)$ and $H_v(x)$ parameterize the $v\!\!\!/ = +1$ and $v\!\!\!/ = -1$ components, respectively, i.e.:

$$v\!\!\!/ h_v(x) = h_v(x)\,, \quad v\!\!\!/ H_v(x) = -H_v(x)\,. \tag{2.8}$$

At this point, it is important to emphasize that (2.7) is a completely general rewriting of the usual Dirac spinor and no approximation has been made so far. Only the fast oscillation of the particle's wavefunction has been factored out explicitly and $v\!\!\!/$ was used as a projector

[1] Instead of "cloud", the subsystem of light degrees of freedom is also often referred to as "brown muck". This term goes back to Nathan Isgur and expresses the fact that due to the non-perturbative nature of light colored systems, "clean" analytically calculable predictions are impossible. The virtue of HQET consists of providing a systematic way to factorize perturbative heavy quark physics from the computationally inaccessible effects in the "brown muck".

to separate the mostly-particle mode h_v from the mostly-antiparticle mode H_v. Using this ansatz, the QCD lagrangian reads

$$\begin{aligned}\mathcal{L} =&\bar{\psi}(\mathrm{i}\not{D} - m)\psi \\ =&\mathrm{i}\bar{h}_v\, v\cdot D h_v - \bar{H}_v(\mathrm{i}\, v\cdot D + 2m)H_v + (\mathrm{i}\bar{h}_v \not{D}_\perp H_v + \mathrm{c.c.})\end{aligned} \tag{2.9}$$

where $D_{\perp\mu} \equiv \partial_\mu - (v\cdot\partial)v_\mu$. The field h_v is massless, while H_v has mass $2m$. Soft interactions with energy $\sim \Lambda_{\mathrm{QCD}}$ therefore cannot excite H_v and it can be integrated out. At tree level, this means to express H_v in terms of h_v via the equation of motion

$$(\mathrm{i}v\cdot D + 2m)H_v = \mathrm{i}\not{D}_\perp h_v \tag{2.10}$$

The HQET lagrangian reads

$$\begin{aligned}\mathcal{L} =&\bar{h}_v\left\{\mathrm{i}v\cdot D + \mathrm{i}\not{D}_\perp \frac{1}{2m + \mathrm{i}v\cdot D}\mathrm{i}\not{D}_\perp\right\} h_v \\ =&\bar{h}_v \mathrm{i}v\cdot D h_v - \frac{1}{2m}\bar{h}_v D_\perp^2 h_v - \frac{g}{4m}\bar{h}_v \sigma^{\mu\nu} G_{\mu\nu} h_v + \mathcal{O}\left(\frac{1}{m^2}\right) \\ =&\mathcal{L}^0 + \mathcal{L}^{1,\mathrm{kin}} + \mathcal{L}^{1,\mathrm{mag}} + \mathcal{O}\left(\frac{1}{m^2}\right)\end{aligned} \tag{2.11}$$

where $\sigma^{\mu\nu} \equiv \frac{1}{2}[\gamma^\mu, \gamma^\nu]$ and $igG_{\mu\nu} \equiv [D_\mu, D_\nu]$. The covariant derivative in (2.11) is understood to only contain soft gluon fields. Hard gluons have been integrated out and their effects are contained in the various operator coefficients of the effective theory.

The effective lagrangian (2.11) allows to draw important conclusions about the heavy quark system. The leading order term

$$\mathcal{L}^0 = \bar{h}_v \mathrm{i}v\cdot D h_v$$

is independent of m as well as of the spin of the heavy quark. This is known as spin-flavor symmetry: All heavy quarks with the same 4-velocity behave the same way, independent of their respective masses and spins. This spin-flavor symmetry is peculiar in the sense that it relates states with the same velocities but different momenta.

The spin-flavor symmetry is broken by $1/m$-suppressed terms. The terms in first order of $1/m$ are the heavy quark kinetic energy $\mathcal{L}^{1,\mathrm{kin}}$ and the magnetic moment interaction $\mathcal{L}^{1,\mathrm{mag}}$, respectively. Being explicitly m-dependent, both violate flavor symmetry. In addition, the magnetic moment interaction $\mathcal{L}^{1,\mathrm{mag}} = \frac{g}{4m}\bar{h}_v \sigma^{\mu\nu} G_{\mu\nu} h_v$ violates spin symmetry.

2.3.2 Reparameterization Invariance

The decomposition of the heavy quark momentum

$$p^\mu = mv^\mu + k^\mu \tag{2.12}$$

into mv and the residual momentum k is a useful book-keeping choice, but it is not unique. There is an arbitrariness of order m/Λ_{QCD} in the choice of v^μ. Concretely, this means that

$$\begin{aligned}&v \to v' = v + \varepsilon/m \quad \text{where } v\cdot\varepsilon = 0 \text{ such that } v'\cdot v' = 1 \\ &k \to k' = k - \varepsilon\end{aligned} \tag{2.13}$$

is a symmetry transformation. The symmetry under the "gauge choice" of v is called Reparameterization Invariance (RPI) and should, like any other symmetry, directly constrain the HQET lagrangian [57].

The field h_v transforms under (2.13) as

$$h_v \to h_{v'} = e^{i\varepsilon x}\left(1 + \frac{\not{\varepsilon}}{2m}\right) h_v. \tag{2.14}$$

such that the condition $\not{v}' h_{v'} = h_{v'}$ is preserved [57]. The leading term of the HQET lagrangian transforms as

$$\mathcal{L}^0 \to \mathcal{L}'^0 = \mathcal{L}^0 + \frac{1}{m}\bar{h}_v \mathrm{i}\varepsilon \cdot D_\perp h_v + \mathcal{O}\left(\frac{1}{m^2}\right), \tag{2.15}$$

while the next-order kinetic term transforms as

$$\mathcal{L}^{1,\mathrm{kin}} \to \mathcal{L}'^{1,\mathrm{kin}} = \mathcal{L}^{1,\mathrm{kin}} - \frac{1}{m}\bar{h}_v \mathrm{i}\varepsilon \cdot D_\perp h_v + \mathcal{O}\left(\frac{1}{m^2}\right). \tag{2.16}$$

The transformations of $\mathcal{L}^0$ and $\mathcal{L}^{1,\mathrm{kin}}$ cancel each other out, as required by the statement of Reparameterization Invariance. Because of RPI, this cancellation must hold to all orders in perturbation theory and therefore the coefficient of $\mathcal{L}^{1,\mathrm{kin}}$ does not get renormalized. By expanding to higher orders in $1/m$ one can identify similar cancellations between operators of successive orders $\mathcal{L}^{n,i}$ and $\mathcal{L}^{n+1,j}$ and thus reduce the number of matching coefficients that need to be calculated.

The full proof of Reparameterization invariance to all orders is not entirely straightforward, and in fact the original proposal [57] was shown to be inconsistent [58]. A valid form of RPI to all orders was first found in [59]. In 1997, Ref. [60] by Raman Sundrum appeared identifying where the early attempts of formulating RPI went wrong and giving an elegant proof of RPI validity to all orders. The crucial observation is that, as h_v and H_v mix under the RPI transformation $v \to v + \varepsilon/m$, H_v needs to be kept as auxiliary field and only be integrated out *after* the RPI transformation has been performed. Then, the relation

$$e^{-\mathrm{i}mv'\cdot x}(h_{v'} + H_{v'}) = e^{-\mathrm{i}mv\cdot x}(h_v + H_v) \tag{2.17}$$

suffices to demonstrate the validity of RPI up to all orders in $1/m$.

2.3.3 Applications of HQET

The spin-flavor symmetry of the leading term of HQET is a powerful tool to constrain the properties of hadrons containing a heavy quark. Probably the most famous application of HQET is the prediction of relations between weak decay form factors of heavy mesons. Based on ideas by Nussinov and Wetzel [61] as well as Voloshin and Shifman [49, 50], Isgur and Wise [51, 52] showed that form factors parameterizing matrix elements of hadronic currents between two meson states each containing a heavy quark can be expressed in terms of a universal function. This function, the Isgur-Wise-function, depends only on the initial and final state velocities v and v'. At zero recoil $v = v'$, the Isgur-Wise-function is

Table 2.2: Overview of D-meson $c\bar{q}$ states, for the light antiquark in s- or p-wave. The parity assignments of the respective states are given in parenthesis.

		light system in		
		s-wave	p-wave	
		$s_l = \frac{1}{2}$	$s_l = \frac{1}{2}$	$s_l = \frac{3}{2}$
Spin s	0	D $(-)$	D_0^* $(+)$	-
	1	D^* $(-)$	D_1^* $(+)$	D_1 $(+)$
	2	-	-	D_2^* $(+)$

normalized to one, which is used to obtain a model-independent measurement of the $|V_{cb}|$ Cabibbo-Kobyashi-Maskawa (CKM) matrix element from the $\bar{B} \to D^* l \bar{\nu}$ decay rate. Precise knowledge of CKM matrix elements such as V_{cb} is essential for the understanding of CP violation in nature. The derivation of the Isgur-Wise form factor relations is discussed in most of the HQET reviews as well as in the original publications. Instead of repeating it here, we will give two different examples for the predictiveness of HQET.

The first application concerns the spectroscopy of ground state D and B mesons, which consist of a heavy c or b quark, respectively, and a "cloud" of colored degrees of freedom, namely the antiquark, sea-quarks and gluons. The flavor symmetry relates the states with different flavor, and the spin symmetry connects the $J = 0$ pseudoscalar and the $J = 1$ vectormeson states. More precisely, the masses of the pseudoscalar and vector modes are expected to be equal up to hyperfine corrections of the order of $1/m$. Therefore, one expects $m_{B^*} - m_B \simeq \mathcal{O}(1/m_b)$ and $m_{D^*} - m_D \simeq \mathcal{O}(1/m_c)$. This leads to the HQET prediction of the relation

$$m_{B^*}^2 - m_B^2 \simeq m_{D^*}^2 - m_D^2 \tag{2.18}$$

which is in approximate agreement with the experimental results $m_{B^*}^2 - m_B^2 \simeq 0.49\,\mathrm{GeV}^2$ and $m_{D^*}^2 - m_D^2 \simeq 0.55\,\mathrm{GeV}^2$.

A second example for the use of symmetry arguments in the heavy quark limit is the explanation for the non-observation of certain D mesons [54].

D mesons are $Q\bar{q}$ systems with $Q = c$. Because c is a spin-1/2 particle, the mesons have spin $s = s_l \pm \frac{1}{2}$ were s_l is the total spin of the light subsystem containing the light antiquark $\bar{q}$. The different D-meson excitations, together with their spin and parity assignments, are shown in Table 2.2.

From experiment it is known that the mesons D_1 and D_2^*, which have the light antiquark in a p-wave with $s_l = \frac{3}{2}$, are observed as clear peaks in the spectrum while the $s_l = \frac{1}{2}$ doublet states D_0^* and D_1^*, decay with widths greater than 100 MeV, are not resolved in the spectrum and are thus difficult to observe. The reason is the following: The doublets with positive parity decay to the negative parity ground state mesons by emission of a single pion. Spin and parity conservation then imply that these decays can occur in even partial

waves $L = 0, 2, \ldots$. Specifically, the decays of the D_2^*

$$D_2^* \to D^*\pi \qquad\qquad D_2^* \to D\pi$$

can only happen in the $L = 2$ partial wave and are therefore suppressed. This explains why the D_2^* resonance is narrow. The decays

$$D_0^* \to D\pi \qquad\qquad D_1^* \to D^*\pi \qquad\qquad D_1 \to D^*\pi$$

are allowed to take place in the s-wave by spin and parity conservation. However, the spin-flavor symmetry of HQET implies that in the $m_c \to \infty$ mass limit, the D_1 and D_2^* decay widths have to be equal, so in this limit the s-wave decay of D_1 is forbidden. Therefore, both D_1 and D_2^* have narrow decay widths and are observed as defined peaks, while the D_0^* and D_1^* widths are broader and difficult to resolve experimentally.

CHAPTER 3

EFFECTIVE THEORY FOR A HEAVY MAJORANA FERMION

3.1 Introduction

While all fermions in the standard model — except possibly for neutrinos — are Dirac fermions, in theories beyond the SM massive Majorana fermions are very common. One well-known example are gauginos in minimally supersymmetric extensions of the SM [62]. The gluino, a heavy color-octet Majorana fermion, can exhibit a particularly interesting collider signature: If the gluinos lifetime exceeds the timescale of QCD confinement of $\sim 10^{-24}$ s, it will form a heavy QCD bound state with gluons and quarks [63]. Gluinos with such long lifetimes appear for instance in split supersymmetry [64, 65]. The resulting bound states of a new heavy colored particle with a "cloud" of light partons are called R-hadrons and are actively searched for by experiments at the Large Hadron Collider [66, 67]. Therefore, it is important to develop a theoretical framework to systematically analyze the system of a heavy Majorana fermion interacting with light particles, i.e. an analogue of HQET for heavy Majorana fermions. Albeit the fact that the usual derivation of HQET explicitly breaks the Majorana condition, it is clear that an analogue version of HQET must also exist for Majorana fermions: At energy ranges much below the fermion mass, where particle-antiparticle creation is not feasible, it should not matter whether the heavy quark is its own antiparticle or not.

In this chapter, we discuss our contribution Ref. [39], in which we derive an effective theory for a heavy Majorana particle. Particular attention is paid to the symmetry structure. The similarities between Majorana and Dirac HQETs are emphasized by demonstrating that Majorana HQET possesses an emergent $U(1)$ symmetry as if it came from a Dirac fermion, even though Majorana fermions by definition cannot transform under any fundamental $U(1)$ symmetry. The emergence of the effective $U(1)$ symmetry should in fact be viewed as a consistency check, since Majorana HQET trivially conserves particle number as being an effective theory for one-fermion states. We also show that reparameterization invariance [57–60] works in the same way in Majorana and Dirac HQETs.

Despite these common features, the two effective theories *are* different. We show that any Majorana HQET must also be equipped with an emergent charge conjugation symmetry, even if the full theory lacks this charge conjugation symmetry. This effective charge conjugation symmetry is an exact, intrinsic property of Majorana HQET that reflects the

absence of a particle-antiparticle distinction in the original Majorana fermion. This contrasts the Dirac case, where a Dirac HQET is symmetric under charge conjugation only if the full theory exhibits the same symmetry. Therefore, this feature potentially provides low energy probes to distinguish between R-hadrons containing a Majorana gluino and those containing a Dirac gluino that appears in many non-minimal models of supersymmetry, for example.

3.2 Degrees of freedom

We first derive the kinetic and mass terms of Majorana HQET. It will be shown that the quadratic terms of the Majorana HQET lagrangian exactly agree with those of Dirac HQET, so the degrees of freedom of the two effective theories are identical in content and propagate in the same manner.

To perform a side-by-side comparison between the Majorana and Dirac cases, consider a Majorana fermion $\psi_M(x)$ and a Dirac fermion $\psi_D(x)$ with the same mass m and identical quantum numbers under all symmetries, except for $U(1)_D$, the very $U(1)$ that defines the Dirac fermion by providing particle number conservation. Being Majorana, $\psi_M(x)$ obeys the constraint

$$\psi_M(x) = \mathcal{B}\psi_M^*(x), \tag{3.1}$$

with the Majorana conjugation matrix $\mathcal{B}$ satisfying

$$\mathcal{B}\gamma^{\mu *}\mathcal{B}^{-1} = -\gamma^\mu\,, \quad \mathcal{B}^* = \mathcal{B}^{-1}\,, \quad \mathcal{B}^T = \mathcal{B}\,. \tag{3.2}$$

As described in Sec. 2.3, in HQET one is interested in the states of a single ψ particle and arbitrary numbers of other particles with masses much smaller than m. In that limit, interactions are transferring only small momenta ($\ll m$) to the ψ particle, hence never exciting another ψ particle. Thus, perturbation theory should have a free ψ particle with a 4-momentum mv as starting point, where v is the timelike 4-velocity. This state is described by the following solutions of the free Dirac equations $(i\partial\!\!\!/ - m)\psi_{D,M} = 0$:

$$\psi_D(x) = e^{-imv\cdot x}u_v\,, \tag{3.3}$$

$$\psi_M(x) = e^{-imv\cdot x}u_v + e^{imv\cdot x}\mathcal{B}u_v^*\,, \tag{3.4}$$

where u_v is a constant spinor obeying the constraint $v\!\!\!/\, u_v = u_v$.

Now, turning on the interactions, the fluctuations of $\psi_{D,M}(x)$ around the solutions (3.3) and (3.4) need to be parameterized. To do so, the constant spinor u_v has to be replaced by an arbitrary x-dependent spinor with both $v\!\!\!/ = \pm 1$ components, and we are led to the following changes of variables:

$$\psi_D(x) = e^{-\mathrm{i}mv\cdot x}[h_v(x) + H_v(x)]\,, \tag{3.5}$$

$$\begin{aligned}\psi_M(x) = {} & e^{-\mathrm{i}mv\cdot x}[h_v(x) + H_v(x)] \\ & + e^{\mathrm{i}mv\cdot x}\mathcal{B}[h_v^*(x) + H_v^*(x)]\,.\end{aligned} \tag{3.6}$$

where $h_v(x)$ and $H_v(x)$ parameterize the $v\!\!\!/ = +1$ and $v\!\!\!/ = -1$ components, respectively, i.e.:

$$v\!\!\!/\, h_v(x) = h_v(x)\,, \quad v\!\!\!/\, H_v(x) = -H_v(x)\,. \tag{3.7}$$

Note that the Majorana condition (3.1) is kept manifest in the parameterization (3.6).

In terms of these new variables, the quadratic part of the full lagrangian for the Dirac theory can be rewritten as

$$\begin{aligned}\mathcal{L}^{(2)}_{\text{D,full}} &= \bar{\psi}_D(\mathrm{i}\not{\partial} - m)\psi_D \\ &= \mathrm{i}\bar{h}_v\, v\cdot\partial h_v - \mathrm{i}\bar{H}_v\, v\cdot\partial H_v - 2m\,\bar{H}_v H_v \\ &\quad + (\mathrm{i}\bar{h}_v\,\sigma^{\mu\nu} v_\mu \partial_{\perp\nu} H_v + \text{c.c})\,,\end{aligned} \tag{3.8}$$

where $\sigma^{\mu\nu} \equiv [\gamma^\mu, \gamma^\nu]/2$ and $\partial_{\perp\mu} \equiv \partial_\mu - (v\cdot\partial)v_\mu$. Here, we have suppressed the kinetic and mass terms of other fields, e.g., the gluon. Similarly, the quadratic part of the full Majorana lagrangian can be rewritten as

$$\begin{aligned}\mathcal{L}^{(2)}_{\text{M,full}} &= \frac{1}{2}\,\bar{\psi}_M(\mathrm{i}\not{\partial} - m)\psi_M \\ &= \mathcal{L}^{(2)}_{\text{D,full}} + \left(e^{-2\mathrm{i}mv\cdot x} P(h_v, H_v) + \text{c.c}\right)\,,\end{aligned} \tag{3.9}$$

where $P(h_v, H_v)$ is a quadratic polynomial of $h_v(x)$, $H_v(x)$ and their derivatives, with constant coefficients (i.e., no explicit x-dependence like $e^{-2\mathrm{i}mv\cdot x}$ inside P), which stems from picking up the $e^{-\mathrm{i}mv\cdot x}$ term of (3.6) twice.

We are now ready to construct effective theories that reproduce these full theories when we specialize in the states of a single ψ fermion with momentum close to mv, plus arbitrary numbers of other light particles with masses and momenta much less than m. The effective theories can be derived from the full theories by restricting the fields $h_v(x)$ and $H_v(x)$ to only contain "slowly varying" modes with wavelengths $\gg m^{-1}$. This does not correctly take into account loop diagrams, where the loop momenta with values up to infinity enter the relevant integrals, but this mismatch can be fully corrected for in the effective theory by adding local operators with appropriate coefficients (i.e. performing the matching procedure, c.f. Sec. 2.2.2).

For the purpose of studying the field content and the form of propagators in the effective theory, tree-level matching is sufficient. Thus, the quadratic terms of the effective lagrangian for the Dirac case can simply be given by the lagrangian (3.8) with the understanding that h_v and H_v only contain modes with wavelengths $\gg m^{-1}$. So,

$$\begin{aligned}\mathcal{L}^{(2)}_{\text{D,eff}} &= \mathrm{i}\bar{h}_v\, v\cdot\partial h_v - \mathrm{i}\bar{H}_v\, v\cdot\partial H_v - 2m\,\bar{H}_v H_v \\ &\quad + (\mathrm{i}\bar{h}_v\,\sigma^{\mu\nu} v_\mu \partial_{\perp\nu} H_v + \text{c.c})\,.\end{aligned} \tag{3.10}$$

In the Majorana case, the effective lagrangian obtained from the lagrangian in Eq. (3.9) contains additional terms, $e^{-2\mathrm{i}mv\cdot x} P(h_v, H_v) + \text{c.c.}$. However, these terms actually vanish once integrated over spacetime to obtain the effective action. In momentum space, they are transformed into δ-functions of the form $\delta^4(2mv + k)$, where k is the momentum carried by $P(h_v, H_v)$. However, since $h_v(x)$ and $H_v(x)$ in the effective theory are restricted to be slowly varying, necessarily $k \ll mv$ and the δ-functions simply vanish. Therefore, we obtain

$$\mathcal{L}^{(2)}_{\text{M,eff}} = \mathcal{L}^{(2)}_{\text{D,eff}}\,. \tag{3.11}$$

We conclude that the field content and propagators of Majorana HQET are identical to those of Dirac HQET. This in particular implies that the spin symmetry of HQET in the limit of decoupling H_v is intact in Majorana HQET, contrary to the claim made in [68].

3.3 Symmetries

In this section, we compare symmetries of the two effective theories. First, the full Dirac and Majorana theories we started with have identical symmetries by assumption, except for $U(1)_D$ of the Dirac fermion. Clearly, all these symmetries of the full theories are passed down to their respective HQETs.

In addition, HQET possesses the emergent "gauge symmetry" of reparameterization invariance (RPI), which is a redundancy in the HQET description in that choosing a different v should not change the physics. Below, we will show that RPI works in exactly the same way in the Majorana and Dirac HQETs.

Furthermore, in Majorana HQET, the $U(1)_D$ global symmetry emerges as an exact symmetry. Being an effective theory of one-particle states, Majorana HQET trivially conserves particle number, even though the full Majorana theory has no particle number conservation. Below, we will demonstrate explicitly how this $U(1)$ arises in Majorana HQET.

Remarkably, yet another symmetry is emerging in Majorana HQET, so that the symmetry content of Majorana HQET is actually larger than that of Dirac HQET. This symmetry is an effective charge conjugation symmetry that reflects the very Majorana nature of the full theory, namely the absence of particle/antiparticle distinction. Thus, this is an exact symmetry of any Majorana HQET, even without a charge conjugation symmetry in the full theory. In contrast, charge conjugation symmetry is optional for Dirac fermions and for Dirac HQETs. This emergent charge conjugation symmetry forbids a class of operators in Majorana HQET that are allowed in Dirac HQET. Therefore, discovering the effects of those operators in experiment can tell us that the underlying fermion must be Dirac.

3.3.1 Reparameterization Invariance

The RPI redundancy in choosing v is manifest in relations (3.5) and (3.6), where the left-hand sides have no reference to v. For the Dirac case, this readily implies that the fields labelled by $v' \equiv v + \varepsilon/m$ must be related to those labelled by v through

$$e^{-\mathrm{i}mv'\cdot x}(h_{v'} + H_{v'}) = e^{-\mathrm{i}mv\cdot x}(h_v + H_v)\,, \tag{3.12}$$

provided that $\varepsilon \ll m$ so that we maintain the requirement that $h_{v'}(x)$ and $H_{v'}(x)$ should vary slowly in x with wavelengths much larger than m^{-1}, just like $h_v(x)$ and $H_v(x)$ themselves. This is exactly the form of RPI proven to be valid to all orders in Dirac HQET by Ref. [60].

For the Majorana case, the v-independence of the left-hand side of (3.6) implies that

$$\begin{aligned} &e^{-\mathrm{i}mv'\cdot x}(h_{v'} + H_{v'}) + e^{\mathrm{i}mv'\cdot x}\mathcal{B}(h^*_{v'} + H^*_{v'}) \\ &= e^{-\mathrm{i}mv\cdot x}(h_v + H_v) + e^{\mathrm{i}mv\cdot x}\mathcal{B}(h^*_v + H^*_v)\,. \end{aligned} \tag{3.13}$$

This naively appears different from the Dirac RPI (3.12). However, since the fields $h_{v'}$, $H_{v'}$, h_v and H_v only carry momenta $\ll mv$, the first term on each side of (3.13) only contains positive frequency modes, while the second term on each side only contains negative frequency modes. Thus, the first and second terms are linearly independent and can be equated separately. This leads to a relation identical to the Dirac RPI (3.12). We conclude that RPI works identically in Dirac and Majorana HQETs.

3.3.2 Emergent $U(1)_D$ in Majorana HQET

The equality (3.11) trivially implies that the quadratic part $\mathcal{L}^{(2)}_{\text{M,eff}}$ respects the same $U(1)_D$ global symmetry as the Dirac counterpart, with both h_v and H_v carrying a unit charge, even though the full Majorana theory (3.9) possesses no $U(1)$ symmetry. We proceed now to show that $U(1)_D$ is an exact symmetry of the entire Majorana HQET lagrangian, not only of the quadratic part, as is expected due to the fact that Majorana HQET is a theory for a fixed number of particles (namely one).

The emergence of $U(1)_D$ can be demonstrated elegantly by using RPI. Since we have shown that Majorana RPI is the same as Dirac RPI, Majorana HQET has the same "RPI invariant" as the Dirac RPI. Namely, the RPI relation (3.12) implies that the linear combination defined as

$$\chi(x) \equiv e^{-\mathrm{i}mv\cdot x}[h_v(x) + H_v(x)] \tag{3.14}$$

(not to be conceptually confused with the full-theory Dirac field ψ_D) is invariant under $v \to v + \varepsilon/m$. Therefore, RPI can be made manifest by writing the lagrangian solely in terms of χ.

Now, since HQET is an effective theory for single-particle states, we only need to look at operators that are bilinear in χ. Thus, all operators in Majorana HQET are in either one of the following forms:

$$\bar{\chi}\mathcal{O}\chi\,, \quad \chi^T\mathcal{C}\mathcal{O}\chi\,, \tag{3.15}$$

where $\mathcal{O}$ contains Gamma matrices, derivatives and the light fields in the theory, while the charge conjugation matrix $\mathcal{C}$ satisfies

$$\mathcal{C}\gamma^{\mu T}\mathcal{C}^{-1} = -\gamma^\mu\,, \quad \mathcal{C}^* = -\mathcal{C}^{-1}\,, \quad \mathcal{C}^T = -\mathcal{C}\,. \tag{3.16}$$

The operators of the 1st type in (3.15) are invariant under $U(1)_D$, while those of the 2nd type are not. Notice, however, that the latter do not exist in the effective action, because they contain rapid oscillations $e^{\pm 2\mathrm{i}mvx}$ and thus vanish under the integration over spacetime, just like what happened to $P(h_v, H_v)$ previously. Therefore, $U(1)_D$ is indeed respected by all operators in Majorana HQET.

3.3.3 Emergent $\mathbb{Z}_2$ Symmetry in Majorana HQET

Notice that the right-hand side of (3.6) is unchanged by the simultaneous operations of

$$v \leftrightarrow -v\,, \quad h_v \leftrightarrow \mathcal{B}h_v^*\,, \quad H_v \leftrightarrow \mathcal{B}H_v^*\,. \tag{3.17}$$

Majorana HQET must be invariant under these charge conjugation operations, because, like RPI, this is a redundant operation, doing nothing to the full-theory field ψ_M. This redundancy makes sense intuitively, because the original Majorana fermion does not distinguish particle and antiparticle so the theory should be independent of the choice v or $-v$ to write the effective theory.

In contrast, Dirac HQET does not in general respect the charge conjugation symmetry (3.17), unless the full theory happens to be invariant under the charge conjugation $\psi_D \leftrightarrow \mathcal{B}\psi_D^*$. It should be stressed, however, that such a symmetry may or may not be present in a given Dirac theory, while any Majorana HQET must obey the symmetry (3.17),

regardless of the presence or absence of charge conjugation symmetry in the full theory, as it is merely a redundancy of the formulation, comparable to RPI.

The emergent charge conjugation symmetry (3.17) imposes nontrivial constraints on the structure of the Majorana HQET lagrangian. As a theoretical illustration, consider a toy model consisting of a heavy, color-octet Majorana fermion $\psi_M = \psi_M^a T^a$ ($a = 1, \cdots, 8$), where $T^a \equiv \lambda^a/2$ with the Gell-Mann matrices λ^a. Suppose that there is also a color-octet real scalar $\phi = \phi^a T^a$ much lighter than ψ. Then, in the full theory, symmetry permits the Yukawa interaction of the form

$$d^{abc}\, \phi^a (\psi_M^b)^T \mathcal{C} \psi_M^c \,, \tag{3.18}$$

with the totally symmetric $d^{abc} \propto \mathrm{tr}[T^a\{T^b, T^c\}]$.
The analogous term $f^{abc}\, \phi^a (\psi_M^b)^T \mathcal{C} \psi_M^c$ with the totally antisymmetric
$f^{abc} \propto \mathrm{tr}[T^a[T^b, T^c]]$ vanishes simply due to the *algebraic* identity reflecting the Fermi-Dirac statistics, $(\psi_M^b)^T \mathcal{C} \psi_M^c = (\psi_M^c)^T \mathcal{C} \psi_M^b$, without owing to any symmetry. This interaction matches at tree level onto the HQET operator

$$d^{abc}\, \phi^a \bar{h}_v^b h_v^c + \cdots \,, \tag{3.19}$$

where the ellipses indicate similar terms containing H_v.

In stark contrast, if the Majorana fermion were instead a color-octet Dirac fermion $\psi_D = \psi_D^a T^a$, both types of the interactions would be allowed:

$$d^{abc}\, \phi^a \bar{\psi}_D^b \psi_D^c + f^{abc}\, \phi^a \bar{\psi}_D^b \psi_D^c \,, \tag{3.20}$$

since this time $\bar{\psi}_D^b \psi_D^c \neq \bar{\psi}_D^c \psi_D^b$. These interactions match at tree level onto the HQET operators

$$d^{abc}\, \phi^a \bar{h}_v^b h_v^c + f^{abc}\, \phi^a \bar{h}_v^b h_v^c + \cdots \,, \tag{3.21}$$

where the ellipses indicate similar terms containing H_v.

Now, without the emergent charge conjugation symmetry (3.17), one would think that the f^{ijk} operator as in (3.21) should also be generated in Majorana HQET at loop level, since Majorana HQET would have exactly the same symmetries and same degrees of freedom as Dirac HQET.[1] However, under the symmetry (3.17), the d^{abc} operator is allowed but the f^{abc} operator is not, because the operation (3.17) gives

$$\bar{h}_v^b h_v^c \longrightarrow (h_v^b)^T \mathcal{B}^{-1} \gamma^0 \mathcal{B} h_v^{c*} = \bar{h}_v^c h_v^b \,, \tag{3.22}$$

so the f^{abc} operator would change sign. Therefore, the emergent charge conjugation of Majorana HQET guarantees that the f^{ijk} operator is never generated at any order in loop expansion.

We conclude that emergent charge conjugation symmetry of Majorana HQET offers the interesting opportunity to tell apart Dirac and Majorana fermions from only low energy measurements performed at scales much below the fermion mass threshold. Namely, probing the presence of the HQET operators forbidden by (3.17) can rule out the possibility that the fermion is Majorana.

[1] If we assume renormalizability in the full Majorana theory, we would have the accidental charge conjugation symmetry $\psi^a T^a \to \pm \psi^a (-T^a)^T$, $\phi^a T^a \to -\phi^a (-T^a)^T$ and $G_\mu^a T^a \to G_\mu^a (-T^a)^T$, with G_μ being the gluon field. Then, correspondingly in Majorana HQET, the symmetry $h_v^a T^a \to \pm h_v^a (-T^a)^T$, etc., would forbid the f^{abc} term. However, this accidental symmetry can easily be broken by non-renormalizable interactions, e.g., $f^{abc} d^{cde}\, \phi^a (\partial_\mu \phi^b) \bar{\psi}^d \gamma^\mu \psi^e$, which we assume to be present.

3.4 Conclusion & applications

Majorana HQET possesses an emergent $U(1)$ symmetry as if it came from a Dirac fermion, even though Majorana fermions by definition cannot have any fundamental $U(1)$ symmetry. The famous reparameterization invariance [57–60], from which HQET derives much of its predictive power, applies in the same way for the Dirac as well as the Majorana case. However, there is a difference between the two effective theories. We showed that in the Majorana case, an additional effective charge conjugation symmetry emerges. This effective charge conjugation symmetry is an exact, intrinsic property of Majorana HQET that reflects the absence of particle-antiparticle distinction in the original Majorana fermion. This contrasts to the Dirac case, where a Dirac HQET would have a charge conjugation symmetry only if the full theory has one. This new $\mathbb{Z}_2$ symmetry of the effective lagrangian, emerging from the charge conjugation symmetry of the full theory is the one new aspect of Majorana HQET as compared to usual Dirac HQET and therefore potentially provides the opportunity to distinguish between the two cases experimentally.

To distinguish directly between R-hadrons containing a Majorana gluino and those containing a Dirac gluino that appears e.g. in many non-minimal models of supersymmetry, using the above approach, however would seem difficult: The strategy would be to search for energy levels in the gluino R-hadron spectrum that are forbidden by the $\mathbb{Z}_2$ symmetry (3.17), and if those can be found then the gluino must be a Dirac fermion. The spectrum of the R-hadrons at leading order however is just colombic, which is unrelated to charge conjugation. The spectral differences between Dirac and Majorana R-hadrons are therefore expected to only appear at the fine-structure level.

The emergent $\mathbb{Z}_2$ symmetry can however be crucial for other phenomenological aspects. An example is presented in Ref. [69], in which the authors apply HQET to determine the cross section for low-velocity scattering of $SU(2)$ charged weakly interacting massive particles (WIMPs) on nuclear targets. Using a real $SU(2)$ triplet scalar as a WIMP, the appropriate version of scalar HQET exhibits the same $\mathbb{Z}_2$ symmetry (3.17) as Majorana HQET, which reduces the number of effective operators and corresponding matching conditions.

CHAPTER 4

LHC IMPLICATIONS OF WIMP DARK MATTER AND GRAND UNIFICATION

The existence of dark matter (DM) is well established through numerous independent astrophysical observations. DM has been experimentally determined to be electrically neutral, non-relativistic (cold) and to at most weakly interacting with baryonic matter. None of particles in the standard model satisfy these requirements. Dark matter thus is arguably the most compelling evidence for new physics beyond the standard model.

In this chapter we motivate, devise and analyze a specific extension of the standard model incorporating dark matter which we worked out originally in Ref. [38]. The scenario we discuss is based on two well-known and extensively studied concepts: (i) that a so-called weakly interacting massive particle (WIMP) constitutes dark matter and (ii) the concept of Grand Unification postulating that the SM gauge groups are subgroups of a single larger symmetry group. The novel aspect of our work is to demonstrate that robust phenomenological trends arise when combining these otherwise independent concepts. Specifically, new colored particles are expected at the TeV scale. These new particles are either collider-stable or decay to final states including a Higgs boson. Both possibilities promise interesting collider signatures.

We preface our discussion with two sections which provide the relevant background. In the first one, we introduce the topic of dark matter, with emphasis on weakly interacting massive particles as dark matter candidater, and in the second one we discuss the concept of Grand Unification. We then proceed to combine the two concepts and work out the resulting phenomenology, following closely our contribution Ref. [38].

Since this work was published, the LHC has delivered improved lower mass bounds on the masses of the colored particles proposed in [38], excluding several of the benchmark points presented. Also, in exploring the prospects of these new colored states to provide an additional Higgs production mode, we assume $m_h = 200\,\text{GeV}$ which is not upheld by the recent LHC result of $m_h = 125\,\text{GeV}$. We nevertheless include our original collider analysis in order to provide a complete and comprehensive picture of our work. We comment on improved bounds and the appropriate changes in the collider analysis of our scenario in Sec. 4.8.

4.1 Dark matter

The earliest evidence for DM was found in observations of galactic rotation curves: Objects on stable Keplerian orbits with radius r outside the visible part of the galaxies are observed to have rotational velocities $v(r)$ that do not decrease as $v(r) \propto 1/\sqrt{r}$ as is predicted by Kepler's Law assuming the gravitational attraction stems solely from the visible mass inside the galaxy. Instead $v(r)$ remains approximately constant out to the largest values of r where the rotation curve are measured. This suggests that the existence of an additional source of gravitational attraction. The rotation curves are explained by the existence of a *dark matter halo* with mass density $\rho(r) \propto 1/r^2$ [34].

The observation of the Bullet cluster passing through another cluster provides particularly persuasive evidence for DM. Whereas the hot baryonic gas masses of the two clusters collided and decelerated, gravitational lensing shows that most of the total mass continues to move on ballistic trajectories. In addition to confirming the existence of a DM halo surrounding the visible galaxy, this observation illustrates directly that DM interacts weakly with visible matter as well as with itself.

The most accurate estimate of the DM density is obtained from global fits of cosmological parameters to a variety of astronomical observations such as the anisotropy in the Cosmic Microwave Background (CMB). The density of cold non-baryonic matter is determined to be [70]

$$\Omega_{\mathrm{nbm}} h^2 = 0.112 \pm 0.006, \tag{4.1}$$

where h is the Hubble constant.

4.1.1 WIMP dark matter

From the discussion above it is clear that candidates for dark matter must satisfy several criteria: First, it has to have little interaction with ordinary matter. More specifically, a DM particle cannot carry electromagnetic charge and has to interact very weakly with baryonic matter. Second, analysis of structure formation in our universe further requires DM to be cold, i.e., non-relativistic. Specifically, if DM consisted of light relativistic particles, the formation would have proceeded in a top-down way and large scale structures such as galaxy clusters would have formed before small scale ones like stars. Since it is established that structure formation instead proceeded in a hierarchical, bottom-up way, relativistic particles cannot make up a signigicant portion of the observed DM density. This requirement excludes SM neutrinos as valid DM candidates. Lastly, DM needs to be stable at cosmological time scales, otherwise it would have decayed away already.

As compelling as the existing data is in confirming the existence of dark matter and establishing the properties just discussed, it provides little insight into the identity and nature of the dark matter particles. The requirements listed above leave room for a wide range of possibilities for the nature of dark matter. Among the most promising DM candidates are axions, sterile neutrinos and weakly interacting massive particles (WIMPs).

As the acronym indicates, WIMPs are particles with mass in the range of $10\,\mathrm{GeV} - 10\,\mathrm{TeV}$ and cross sections governed by weak interactions. In the early universe, WIMPs are assumed to be in thermal equilibrium with the visible (standard model) matter. The

equilibrium is established through WIMP pair annihilation into SM particles and vice versa. The reaction rate is proportional to the product of WIMP number density and the thermally averaged annihilation cross section times velocity $\langle \sigma_A v \rangle$. As the universe expands and the temperature drops below the WIMP mass, the thermal production of WIMPs becomes Boltzmann-suppressed. The WIMPs drop out of thermal equilibrium once their reaction rate drops below the Hubble expansion rate H. This effect is called *freeze-out*. After freeze-out, the WIMP number density per co-moving volume remains practically constant, as any given WIMP is unlikely to find another WIMP to annihilate. The present relic density Ω_{WIMP} is evaluated [71] to be approximately

$$\Omega_{\mathrm{WIMP}} h^2 \simeq \text{const.} \frac{T_0^3}{M_{\mathrm{Pl}}^3 \langle \sigma_A v \rangle} \simeq \frac{0.1\,\mathrm{pb} \cdot c}{\langle \sigma_A v \rangle}\,, \tag{4.2}$$

where $T_0 = 2.7255(6)\,K$ [70] is the present day CMB temperature. Thus, the WIMP relic density has the correct order of magnitude to explain dark matter if its annihilation cross section is about 0.1 pb. This is precisely the size of typical cross sections governed by the weak interaction. The fact that two astrophysical parameters T_0 and M_{Pl} in combination point to a purely particle physics quantity is quite remarkable. This so-called *WIMP Miracle* is an encouraging trait of the WIMP DM candidate.

WIMPs are encountered in many extension of BSM physics. The arguably most prevalent dark matter candidate in the literature is the lightest superparticle (LSP) in supersymmetric models [72, 73]. Typically the LSP is stabilized by imposing an exact R-parity in these models [62].

In Ref. [2], the concept of WIMP DM has been analyzed from a purely effective field theory point of view. Instead of being embedded into a framework aimed at solving e.g. the hierarchy problem and predicting an entire spectrum of new particles at the weak scale, [2] takes a minimalistic approach to WIMP DM. The proposed *minimal dark matter* scenario extends the SM particle content only by a single n-tuplet of $SU(2)$ that does not carry color charge and has a hypercharge such that an electrically neutral component of the n-tuplet exists can be dark matter.

4.1.2 Direct detection searches for WIMPs

The strongest experimental limits on WIMP dark matter particles arise from direct detection experiments.

From the rotation curves it is inferred that dark matter is gravitationally trapped inside of galaxies, including our own. The earth on its orbit around the sun is thus moving through a *dark matter wind*. WIMPs are expected to interact with matter inside of detectors via elastic scattering with typical recoil energies of the order of 1 to 100 keV. The shape of the predicted nuclear recoil spectrum results from the convolution of the velocity distribution of the WIMP with the angular scattering distribution. The WIMP velocity distribution is usually taken to be Maxwellian, an assumption which however does not take into account the possibility of streams. Also, the local dark matter density is not known precisely: The canonical value of $\rho_0 = 0.3\,\mathrm{GeV/cm^3}$ is subject to an uncertainty factor of order one depending on the modelization of the halo.

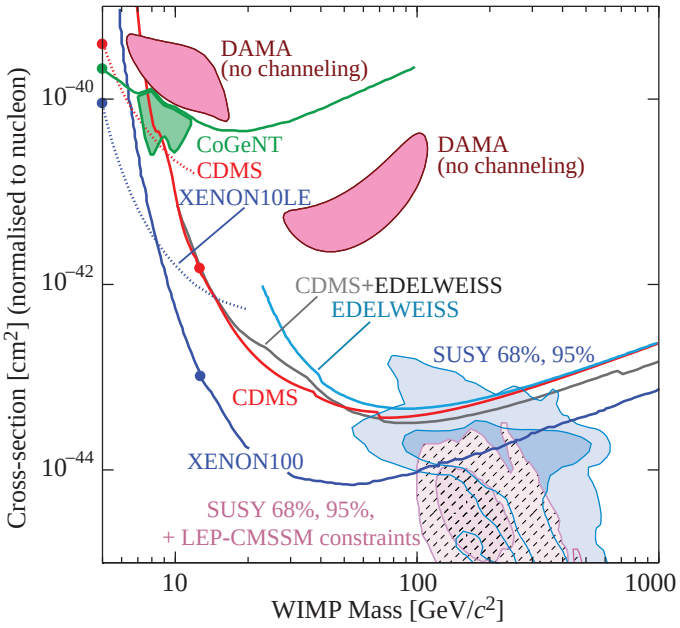

Figure 4.1: Exclusion limits / claims of signal regions for WIMPs, in the plane of spin-independent cross section (normalized to nucleon mass) versus WIMP mass. The shaded regions correspond to SUSY predictions for LSP WIMP cross sections. The cross-shaded regions correspond to LHC exclusion bounds obtained for the cMSSM. Figure taken from Ref. [1].

The spin-independent part of the cross section scales approximately as square of the mass of the nucleus as a result of coherence effects between the individual nucleons, so heavier target nuclei are preferred. Unless the spin-dependent part of the DM-nucleon scattering cross section vanishes, it dominates over the spin-independent component. Several direct detection experiments exist with a range of target nuclei including ^{19}F, ^{23}Na, ^{73}Ge, ^{127}I, ^{129}Xe and ^{133}Cs. Since the typical cross sections of DM recoiling against the target nuclei do not exceed 1 evt day^{-1} kg^{-1}, the experiments need to be performed underground to shield against cosmic ray induced backgrounds and the selection of radio-pure materials for the construction of the detector is crucial.

The current observations at the various DM experiments are conflicting. The longstanding claim by the DAMA/LIBRA experiment to have observed an annually modulated WIMP signal [74,75] and the tentative signal found by the CoGeNT collaboration [76,77] are contradicted by the null results from CDMS [78,79], EDELWEISS [80,81] and XENON [82,83]. Whether the disagreement stems from unaccounted backgrounds that are being mistaken for signal events or from non-standard physical effects that modify the WIMP-nucleus interactions in specific experiments is still a subject of intense discussion. The current XENON and CDMS exclusion limits are starting to exclude the typical lightest supersymmetric particle (LSP) WIMP DM candidates predicted in many supersymmetric models, c.f. Fig. 4.1. The *minimal dark matter* hypothesis is less constrained, see Fig. 4.2. The improved reach

of the upcoming experiments XENON-1T [84] and Super-CDMS [85] will provide crucial further tests for WIMPs as DM candidates.

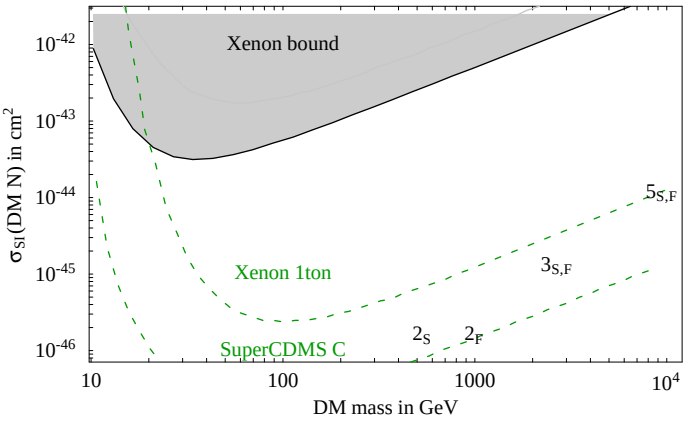

Figure 4.2: Direct detection limits are not yet sensitive to *minimal dark matter* WIMP candidates as defined in [2] and [3]. Fermionic (scalar) n-tuplets of $SU(2)_L$ are denoted by n_F (n_S). The scenario will be probed by the upcoming XENON-1T and SuperCDMS experiments. Figure taken from Ref. [3].

4.2 Grand Unification

The standard model is characterized by its symmetry structure, namely the tensor product of three Gauge Symmetry groups, $SU(3)_C \times SU(2)_L \times U(1)_Y$ with the respective gauge couplings g_3, g and g'. The SM fermions are in the following representations of the gauge symmetries:

$$\begin{array}{lllll} \text{quarks:} & q \sim (\mathbf{3},\mathbf{2})_{1/6} & u^c \sim (\bar{\mathbf{3}},\mathbf{1})_{-2/3} & d^c \sim (\bar{\mathbf{3}},\mathbf{1})_{1/3} & \\ \text{leptons:} & l \sim (\mathbf{1},\mathbf{2})_{-1/2} & e^c \sim (\mathbf{1},\mathbf{1})_1 & & \end{array} \tag{4.3}$$

We use the standard notation $(SU(3)_C\,,\, SU(2)_L)_Y$ to specify the representations. Three generations exist of each quark and lepton species. The SM model particle spectrum is completed by a single Higgs boson in the representation

$$H \sim (\mathbf{1},\mathbf{2})_{1/2}. \tag{4.4}$$

In general, the presence of chiral fermions leads to so-called *anomalies*. The transformations of an anomalous symmetries leave the action invariant but do change the path integral. The SM however is anomaly-free, since the individual contributions from the five fermion families precisely cancel each other. This is a highly non-trivial feature and can be interpreted as a sign for an underlying organizing principle governing the particle content and the symmetry structure of the SM.

Grand Unified theories (GUTs) provide such a principle. Grand Unification stipulates that the $SU(3)_C \times SU(2)_L \times U(1)_Y$ gauge group is embedded in a larger and simpler gauge group. Georgi and Glashow proposed specifically $SU(5)$ to be this more fundamental symmetry group [86], based on the observation that the five SM fermion families can be grouped into two simple representations of $SU(5)$:

$$\bar{\mathbf{5}} = [d^c, l] \qquad\qquad \mathbf{10} = [q, u^c, e^c]\,. \tag{4.5}$$

In this picture, anomaly cancellation in the SM is the direct result of the fact that the chiral representations $\bar{\mathbf{5}}$ and $\mathbf{10}$ of $SU(5)$ have opposite contributions to the gauge anomaly. Unification also explains the absence of fractionally charged hadrons: If the SM gauge groups result from a spontaneous breaking $SU(5) \to SU(3)_C \times SU(2)_L \times U(1)_Y$, the gauge representations of the SM particles are fully determined by the respective $SU(5)$ representation in the unbroken limit. Specifically, the resulting $U(1)_Y$ charges are automatically quantized. Unification thus offers a way to explain the absence of fractionally charged hadrons as well as the fact that the electric charges of protons and electrons are exactly opposite, resulting in exactly neutral atoms.

Embedding the three SM gauge groups into a single $SU(5)$ with gauge coupling g_U requires the gauge couplings to obey the relation

$$g_3 = g_2 = g_1 = g_U \qquad \text{where } g_2 = g \text{ and } g_1 = \sqrt{\frac{5}{3}} g'\,. \tag{4.6}$$

Unification of the gauge couplings in the sense of Eq. (4.6) is clearly not observed in the experimentally determined values of the three gauge couplings, which show a distinct hierarchy. This hierarchy can be understood in terms of effective field theories: The $SU(5)$ symmetry is valid only above M_{GUT}, the scale at which it is broken spontaneously. All particles which are not in the SM subgroup of $SU(5)$ acquire masses of order M_{GUT} while all SM particles remain light. In the EFT picture the GUT particles are integrated out at the scale M_{GUT}. The gauge couplings, starting from a common value $g_U(M_{\text{GUT}})$, evolve independently below M_{GUT} all the way down to the EWSB scale. While the $SU(3)$ and $SU(2)$ gauge couplings increase at lower energy scales according to their asymptotically free renormalization group equations (RGEs), the $U(1)_Y$ coupling decreases. This explains the observed hierarchy $g_3 \gg g \gg g'$.

A closer look at the solutions to the SM renormalization group equations reveals that the three gauge couplings' trajectories do come close together at energies of about 10^{15} GeV but the unification is not exact. In the minimal supersymmetric extension of the standard model, or MSSM, additional contributions from superparticles modify the RG equations in such a way that the three couplings meet almost precisely at $M_{\text{GUT}} \simeq 10^{16}$ GeV with a value of $\alpha_U(M_{\text{GUT}}) \equiv g_u^2(M_{\text{GUT}})/(4\pi) \simeq 1/24$. The remaining deviation from exact gauge coupling unification is small enough to be explained by threshold corrections from integrating out GUT particles at M_{GUT}. Perturbative gauge coupling unification allows the interpretation that supersymmetry is embedded into a GUT framework and is considered to be one of the main motivating features of supersymmetry.

Because quarks and leptons are combined into GUT multiplets, baryon number is necessarily violated in any Grand Unified theory. Nucleons can decay via the exchange of gauge bosons with GUT scale masses. The relevant baryon number violating effective operators have mass dimension six and are suppressed by $1/M_{\rm GUT}^2$. The Super-Kamiokande limit of the decay rate $\tau(p \to \pi^0 e^+) > 5.3 \cdot 10^{33}$yr [87] then translates into a bound on the GUT scale of $M_{\rm GUT} \gtrsim 10^{15}\,$GeV.

Grand Unified theories are also often based on larger symmetry groups, containing the $SU(5)$ as subgroup. A prominent example is the symmetry group $SO(10)$. The 16 dimensional spinor representation transforms as

$$\mathbf{16} = \mathbf{10} + \bar{\mathbf{5}} + \mathbf{1} \tag{4.7}$$

under the subgroup $SU(5)$. Thus all SM families can be placed into a single $SO(10)$ spinor representation. The $SU(5)$ singlet is identified as the right-handed neutrino ν^c, whose presence allows to write down a renormalizable neutrino mass term.

4.3 Combininig the concepts of WIMP dark matter and gauge coupling unification

We have provided the background to present our work [38], in which we identify robust phenomenological trends that can be derived from combining the concepts presented in the preceding sections, namely gauge coupling unification and dark matter being realized in form of a simple WIMP. In addition to a WIMP candidate in the triplet representation of $SU(2)$, our scenario predicts new colored states within LHC reach.

The motivation to combine WIMP DM with gauge coupling unification originates from the following train of thought. The existence of dark matter is unequivocal evidence for new physics beyond the standard model and a weakly interacting massive particle is a simple and robust DM candidate as discussed in Sec. 4.1. Since the null results from direct DM search experiments have excluded a WIMP with nonzero hypercharge [88], the simplest WIMP DM candidate is an $SU(2)_L$-triplet with $Y = 0$, denoted as a V hereafter. The V can be stabilized by imposing e.g. $\mathbb{Z}_2$ parity transforming $V \to -V$. A careful calculation of the relic abundance of a V is performed in Ref. [3], including non-perturbative effects and possible co-annihilations, finding that the V mass should be 2.5 TeV if the V is spin-0, or 2.7 TeV if it is spin-1/2, assuming that the V accounts for the entire missing mass of the universe. Unfortunately, since the V is heavy and color-neutral, it is virtually impossible to be directly produced in pp collisions at the Large Hadron Collider and direct detection limits are not restrictive enough to confirm or exclude it (the V particle corresponds to the point marked by 3_F in Fig. 4.2). However, V may well be part of a bigger, well-motivated extension of the SM containing other new particles that can give rise to observable LHC signals. We select gauge coupling unification [86, 89] as to be that guiding principle besides WIMP DM.

Although this is still not constraining enough to point to one single model, it is possible to identify generic, robust phenomenological trends in such extensions of the SM. Specifi-

cally, we adopt the V as a dark matter candidate and demand perturbative gauge coupling unification.[1] We assume no extra mass scales other than the unification scale and the TeV scale as dictated by the WIMP miracle. Finally, we assume that new particles, including the V, are all fermions to avoid extra fine-tuning issues associated with scalar masses. These assumptions readily imply the existence of additional new particles at the TeV scale since the gauge couplings in the SM+V theory do not unify. In particular, we find that there must exist new colored particles at the TeV scale. We also find that the new colored particles generically allow Yukawa couplings to quarks and the Higgs boson.

At this point we want to comment on the connection between our setup and the scenario called *split supersymmetry* [64, 65]. Split supersymmetry is a well-studied scenario, which is also based on WIMP DM and gauge coupling unification. Similar to our scenario it lacks supersymmetry at the TeV scale. There are two major differences, however. First, contrary to one of our assumptions above, split supersymmetry has an extra threshold between the TeV and the unification scale, where all the squarks and sleptons, and most importantly, the second Higgs doublet reside, which affects unification. Second, in split supersymmetry, WIMP DM has to be a nontrivial composition of the higgsinos, wino and/or bino; if we assume that dark matter in split supersymmetry is a pure wino (i.e. the V) as in our scenario, gauge coupling unification would not work well (using the same criteria for precision as we use in Sec. 4.4) unless there is a hierarchy larger than two orders-of-magnitude between the higgsino and gluino masses.

The existence of new colored particles with Yukawa couplings λ to quarks and the Higgs boson suggests the following two scenarios for the LHC. If λ is sufficiently small, the new colored particles will be collider stable, appearing as massive stable hadrons called R-hadrons. Since R-hadron signals can be quite spectacular, this is an exciting possibility already for the *early* LHC run at $\sqrt{s} = 7\,\text{TeV}$ with an integrated luminosity $\approx 1\,\text{fb}^{-1}$. On the other hand, if λ is not so small, the new colored particles will decay promptly via λ, with an $\mathcal{O}(1)$ fraction of their decays containing Higgs bosons. This is an interesting new production channel for the Higgs boson, where the size of the cross section is governed by the *strong* interaction, potentially making the LHC a "Higgs factory".

To perform quantitative benchmark studies of these characteristic phenomenological features of WIMP DM and unification, we choose a simple benchmark model consisting of a DM candidate V and new colored particles X (to be specified more explicitly later). Among all models with WIMP DM and unification, this benchmark model contains the smallest number of new multiplets beyond the SM, but it already exhibits the two classes of generic collider signatures mentioned above.

Our analysis on this benchmark model as shows that, for the range $m_X = 360\text{-}650\,\text{GeV}$, the early LHC phase ($7\,\text{TeV}$, $1\,\text{fb}^{-1}$) should have sufficient discovery potential for the R-hadron case. Since our work was published, the experimental search strategy for R-hadrons has been improved [67], and in fact the benchmark points analyzed for the R-hadron case

[1] Note that a V is not only the simplest WIMP DM candidate possible but also the only $SU(2)_L$ multiplet with zero hypercharge that appears within the simple $SU(5)$ multiplets, **5**, **10**, **15**, and **24**.

have already been excluded [90,91]. Even in light of this, the analysis presented here is still relevant as it shows the generic properties of the underlying model and demonstrates its predictive power.

For the Higgs factory case, we will lay out an experimental strategy for the full LHC at $\sqrt{s} = 14\,\text{TeV}$. This consists of two parts, the discovery of the X and measurement of m_X, and the discovery of the Higgs bosons from the X decays. We show that with $10\,\text{fb}^{-1}$ of data at the LHC (14 TeV), it should be possible to discover the X and the Higgs bosons from the X decays in the range $300\,\text{GeV} < m_X \lesssim 550\,\text{GeV}$ for a moderately heavy Higgs (i.e. decaying to weak gauge bosons).[2]

The remainder of this chapter is organized as follows. In Sec. 4.4 we survey possible extensions of the SM that feature gauge coupling unification and WIMP DM. In Sec. 4.5 we describe our simple benchmark model that phenomenologically represents all such extensions. The couplings λ of the new colored particles to quarks and the Higgs are expected to have an upper bound from flavor/CP/electroweak constraints, which is analyzed in Sec. 4.6 using the benchmark model. The collider signatures of the R-hadron case and the Higgs factory case are studied in detail in Sec. 4.7.1 and Sec. 4.7.2, respectively. In Sec. 4.8 we summarize our analyses and comment on how our scenario is affected by more recent LHC searches. As an aside, in Appendix A we discuss how proton decay can be avoided in the class of models we are considering.

4.4 Extensions of the SM featuring WIMP DM and unification

In this section we enumerate possible extensions of the SM that contain the WIMP DM candidate V and are consistent with gauge coupling unification, and identify generic features shared by such extensions. This analysis will serve as a basis for our choice of a benchmark model in Sec. 4.5.

Let us assume unification of the SM gauge group into a simple group, such as $SU(5)$, to fix the normalization of hypercharge. The DM candidate V can be embedded into a **24** of $SU(5)$, consistent with this assumption. Moreover, let us assume that all new particles, including the V, are spin-1/2 fermions in order to avoid unnecessary extra fine-tuning problems associated with scalar masses besides the notorious existing problem with the Higgs mass. As calculated in Ref. [3], the fermionic V mass is fixed by the relic abundance to be $m_V = 2.7\,\text{TeV}$, which we will assume to be the case hereafter.

This cannot be the end of the story, however, because the SM augmented by only the V is not consistent with gauge coupling unification. There must be additional new particles. In principle, these additional particles could appear anywhere below the unification scale. However, since we must presume some underlying dynamics that generates the TeV scale in order for the WIMP miracle not to be a mere coincidence, we adopt the simplest assumption

[2]The assumption of a moderately heavy Higgs decaying predominantly to WW and ZZ was valid when [38] was published, but is outdated since the Higgs boson has been discovered to be light, $m_h \sim 125\,\text{GeV}$. We discuss how this affects the phenomenology of our scenario in Sec. 4.8.

that the same dynamics also provides TeV-scale masses to the additional new particles, with no extra mass scale other than the TeV scale and the unification scale. We take the new fermions to be vectorlike, because chiral fermions would require electroweak symmetry breaking to acquire TeV-scale masses, which would generically lead to dangerously large corrections to precision electroweak observables, in particular the ρ parameter [92, 93]. Let us further restrict ourselves to the case where the vectorlike fermions can be embedded into the simplest $SU(5)$ multiplets, $\mathbf{5} \oplus \overline{\mathbf{5}}$, $\mathbf{10} \oplus \overline{\mathbf{10}}$, $\mathbf{15} \oplus \overline{\mathbf{15}}$ and $\mathbf{24}$. Thus, we consider

$$\begin{array}{lll} Q \sim (\mathbf{3},\mathbf{2})_{1/6}\,, & U \sim (\mathbf{3},\mathbf{1})_{-2/3}\,, & D \sim (\mathbf{3},\mathbf{1})_{-1/3}\,, \\ L \sim (\mathbf{1},\mathbf{2})_{+1/2}\,, & E \sim (\mathbf{1},\mathbf{1})_{+1}\,, & X \sim (\mathbf{3},\mathbf{2})_{-5/6}\,, \\ S \sim (\mathbf{6},\mathbf{1})_{-2/3}\,, & T \sim (\mathbf{1},\mathbf{3})_{1}\,, & V \sim (\mathbf{1},\mathbf{3})_{0}\,, \\ G \sim (\mathbf{8},\mathbf{1})_{0}\,, & & \end{array}$$

as well as the conjugates Q^c, U^c, $\cdots$, T^c, except for V and G, which are real. (Our convention is such that H has the quantum numbers $(\mathbf{1},\mathbf{2})_{1/2}$. The SM fermions are denoted by lower-case letters, q, u^c, d^c, l, e^c.) As we will see below, this already provides a sufficient number of candidate models for us to observe generic trends in extensions of the SM with WIMP DM and gauge coupling unification.

In searching for possible field contents that can lead to unification, there are various uncertainties that must be taken into account when we "predict" the $SU(3)_C$ coupling α_3 in terms of $\alpha_{1,2}$, which we regard as precise. First, in our RG analysis, which we perform at the 1-loop level, there is a threshold ambiguity at $m_V = 2.7\,\text{TeV}$. We estimate this uncertainty by varying the $\overline{\text{MS}}$ subtraction scale μ from $m_V/\sqrt{2}$ to $\sqrt{2}\,m_V$. Second, unlike the V mass, the masses of the additional fermions cannot be fixed a priori and can be anywhere at the TeV scale, from a few hundred GeV to several TeV. Therefore, we scan over the additional fermions' masses in the range between 300 GeV and 10 TeV, where for simplicity we assume a single common mass for all of them.[3] These two sources of uncertainty each shift our α_3 prediction at the level of a few times $\Delta\alpha_3^{(\text{exp})}$, the experimental uncertainty in the measurement $\alpha_3^{(\text{exp})} = 0.1184 \pm 0.0007$ [94]. We demand that the "band" in our α_3 prediction combining these two uncertainties have an overlap with the band corresponding to $3\Delta\alpha_3^{(\text{exp})}$ (i.e. 3σ). There are also threshold effects from unspecified GUT physics, but we assume that they are similar in size to the uncertainties mentioned above and simply neglect them. Finally, we demand that the coupling at the unification scale be perturbative, $\alpha_{\text{GUT}} < 1$.

A similar analysis was performed in Ref. [65], where the main difference lies in the treatment of proton decay. While Ref. [65] demands the unification scale to be higher than $\sim 10^{16}\,\text{GeV}$ in order to sufficiently suppress proton decay, we choose to impose a symmetry to forbid proton decay, and only demand the GUT scale to be higher than $10^5\,TeV$ (and lower than the Planck scale $\sim 10^{18}\,\text{GeV}$) to avoid having to address possible conflicts between GUT physics and flavor/CP bounds. The use of a symmetry to forbid proton decay requires some model building at the unification scale, but it has no observational consequences for the TeV-scale physics, so we leave the model building to Appendix A. Another

[3] New charged/colored particles below 300 GeV are likely to be already excluded, as will be illustrated by the analysis of the benchmark model below.

Table 4.1: Possible combinations of new fermions that, together with the DM V, could lead to unification. It is understood that the new fermions are vectorlike, so in writing X, U, $\cdots$, the presence of their charge conjugates X^c, U^c, $\cdots$ is also implied, except for the Majorana fermions V and G.

$2X$	$2X + D + L$	$2U + T + E$
$U + S + 2T$	$2X + 2U + T$	$3X + L + E$
$3X + G + V$	$3U + T + L$	$\cdots$

difference between our analysis and that of Ref. [65] is that in calculating the running of the gauge couplings, Ref. [65] assumes that all new particles have masses near m_Z, while our masses span a wide range around a TeV, as we described above.

There are 22 models satisfying the above criteria with no more than 3 types of multiplets in addition to the V and no more than 3 generations per type. Particularly simple ones are listed in Table 4.1. All the 22 models share the following features:

(1) There exist new colored particles.

(2) The quantum numbers of these new colored particles allow Yukawa couplings to quarks and the Higgs.

Property (1) is clearly favorable for hadron colliders. Even better, all the 22 models actually survive even if we restrict the additional fermions' masses to the range 300 GeV-1 TeV, so they all can be potentially within the LHC reach. Property (2) is not satisfied by S and G, but they only appear twice each among the 22 models, and even those models contain other colored particles that do satisfy property (2). We therefore identify these properties as robust LHC implications of WIMP DM and unification.[4]

To assess the robustness of the above features further, one can repeat the exercise with more conservative estimates on the uncertainties in the prediction of α_3. For example, if we vary the matching scale μ from $m_V/2$ to $2m_V$ (with everything else treated as above), we obtain 63 models, of which there is only one model $(V + E)$ without colored particles,[5] and only 6 colored models without property (2). Again, most models survive even if we restrict the search in the "LHC-accessible" range 300 GeV-1 TeV; 44 models in total, only one colorless model, and only one colorful model without property (2).

In the next section, we choose a benchmark model that represents characteristic phenomenologies of all these models which follow from properties (1) and (2). We will then use the benchmark model for further, more quantitative analyses in later sections.

[4]Recall the crucial role of the WIMP miracle in selecting the TeV scale as the mass scale for the new particles.

[5]Actually, a closer inspection reveals that unification favors the E in the $V + E$ model to be lighter than ≈ 300 GeV. The quantum numbers of the E allow it to decay to $l + Z$ in particular, so this model is already excluded.

4.5 The benchmark model

Given the insights worked out in the previous Sec. 4.4, we select the model with the dark matter V and two generations of $X \oplus X^c$ as our benchmark. This is the simplest of all models with a V featuring unification, having the smallest number of new multiplets beyond the SM. But most importantly, the collider phenomenology of this model is representative of all models identified in Sec. 4.4 as far as the LHC phenomenology is concerned.

The most general renormalizable lagrangian for the $2X + V$ model consistent with the $\mathbb{Z}_2$ symmetry $V \to -V$ reads

$$\begin{aligned} \mathcal{L} &= \mathcal{L}_{\rm SM} + \bar{V}\bar{\sigma}^\mu \mathrm{i}\mathrm{D}_\mu V - \frac{m_V}{2} VV \\ &\quad + \sum_a \Big[\bar{X}_a \bar{\sigma}^\mu \mathrm{i}\mathrm{D}_\mu X_a + X_a^c \sigma^\mu \mathrm{i}\mathrm{D}_\mu \bar{X}_a^c \\ &\quad - \Big(m_{X_a} X_a^c X_a + \sum_i \lambda_{ia}\, H d_i^c X_a^c + c.c \Big) \Big] , \end{aligned} \tag{4.8}$$

where $a = 1, 2$ and $i = 1, 2, 3$ denote generations of the X and d-type quark, respectively. We also use $X_{-1/3}$ and $X_{-4/3}$ to refer to the upper and lower $SU(2)_L$ components of X, respectively, where the subscripts denote the electric charges.

It is technically natural for λ to take any value, but there are obvious phenomenological constraints. First, λ has to be nonzero because the Xs must eventually decay to avoid cosmological problems. (However, the Xs could decay via higher dimensional operators. We will comment on that possibility in a separate note at the end of this section). Second, λ must be much less than $\mathcal{O}(1)$ because λ breaks the $U(3)^5$ flavor symmetry of the SM, providing new sources of flavor/CP violations in addition to the SM Yukawa couplings. We will return to flavor/CP constraints in Sec. 4.6.

The leading decays of X induced by λ can be most easily understood by the Goldstone equivalence theorem. In the limit of keeping only the X mass, the equivalence theorem tells us that $X_{-1/3}$ will decay as

$$X_{-1/3} \to Z + d\,, \quad X_{-1/3} \to h + d \tag{4.9}$$

with equal probabilities, where d can be any down-type quark.[6] Note that the equivalence theorem holds only in this limit. When the finite masses of the Higgs and Z bosons are taken into account, the branching fraction for the Z channel is expected to be somewhat larger due to phase space. For low X masses, this can have a significant impact on the phenomenology. Similarly, $X_{-4/3}$ can decay as

$$X_{-4/3} \to W^- + d\,, \tag{4.10}$$

which will be the dominant decay mode as long as the corresponding rate can be regarded as prompt on the collider time scale. When this rate drops below the displaced-vertex range, the dominant decay of the $X_{-4/3}$ will be through the weak interaction to an $X_{-1/3}$,

[6]The small violation of the equivalence theorem induces additional decays such as $X_{-1/3} \to W^- + u$, which can be thought of as arising from mixing of the Xs with down-type quarks. However, as we will see in Sec. 4.6, flavor/CP bounds constrain such mixings to be tiny, rendering these decay modes negligible.

which becomes slightly lighter than $X_{-4/3}$ after electroweak symmetry breaking, as we will elaborate more in Sec. 4.7.1.

Therefore, depending on the size of λ, we have either of the following collider signatures:

(A) If λ is sufficiently tiny, the X will be stable on collider time scales, and upon production it will hadronize into stable massive hadrons ("R-hadrons"). R-hadrons are easy to observe when they are charged, so X may be discoverable already in the early LHC run (i.e. 7 TeV, 1 fb^{-1}).

(B) If λ is not so small (but small enough to satisfy flavor/CP constraints), the X will decay within the detector, and as we have seen above, roughly a quarter of X particles (a half of $X_{-1/3}$ particles) will decay to a Higgs boson (plus a jet). This is an exciting possibility — a "Higgs factory" — where the Higgs bosons are produced with a characteristic $2 \to 2$ cross section of the *strong* interaction. In the remaining 3/4 of the time, the X will decay to a Z or W boson. Then, leptonic Z decays can be used to discover the X itself.

In Sec. 4.6 we will show that flavor/CP constraints indeed allow a window for the case (B).

Note that possibilities (A) and (B) are common to all the 22 models identified in Sec. 4.4. For example, in models containing Q instead of X, the λ coupling in Eq. (4.8) should be replaced by $\lambda_u H u^c Q + \lambda_d H^* d^c Q$, which would exhibit the same phenomenology as above. In models containing U or D instead of X, the λ coupling is replaced by $\lambda H U^c q$ and $\lambda H^* D^c q$, respectively, which is again phenomenologically equivalent.

Actually, the models with Q, U and/or D have additional potentially interesting modes $Q \to Z + t$, $Q \to W + t$, $U \to Z + t$, or $D \to W + t$. While the appearance of the top constitutes a qualitative difference in the collider phenomenology, a full analysis for such decay channels is more complicated due to the higher final-state multiplicity from the top decay. There are reducible background sources which cannot be simulated reliably at the matrix element level due to the large number of final-state particles, and even for irreducible backgrounds the issue of combinatoric backgrounds makes searches more difficult. Some of these problems may be ameliorated if an $\mathcal{O}(1)$ fraction of tops is produced with large p_T, such that the methods of boosted top-tagging [95–98] can be applied. A comprehensive study of these more complicated cases is beyond the scope of this work. Instead, we will focus on the phenomenology of signatures (A) and (B).

4.5.1 Effects of higher-dimensional operators

Before concluding this section we want to demonstrate explicitly that adding non-renormalizable interactions to the lagrangian (4.8) does not alter our results. In particular, one might worry that a higher-dimensional operator might lead to a prompt decay of the X even when $\lambda = 0$, destroying the R-hadron scenario. Fortunately, this is not the case. The leading non-renormalizable interaction that can let X decay is

$$\frac{1}{\Lambda}(X^c H^*)(q H^*)\,, \tag{4.11}$$

where Λ is some high scale. By our assumption, there is no new threshold between the TeV scale and the unification scale, so Λ must be at least $\sim 10^{11}$ GeV. To avoid a suppression

from three-body phase space, one of the Higgs fields can be put to its VEV. Therefore, the X decay length due to this operator is at least

$$\Gamma^{-1} \sim \left[\frac{m_X v^2}{16\pi(10^{11}\,\mathrm{GeV})^2}\right]^{-1} \simeq 3\ \mathrm{m}\,\frac{1\,\mathrm{TeV}}{m_X}\,. \tag{4.12}$$

Thus even the most conservative estimate gives a decay length comparable to the dimensions of the LHC detectors. Therefore, higher-dimensional operators do not upset our conclusions. Since this X decay is still prompt on a cosmological time scale, setting $\lambda = 0$ in the coupling (4.13) is actually allowed cosmologically, as X can decay via the above operator.

4.6 Flavor/CP and electroweak constraints

In this section, we analyze flavor/CP violations as well as corrections to precision electroweak observables in the benchmark model. These corrections arise due to the coupling

$$\mathcal{L} \supset \lambda_{ia}\, H d_i^c X_a + c.c\,, \tag{4.13}$$

where $a = 1, 2$ and $i = 1, 2, 3$. We will adopt the most conservative assumption that λ is an "anarchic" matrix without any special texture or alignment:

$$(\lambda_{ia}) = \begin{pmatrix} \sim\lambda & \sim\lambda \\ \sim\lambda & \sim\lambda \\ \sim\lambda & \sim\lambda \end{pmatrix}. \tag{4.14}$$

Therefore, the bounds discussed in this section could be relaxed by further model building or extra assumptions on the structure of λ. For example, Ref. [99,100] introduces a model with a single X particle (and no V) with a similar coupling selectively to the third generation, and consequently their model is much less constrained by flavor/CP.

Since the Xs are heavier than all SM particles and we anticipate a small λ, we integrate out the Xs and analyze effective operators in powers of λ/m_X. Strictly speaking, the ratio $\langle H\rangle/m_X$ is not a very small number, so contributions higher order in $\langle H\rangle/m_X$ can change our estimates by an $\mathcal{O}(1)$ factor. However, our interest is to show that a robust "Higgs factory" window can exist for the broad scenario of extending the SM with WIMP DM and unification, rather than placing precise bounds on this particular benchmark model. Therefore, order-of-magnitude estimates suffice for this purpose.

The most stringent bound comes from K^0-$\overline{K}^0$ mixing. The relevant tree and 1-loop diagrams are shown in Fig. 4.3. Upon integrating out X in the diagram on the left-hand side in Fig. 4.3, we generate the operator

$$\sum_{i,j,a} \frac{\lambda_{ia}\lambda_{aj}^\dagger}{m_{X_a}^2}\, d_i^c \sigma^\mu \bar{d}_j^c\, (H^\dagger \overleftrightarrow{D}_\mu H)\,. \tag{4.15}$$

Below the Z mass, using this operator twice with all the four Hs put to VEVs would generate 4-fermion operators with four right-handed down-type quarks with a coefficient of $\sim \lambda^4 v^2/m_X^4$, which is conservatively $\sim \lambda^4/m_X^2$. In particular, the imaginary part of the

Figure 4.3: Contributions to $K^0 - \bar{K}^0$ generated by X. *Left:* Feynman diagram leading to the tree-level operator (4.15). *Right:* Feynman diagram leading to the four fermion operator (4.17).

coefficient of $(d^c\sigma_\mu\bar{s}^c)(d^c\sigma^\mu\bar{s}^c)$ is constrained and has to be less than $(10^4\text{TeV})^{-2}$ [101, 102]. With our assumption of anarchic λ, we expect an $\mathcal{O}(1)$ phase in λ^4, so we obtain the bound

$$\lambda \lesssim 10^{-2}\sqrt{\frac{m_X}{1\,\text{TeV}}}\,. \tag{4.16}$$

Similarly, upon integrating out X in the diagram shown in the right-hand side of Fig. 4.3, we generate the operator

$$\frac{1}{16\pi^2}\sum_{a,i,j,k,l}\frac{\lambda_{ia}\lambda^\dagger_{aj}(y_u^\dagger y_u)_{kl}}{m^2_{X_a}}(d_i^c\sigma_\mu\bar{d}_j^c)(\bar{q}_k\bar{\sigma}^\mu q_l)\,. \tag{4.17}$$

From this, the imaginary part of the coefficient of $(d^c\sigma_\mu\bar{s}^c)(\bar{d}\bar{\sigma}^\mu s)$ can be estimated to be

$$\sim \frac{1}{16\pi^2}\frac{\lambda^2\theta_c^5}{m_X^2}\,, \tag{4.18}$$

where we have used $(y_u^\dagger y_u)_{12} \sim y_t^2\theta_c^5 \approx \theta_c^5$ with the Cabbibo angle $\theta_c \approx 1/5$. This coefficient should be less than $(10^5\,\text{TeV})^{-2}$ [101], which implies

$$\lambda \lesssim 10^{-2}\frac{m_X}{1\,\text{TeV}}\,. \tag{4.19}$$

The bound (4.19) is slightly stronger than the bound (4.16) for $m_X \lesssim 1\,\text{TeV}$, so we adopt Eq. (4.19) as our upper bound on λ.

No other constrains are as strong as Eq. (4.19). For example, let us look at the dipole operators generated from diagrams as in Fig. 4.4:

$$\sim \frac{g_F}{16\pi^2}\sum_{a,i,j,k}\frac{\lambda_{ia}\lambda^\dagger_{ak}(y_d)_{kj}}{m^2_{X_a}}H^\dagger d_i^c\bar{\sigma}^{\mu\nu}F_{\mu\nu}q_j\,, \tag{4.20}$$

where $F = B, W$ denotes the electroweak gauge fields, which in particular contribute to the process $b \to s\gamma$ after electroweak symmetry breaking. Since these operators are suppressed by the small bottom Yukawa coupling $y_b \sim 1/40$, one can think of them as the $b \to s\gamma$ dipole operator in minimal flavor violation [103] with the scale $\Lambda \sim 4\pi\theta_c m_X/(\sqrt{e}\,\lambda)$, where

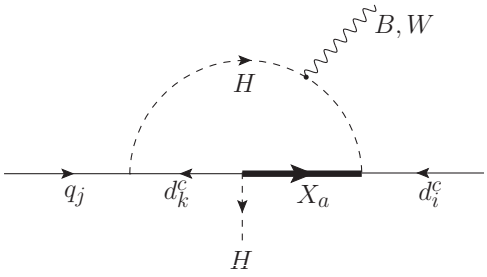

Figure 4.4: One of the Feynman diagrams leading to the dipole operator (4.20).

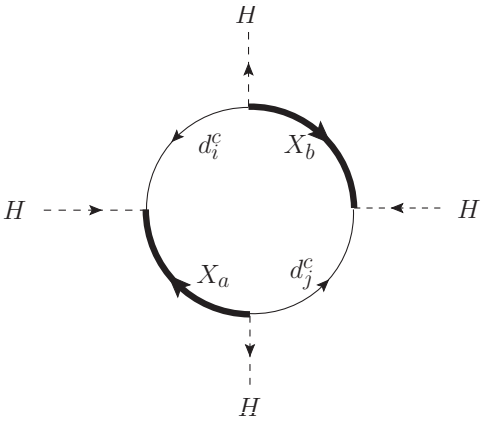

Figure 4.5: Feynman diagram contributing to the ρ parameter (4.22).

e is the QED coupling. Then, the bound $\Lambda \sim 10$ TeV from $b \to s\gamma$ [103, 104] implies $\lambda/m_X \lesssim 10^{-1}\,\mathrm{TeV}^{-1}$, which is again weaker than Eq. (4.19).

Let us also look at precision electroweak constraints. First, the operator (4.15) modifies $Z \to b\bar{b}$:

$$\frac{\Delta g_{Zb\bar{b}}}{g_{Zb\bar{b}}} \sim \frac{\lambda^2}{m_X^2}\,. \tag{4.21}$$

Again, given Eq. (4.19), this is safely below the experimental bound.[7] Second, Fig. 4.5 generates an operator contributing the ρ parameter

$$\sim \frac{\lambda^4}{16\pi^2 m_X^2}(H^\dagger D_\mu H)(H^\dagger D^\mu H)\,. \tag{4.22}$$

The coefficient should be less than $\sim 10^{-3}/v^2$ [105] with the Higgs VEV $v = 174\,\mathrm{GeV}$, implying $\lambda \lesssim \sqrt{m_X/(1\,\mathrm{TeV})}$, which again is much weaker than Eq. (4.19).

Given the bound (4.19), there is clearly a robust "Higgs factory" window where the Xs decay promptly. Keeping only the X mass for simplicity, the decay rate of an X via

[7] Ref. [100] discusses a model with a single generation of X (and without V), in which they exploit this shift in $Z \to b\bar{b}$ to improve precision electroweak fits of the SM.

coupling (4.13) is given by $\Gamma_X \sim \lambda^2 m_X/16\pi$. Therefore, demanding $\Gamma_X^{-1} \lesssim 10^{-12}$s (i.e. the decay length shorter than $\mathcal{O}(0.1)$mm), we obtain the Higgs-factory window

$$10^{-7} \left(\frac{1\text{ TeV}}{m_X}\right)^{\frac{1}{2}} \lesssim \lambda \lesssim 10^{-2} \frac{m_X}{1\text{ TeV}}\,. \tag{4.23}$$

Below the Higgs-factory window, there is a two or three orders-of-magnitude window where an X decays with a displaced vertex or in the LHC detector but with a macroscopic decay length. At a hadron collider, events where new physics only manifests itself at a macroscopic distance from the interaction point but still within the volume of the detector are challenging. Such signatures also appear in supersymmetric theories, c.f. [64, 106–108] and [109], hidden valley models [110–112], quirk models [113], and vectorlike confinement models [114–116]. As discussed in section 16 of Ref. [117] (and references therein), when particles with macroscopic decay lengths are produced, trigger efficiencies can become a concern. A detailed analysis of this scenario is beyond the scope of this work.

4.7 Collider phenomenology

In this section we will investigate in detail the two characteristic collider signatures of our scenario using the benchmark model. For the case of collider stable Xs, we show that the discovery of X is possible up to $m_X = 650\,\text{GeV}$ in the early 7-TeV run with $1\,\text{fb}^{-1}$ of data, and well past 1 TeV with the 14-TeV running. In the case that the Xs decay promptly, we concentrate on the discovery of the X and the Higgs bosons from X decays for early 14-TeV running ($10\,\text{fb}^{-1}$). In order to keep the analysis simple, we restricted the analysis to the case of a moderately heavy Higgs ($m_h = 200\,\text{GeV}$), and found the Higgs discovery potential to be similarly enhanced for a light Higgs as well. Of course, in light of the LHC discovery of the Higgs with $m_h \sim 125\,\text{GeV}$, our analysis is not up to date anymore.

Even though the benchmark model contains two generations of X, we have no reason to expect that they would be exactly degenerate in mass. Since the production cross section will be dominated by the lighter X, we will base our collider analysis on one generation of X only. This is the most conservative choice; if the Xs do happen to be nearly degenerate, this would significantly enhance the results below.

4.7.1 R-hadron Signals at the LHC

When the coupling λ is sufficiently small, the X does not decay within the detector. The signature therefore is that of an "R-hadron", that is, the X hadronizes with light colored degrees of freedom and the color-neutral bound state behaves as a (possibly charged) stable massive particle. Before we present a quantitative analysis, let us dwell on a few qualitative features of this signature.

Firstly, note that even when λ is very small, $X_{-4/3}$ still decays to $X_{-1/3}$ via the weak interactions, and in terms of collider signatures, the production of $X_{-4/3}$ is indistinguishable from that of $X_{-1/3}$ because the decay products are virtually unobservable. As worked out in detail in Ref. [2], $X_{-4/3}$ is expected to be heavier than $X_{-1/3}$ by only $\Delta m_X = 0.60\,\text{GeV}$. The dominant decay mode is $X_{-4/3} \to X_{-1/3} + \pi^-$ through an off-shell W^-, with a partial

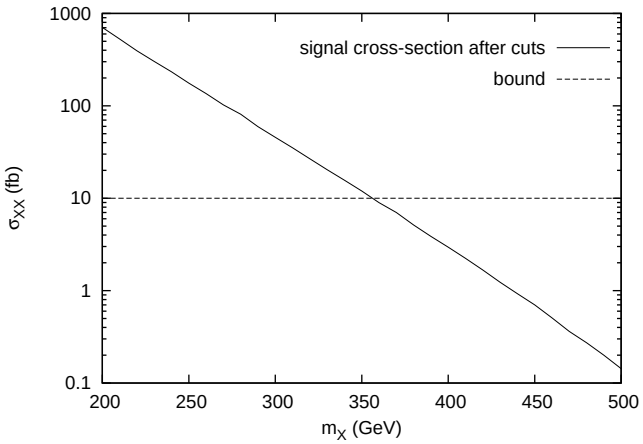

Figure 4.6: The cross section for R-hadron production at the Tevatron after all selection cuts. The bound from the CHAMP search is included for comparison.

width

$$\Gamma^{-1} = 1.3\text{mm}\left(\frac{0.60\,\text{GeV}}{\Delta m_X}\right)^3 \sqrt{\frac{1-\frac{m_\pi^2}{(0.60\,\text{GeV})^2}}{1-\frac{m_\pi^2}{\Delta m_X^2}}}\,. \tag{4.24}$$

The smallness of the mass gap makes the π very soft and thus unobservable at the LHC, and other subdominant decay modes have the same problem. Therefore, in analyzing the discovery potential or checking existing bounds, the production cross section of $X_{-4/3}$ should be added to that of $X_{-1/3}$.

The charge of an R-hadron is crucial for prospects of observing it. In particular, the most effective way to trigger on a stable charged massive particle is via the muon system [118]. The bound states of an $X_{-1/3}$ can be mesons $(X\bar{q})$ or baryons (Xqq). The physics of these bound states can be understood by regarding the $X_{-1/3}$ as a heavy version of the b quark, which is already much heavier than Λ_{QCD}. The lightest B mesons are B^0 and $B^\pm$, with only a few-hundred-keV mass splitting, while the lightest B baryon Λ_b^0 is heavier than the $B^{0,\pm}$ by 340 MeV. Therefore, we expect that the lightest X-meson should be lighter than the lightest X-baryon also by $\sim 340\,\text{MeV}$, with a few-hundred-keV mass splitting between the neutral and charged X-mesons. Since the splitting between the lightest X-meson and X-baryon is on the order of Λ_{QCD} itself, we expect that an X should preferentially hadronize into an X-meson, which can be either charged or neutral with 50% probability because their mass difference is tiny.[8]

In order to estimate the trigger efficiencies, we will use the following assumptions in the rest of our analysis:

[8]The few-hundred-keV mass difference between the $(X_{-1/3}\bar{d})$ meson and the $(X_{-1/3}\bar{u})$ meson might allow one to decay to the other via the weak interaction, if the mass difference is larger than the electron mass. But such a decay would occur with an extremely long lifetime (like the β-decay of the neutron), so it can be ignored on collider time scales.

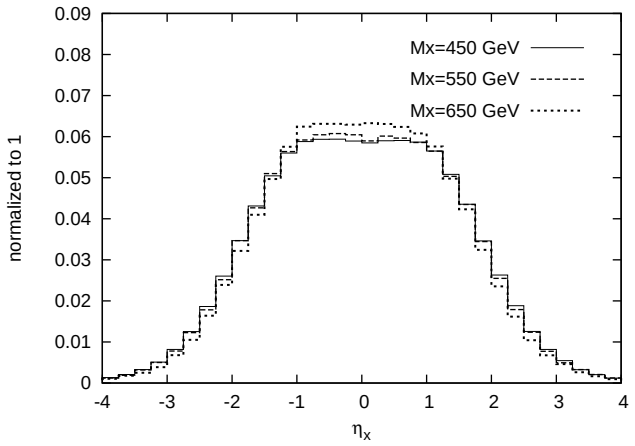

Figure 4.7: The rapidity distribution of the R-hadrons at the LHC (7 TeV) for the three mass points.

- There is a 50% chance that an R-hadron is charged when produced at the primary interaction.
- This charge is retained until the calorimeter is reached.
- One or more charge exchange interactions take place in the calorimeter, randomizing the charge of the R-hadron such that there is a 50% chance that it reaches the muon chamber as a charged particle.[9]

One of the requirements for triggering is that the particle reaches the muon system with nonzero charge.[10] Most experimental searches for massive stable particles also use as a selection criterion that there should be a charged track in the inner part of the detector that matches the hit in the muon chamber, even if this is not required for triggering. Therefore we will also adopt this as one of our event selection criteria.

Finally, an important kinematic variable, especially at the LHC (where the detectors are physically larger and the time between bunch crossings is short), is the "time-lag". This is defined as how much later the massive R-hadron ($\beta < 1$) arrives at the muon

[9] In addition to conversion between the charged and neutral X-mesons, for which there is a tiny energetic cost of a few hundred keV, there is also a process where an X-meson scatters into an X-baryon in the calorimeter [119], which, however, requires an energy of at least ~ 340 MeV. Using the analogy with the b system, the lightest X-baryon (analogous to Λ_b^0) should be neutral, while the lightest charged X-baryon (analogous to $\Sigma_b^{\pm}$) should be heavier by ~ 190 MeV. So, a charged X-baryon, even if produced, would promptly decay to a neutral X-baryon (by emitting a pion) which would then not be caught by the muon chamber, potentially hurting our R-hadron signal. The question of how frequently this meson-to-baryon conversion occurs is highly nontrivial and beyond the scope of this work. However, note that a meson-to-baryon conversion would not occur to the $\bar{X}$ due to the lack of anti-nucleons in the calorimeter. Therefore, even in the worst case where we always lose the R-hadrons from the X, we still have those from the $\bar{X}$, so the effective cross section would be roughly halved, which would correspond a small shift ($\sim \mathcal{O}(10)$ GeV) in the mass scale.

[10] This requirement is not imposed anymore in the improved CMS search strategy [67].

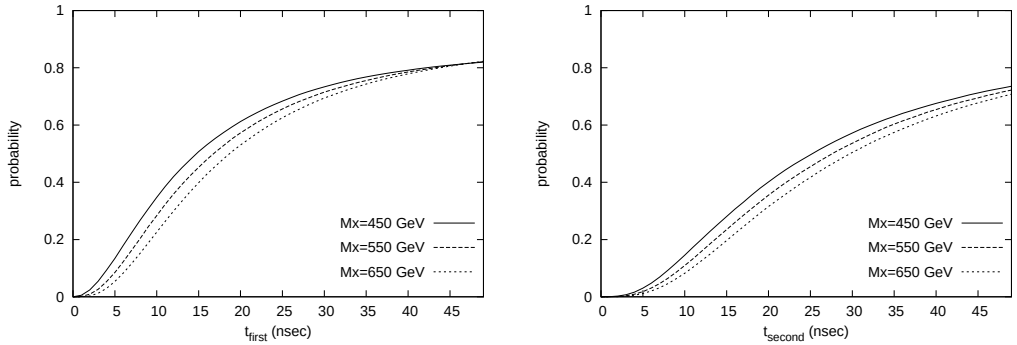

Figure 4.8: Time-lag distribution of the R-hadrons to arrive in the muon system at the LHC (7 TeV). *Left:* Time-lag distribution of the first R-hadron. *Right:* Time-lag distribution of the second R-hadron.

chamber compared to a relativistic particle (e.g. a muon). To be conservative, we use the physical dimensions of the ATLAS detector (which is larger than CMS) as described in Ref. [118]. Specifically, we differentiate the barrel region ($|\eta| < 1.4$) from the end-cap region ($1.4 < |\eta| < 2.5$). For the barrel region we calculate the time to get to a radius of 7.5 meters from the interaction point, and for the end-cap we calculate the time to get to $|z| = 14.5$ meters. For the LHC search, we will use as one of the event selection criteria that at least one of the R-hadrons reaches the muon chamber before relativistic particles from the next bunch crossing, i.e., with a time-lag of less than 25ns.

Before we investigate the discovery potential of X at the early LHC, let us address constraints on R-hadron production from the Tevatron [120, 121]. We will use the event selection criteria described in Ref. [120] in order to estimate acceptance and trigger rates in the benchmark model. In particular we demand that events contain at least one particle that has $|\eta| < 0.7$, $p_T > 40\,\text{GeV}$ and $0.4 < \beta < 0.9$, leaves a track, and is charged when it arrives at the muon system. For a single R-hadron satisfying these cuts, our above assumptions on the charges of R-hadrons imply a 25% probability for being detected. However, when both of the pair-produced R-hadrons are within acceptance and charged throughout the detector (a 1/16 probability), we need to correct for the fact that the reconstruction and trigger efficiency used in the analysis of Ref. [120] applies to a single R-hadron. Therefore the "effective cross section" for such events needs to be multiplied by a correction factor ξ before the comparison with the bound of Ref. [120]. This correction factor is given by $\xi = (1-(1-\varepsilon)^2)/\varepsilon$, where $\varepsilon = 0.533$ is the reconstruction efficiency for a single R-hadron. We use `CalcHEP 2.5.4` [122] with CTEQ6 parton distribution functions [123] to simulate the parton level process. The effective cross section after the selection cuts is plotted in Fig. 4.6 against the bound of Ref. [120]. We conclude that $m_X > 360\,\text{GeV}$ is not excluded.

We now turn to production of R-hadrons at the early LHC, i.e., for the 7-TeV running with $1\,\text{fb}^{-1}$ of integrated luminosity. We choose to look at mass points $m_X = 450\,\text{GeV}$, 550 GeV and 650 GeV. In Fig. 4.7, we plot the rapidity distribution of the R-hadrons for each mass point to show that R-hadron production is dominantly central. As event selection criteria, we impose that at least one R-hadron must reach the muon detector ($|\eta| < 2.5$)

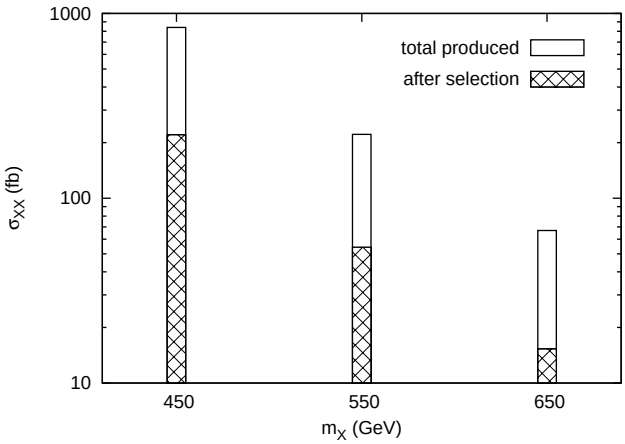

Figure 4.9: Total production cross section of R-hadron production and effective cross section after selection cuts at the LHC (7 TeV) for the three mass points.

with $p_T > 30\,\text{GeV}$ and a time lag of less than 25ns. We further demand that the R-hadron in question leaves a track and is charged when it gets to the muon chamber (a 25% probability per R-hadron as before). In events where both R-hadrons reach the muon chamber with $p_T > 30\,\text{GeV}$, we plot the time-lag of the earlier (later) R-hadron in on the left-hand side (right-hand side) of Fig. 4.8. Folding in the time-lag cut and the probability of being charged (but leaving out reconstruction efficiencies, which are unknown at this time), we plot the effective cross section after all selection cuts in Fig. 4.9. Note that the efficiency of the selection cuts has a slightly decreasing trend at higher mass, because the production occurs closer to threshold and fewer events satisfy the time-lag cut. Requiring at least 10 events for discovery, we see that X masses of up to 650 GeV should be within reach with $1\,\text{fb}^{-1}$ of data from the 7-TeV run.

Using the same selection criteria for the 14-TeV running, we also plot in Fig. 4.10 the effective cross section after cuts in that case. We see that even with early 14-TeV data (e.g. $\approx 10\,\text{fb}^{-1}$), X masses well past 1 TeV should be within reach.

4.7.2 The LHC as a Higgs factory

For λ in the range given by Eq. (4.23), the X decays promptly. For the $X_{-1/3}$, the dominant decay modes are $Z + j$ and $h + j$. Since production proceeds through QCD, this gives rise to a "Higgs factory" if m_X is not too large. The $X_{-4/3}$ decays to $W + j$ and therefore gives no additional contribution to Higgs production. For the rest of this section, we will be interested in the production of $X_{-1/3}$ only. We will show that there is a window in m_X where with $10\,\text{fb}^{-1}$ of 14-TeV running both the X and the Higgs can be discovered.

We will first dwell on the discovery of the X when both of the pair-produced Xs decay to $Z + j$. For the purposes of this analysis, we will restrict ourselves to consider only the decays of Z to charged leptons as they have considerably less background, but a full collider study can combine various channels and extend the reach in m_X.

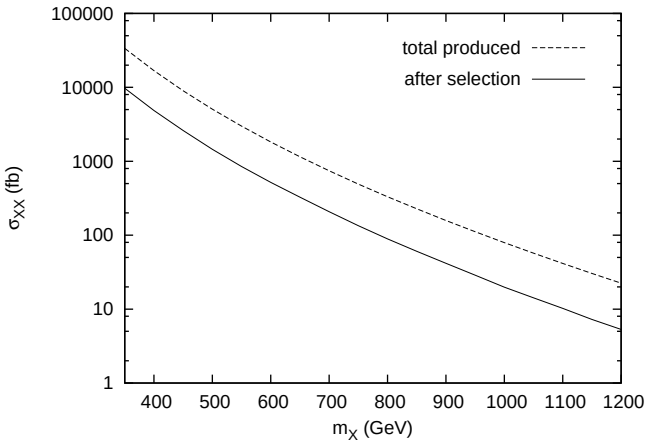

Figure 4.10: Effective R-hadron production cross section after selection cuts at the LHC (14 TeV).

We will then use the value of m_X extracted from this analysis in order to discover the Higgs in the events where one of the Xs decays to $Z + j$ and the other to $h + j$. We will focus on a scenario with a moderately heavy Higgs, with a dominant decay mode to W^+W^-, although discovery of a light Higgs through X production should be competitive with Higgs production from the SM as well. Once again, we will limit ourselves to leptonic decays of the Z as well as the Ws, but in a more detailed analysis, several channels can be combined to extend the discovery reach.

Let us start with the Tevatron bounds on m_X. The strongest constraint arises from a recent analysis of WZ production [124, 125], searching for events with exactly three final state leptons. In our benchmark model, events with pair-produced X decaying to Z, h and jets, followed by $h \to WW$ can be picked up by this search, as well as ZZ plus jet final states when both Z decay leptonically but one lepton fails to be identified. We implemented the cuts described in Ref. [124, 125], which include requiring the presence of an e^+e^- or $\mu^+\mu^-$ pair with invariant mass in the interval [86 GeV, 106 GeV] as well as $p_{T,l_1} > 20$ GeV, $p_{T,(l_2,l_3)} > 10$ GeV and $\not{E}_T > 25$ GeV. We find that for $m_X > 300\,\text{GeV}$, the number of events from X production after the selection cuts falls within one standard deviation of the SM expectation. The WW final state poses a weaker constraint, because in this final state a veto on hard jets is imposed in order to reduce the $t\bar{t}$ background [126, 127]. For $m_X > 300\,\text{GeV}$ the X-production cross section is only a fraction of the $t\bar{t}$ cross section, so there is no additional constraint from searches for $t\bar{t}$ either. Finally, for the same range in m_X, the Higgs production from X decays is significantly below the SM Higgs production cross section for the same m_h, so Higgs searches also do not give additional constraints. In order to stay consistent with these constraints, we will concentrate on the rest of this section on two mass points, $m_X = 300\,\text{GeV}$ and $m_X = 550\,\text{GeV}$, both with $m_h = 200\,\text{GeV}$.

In our analysis, we generate 3×10^5 parton level events (at 14-TeV LHC running) for each value of m_X using the user-mode of `MadGraph` [128] and CTEQ6 parton distribution functions [123]. We decay the X, h, W and Z particles using `BRIDGE` [129] in order for the

angular distributions of the final-state leptons and jets to be accurate. In the signal sample we allow all possible decays of X, h, W and Z in order to take full account of the combinatoric background, while in the background samples we force leptonic decays (including τ's) since hadronically decaying background events will not pass our selection cuts. The hadronization and detector simulation are done with the `PYTHIA` [130] and `PGS` [131] interface in `MadGraph`, with the default CMS parameter set. This parameter set uses a tracker and muon system η coverage up to 2.4, and a minimum lepton p_T of 5 GeV. Cone jets with $\Delta R = 0.5$ are used, note however that our analysis is inclusive and we do not place any cuts on jets. The `PGS` default algorithms are used for lepton isolation as well as other details of detector simulation. As the background for the X search we generated a matched $ZZ+$jets sample containing 53494 events after matching, using the MLM matching in `MadGraph`, and the same tools as were used for the signal. For the Higgs search we generated a matched $t\bar{t}Z+$jet sample with 36120 events after matching in the same way.

Discovering the X. In order to discover the X, we focus on the ZZ final state, where both Zs decay leptonically. For SM backgrounds, we have generated an MLM-matched sample with ZZ, $ZZ+j$, and $ZZ+2j$. As our event selection criteria, we demand that an event contains two (distinct) Z candidates, where a Z candidate is defined as an e^+e^- or a $\mu^+\mu^-$ pair with an invariant mass within 5 GeV of m_Z. We then pair the two Z candidates with the two hardest jets in the event (which in the case of signal are expected to come from the partons of the X decays) and retain the pairing where the Zj pair masses are closer to each other. We then plot the average pair mass m_{Zj}, where the peak from the X is clearly visible and distinguishable from the $ZZ+$jets background. For $m_X = 300\,\text{GeV}$, where the branching fraction $X \to Zj$ is 0.76, the cross section before (after) selection is 36.8 pb (50.5 fb). Similarly, before (after) selection we obtained 1.43 pb (1.32 fb) for $m_X = 550\,\text{GeV}$, where the branching fraction $X \to Zj$ is 0.57. Leptonic branching fractions and selection cuts reduce the SM background cross section from 11.4 pb down to 5.1 fb. The results for the two mass points and for $10\,\text{fb}^{-1}$ are plotted in Fig. 4.11. Since the background peaks towards low values of m_{Zj}, a cut on m_{Zj} can improve signal significance. For the $m_X = 550\,\text{GeV}$ case we use $m_{Zj} \geq 430\,\text{GeV}$ as a selection cut. While a similar cut can also be used for the $m_X = 300\,\text{GeV}$ case, signal is already much larger than background in this case and therefore a cut on m_{Zj} is not essential. With this additional cut, the signal cross section becomes 0.85 fb while background is reduced to 0.074 fb. With an integrated luminosity of $10\,\text{fb}^{-1}$, this translates to an average 9.2 events with a background expectation of 0.74 events. Using Poisson statistics, this corresponds to a probability of 9.4×10^{-8}, equivalent to more than a 5σ upward fluctuation in a Gaussian distribution. We conclude that m_X up to $\approx 550\,\text{GeV}$ is discoverable with $10\,\text{fb}^{-1}$ at $\sqrt{s} = 14\,\text{TeV}$.

Discovering the Higgs. In order to discover the Higgs, we focus on the Zh final state, where the Z as well as the Ws from the Higgs decay to leptons. More concretely, our event selection criteria are:

- The event contains two positively and two negatively charged leptons, with exactly one Z candidate (as defined above).
- The Z candidate and (at least) one of the two hardest jets has an invariant mass within 90 GeV of m_X as determined in the previous section.

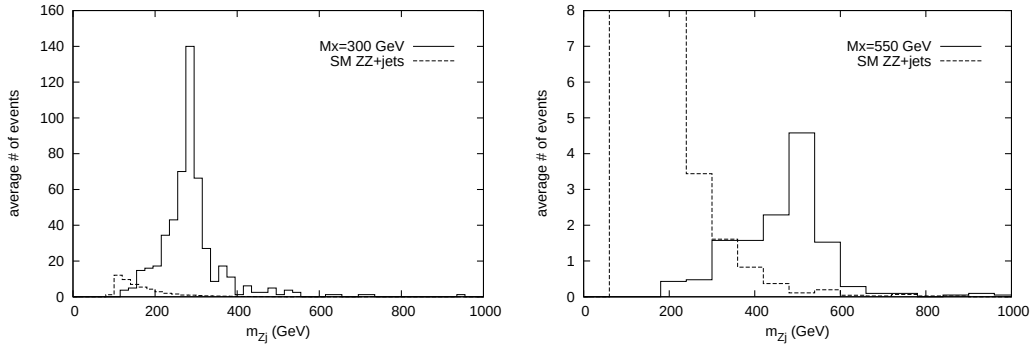

Figure 4.11: Distribution of the average Z+jet pair mass for signal and background in $10\,\mathrm{fb}^{-1}$ of LHC data (14 TeV). *Left:* Signal for $m_X = 300\,\mathrm{GeV}$. *Right:* Signal for $m_X = 500\,\mathrm{GeV}$.

For $m_X = 300\,\mathrm{GeV}$ the selection reduced the signal cross section from 36.8 pb to 22.2 fb, for $m_X = 550\,\mathrm{GeV}$ from 1.43 pb to 0.87 fb. With the first selection criterion, the dominant background is $t\bar{t}Z + \mathrm{jet(s)}$. At parton level, we generated an MLM-matched sample with up to one extra parton, i.e., $t\bar{t}Z$ and $t\bar{t}Z{+}j$. The second selection criterion, which uses the value for m_X obtained with the search strategy described in the previous subsection, then further reduces the background such that we are essentially left with a pure signal sample. Leptonic branching fractions and the selection cuts reduce the background cross section from 0.61 pb to 0.40 fb (0.083 fb), applying the two selection criteria for $m_X = 300\,\mathrm{GeV}$ ($m_X = 550\,\mathrm{GeV}$). For both mass points, this corresponds to discovery level statistical significance. Using Poisson statistics in the heavy mass case, the probability for a background fluctuation to mimic the signal is 2.4×10^{-7}, equivalent to more than 5σ in a gaussian distribution.

We then identify the two leptons which do not belong to the Z candidate, and form the transverse mass variable $M_{T,WW}$ as follows:

$$M^2_{T,WW} = (E_{T,l^+l^-} + E_{T,\nu\bar{\nu}})^2 - (\vec{p}_{T,l^+l^-} + \vec{p}_{T,\mathrm{miss}})^2, \tag{4.25}$$

where

$$\begin{aligned} E^2_{T,l^+l^-} &= p^2_{T,l^+l^-} + m^2_{l^+l^-}\,, \\ E^2_{T,\nu\bar{\nu}} &= p^2_{T,\mathrm{miss}} + m^2_{l^+l^-}\,. \end{aligned} \tag{4.26}$$

Note that $E_{T,\nu\bar{\nu}}$ is only an approximation to the true transverse energy of the neutrino system

$$E^2_{T,\nu\bar{\nu},\mathrm{true}} = p^2_{T,\nu\bar{\nu}} + m^2_{\nu\bar{\nu}}. \tag{4.27}$$

Although this approximation only becomes exact when the W are produced at threshold, for a 200-GeV Higgs the $M_{T,WW}$ distribution still peaks near the Higgs mass. We plot the results for $m_X = 300\,\mathrm{GeV}$ and for $m_X = 550\,\mathrm{GeV}$ in Fig. 4.12.

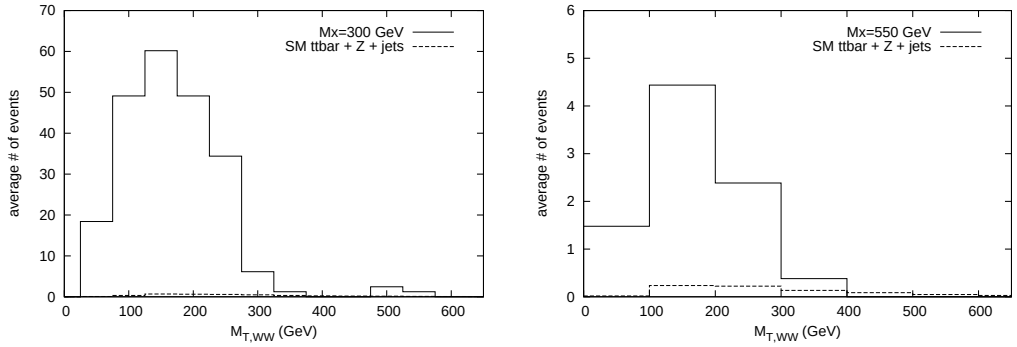

Figure 4.12: Distribution of $M_{T,WW}$ for signal (assuming $m_h = 200\,\text{GeV}$) and background with a luminosity of $10\,\text{fb}^{-1}$. *Left:* Signal for $m_X = 300\,\text{GeV}$. *Right:* Signal for $m_X = 500\,\text{GeV}$.

4.8 Concluding remarks

The minimal way to incorporate a WIMP DM candidate is as the neutral component of an electroweak triplet with zero hypercharge. We have looked for possible extensions of the SM that contain such a triplet as well as additional matter fields as necessary for gauge coupling unification. We have identified the characteristic features of such models. New colored particles at the TeV scale are ubiquitous and they can be produced in large numbers at the LHC. The colored particles allow couplings such that they dominantly decay to a Higgs and a jet, within or outside the LHC detector depending on the size of the couplings. The former possibility gives rise to a new channel for Higgs production, while the latter leads to spectacular R-hadron signals. In order to study these interesting characteristic collider signatures of WIMP DM and unification, we have chosen the model with the simplest matter content as a benchmark. The benchmark model contains two generations of an $SU(2)_L$-doublet color-triplet particle X that decay via Yukawa-type couplings to the SM. In particular, the final states contain Ws, Zs and Higgses, as well as down-type quarks.

We have investigated the constraints from flavor bounds on the size of the Yukawa-type coupling that leads to the X decay. We showed that there is a range where the X can decay promptly, or can be long-lived (stable on collider time scales). We have explored each of these possibilities in turn, showing that in the case of the long-lived X, R-hadrons can be discovered at the early LHC (7TeV) up to $m_X = 650\,\text{GeV}$, and past 1 TeV with a 14-TeV running.

In the case where the X particles decay promptly, a large number of Higgs bosons are produced through the decays, which, depending on the X mass, can be discovered with less luminosity than would be possible from SM Higgs production. We have shown that, for $m_X \lesssim 550\,\text{GeV}$ and with $10\,\text{fb}^{-1}$ of data at the LHC, we can discover the X itself in the leptonic ZZ final state as well as the Higgs bosons from X decays in the leptonic WW final state for a benchmark Higgs mass $m_h = 200\,\text{GeV}$.

In our phenomenological analysis we focus only on signals that are clean and have little background. These studies can be significantly expanded in a more dedicated collider search.

In particular, semi-leptonic decay channels can be combined with the fully leptonic ones to increase the reach. The discovery potential of a light Higgs should be enhanced as well, especially utilizing search methods relying on boosted final states. Finally, models other than the benchmark model we have chosen can be studied for qualitatively different final states. For example, while final states with up-type quarks (in particular the top quark) are rare in the benchmark model, other models can give rise to a large number of tops produced from the decays of the new physics (in addition to the two signals we discussed). Another interesting problem would be the case where X decays within the detector with a displaced vertex or with a macroscopic length. These questions however were beyond the scope of our work.

Finally, we want to comment briefly on how recent LHC results affect the phenomenology of the scenario described so far which has been worked out in 2010 when the LHC operation had just begun. For the case of collider-stable X particles forming R-hadrons, the bounds on m_X have been significantly raised. In addition to increase in the amount of data available, this progress is a result of an improved experimental search strategy which has been proposed in [67]. Instead of relying on muon triggers and thus the details of charge-conversion processes between the calorimeter material and the R-hadron as described in Sec. 4.7.1, R-hadron candidates can now be identified by their large momentum and characteristicly high ionization loss alone. The most recent R-hadron searches using this search strategy [90, 91] place limits on R-hadron masses that reach up to 1 TeV.

For the case of promptly decaying X particles, the benchmark choice of a Higgs boson with $m_h = 200\,\text{GeV}$ should be updated to the experimentally determined value $m_h \sim 125\,\text{GeV}$. The main qualitative difference is that a hypothetical 200 GeV Higgs decays dominantly to $h \to W^+W^-$ and $h \to ZZ$, while these channels are kinematically unavailable for the case of a Higgs boson with $m_h \sim 125\,\text{GeV}$, which decays dominantly to $\bar{b}b$ final states. The general statement that the decays of new colored states predicted in our scenario provide a new Higgs production channel and are of high phenomenological interest, however, remains valid.

CHAPTER 5

SUPERSYMMETRY AND NATURALNESS OF ELECTROWEAK SYMMETRY BREAKING

5.1 The hierarchy problem

Among the many and diverse arguments for the existence of physics beyond the SM, the hierarchy problem enjoys a special status, because any solution requires the introduction of new particles with masses of the order of the weak scale Λ_{EWSB}. Therefore, investigating approaches to solving the hierarchy problem and deriving testable predictions is a central objective in the current LHC era.

While it is easy to find a mechanism to break electroweak symmetry, the hierarchy problem states that it is extraordinarily difficult to explain why EWSB is characterized by the scale $\Lambda_{\text{EWSB}} \sim 100\,\text{GeV}$, which is many order of magnitude below the Planck scale. The standard model way to break electroweak symmetry and give mass to W and Z bosons as well as to the SM fermions is to include a scalar $SU(2)_L$ doublet Higgs field H. When the Higgs acquires a VEV of the order of 100GeV, the $SU(2)_L$ symmetry is spontaneously broken. If the SM could exist in isolation, it would be perfectly viable to define the Higgs mass term to be of the order of $(-m_H^2) \sim (100\,\text{GeV})^2$. Since however the SM is incomplete and should be regarded as the effective theory limit of some more fundamental theory, a light Higgs mass term becomes problematic: Since it is not protected by any symmetries the scalar mass parameter m_H^2 will generally acquire loop-corrections proportional to Λ^2, where Λ is the cutoff scale of the standard model. If Λ is chosen to be the Planck scale, one would expect m_H^2 to be of the order of M_{Pl}^2, or in other words over 30 orders of magnitude larger than the experimentally determined Higgs VEV. This huge, unexplained discrepancy between the physical and the natural Higgs mass constitutes the hierarchy problem.

After decades of active search at different collider experiments, the LHC recently confirmed the existence of a light scalar particle connected to electroweak symmetry breaking. It is not yet fully established whether the newfound particle with mass at around $\sim 125\,\text{GeV}$ really is the Higgs particle or just one part in a more intricate EWSB sector. The discovery however definitely disfavors approaches to circumvent the hierarchy problem by avoiding the existence of an elementary Higgs particle altogether. Examples for theories of this kind are e.g. technicolor, where electroweak symmetry is broken by condensates of new strongly in-

teracting techni-fermions or models with warped extra dimensions in which the electroweak symmetry is broken by boundary conditions.

In the presence of an elementary Higgs particle, the hierarchy problem can be solved by introducing a new symmetry to stabilize a light Higgs mass term m_H. There are two main approaches:

The first option is the Higgs being a pseudo Nambu-Goldstone boson associated with the spontaneous breaking of a larger symmetry group [132] that contains the SM symmetries as a subgroup. In this case the mass term $m_H^2 H^\dagger H$ is forbidden by a shift symmetry under which $H \to H + \varepsilon$.

Alternatively, the Higgs mass can be protected by supersymmetry (SUSY). In supersymmetry, fields differing by spin-1/2 are connected by a new spacetime symmetry to form so-called supermultiplets. In supersymmetric models the hierarchy problem is circumvented due to the fact that fermion masses are protected by chiral symmetry and receive radiative mass corrections that are at most logarithmically divergent. In supersymmetry, this protection mechanism is at work for the entire supermultiplet, i.e. it also applies to the scalar components and specifically Higgs boson.

Supersymmetry is widely considered to be the most compelling scenario for beyond the standard model physics. In addition to solving the hierarchy problem, it provides a candidate for dark matter and exhibits almost-exact gauge coupling unification in the simplest implementation of supersymmetry, the minimal supersymmetric standard model (MSSM). Experimental searches however have not provided any evidence for SUSY. After hopes for the discovery of superparticles at LEP, the Tevatron and LHC so far have been disappointed, the continuing data-taking effort at the LHC will subject SUSY to a critical test: In the coming years of LHC operation, with more center-of-mass energy and more data to be recorded, the discovery reach for colored superparticles will grow substantially and reach the several-TeV regime.

While a non-discovery of superparticles at the LHC would not exclude SUSY per se, it would severely constrain its naturalness: If the superpartners to the SM particles are much heavier than the electroweak symmetry breaking scale, i.e. the scale of SUSY breaking M_{SB} is much larger than Λ_{EWSB}, the Higgs mass is not sufficiently protected from large corrections. This results in the so-called naturalness problem of supersymmetry.

In this chapter, we first introduce basic concepts and notation of supersymmetry and the MSSM. We then proceed to discuss the status of SUSY naturalness in light of LHC exclusion limits. This will provides the foundation for chapter 6, in which a strategy for building supersymmetric models with reduced fine-tuning is presented.

5.2 Basics of supersymmetry

In this section, the concepts of supersymmetry necessary for the remainder of this work will be introduced.

Table 5.1: The field content and nomenclature of the minimal supersymmetric standard model.

		spin 0	spin $\frac{1}{2}$	spin 1	Gauge Rep.
Chiral supermultiplets					
squarks, quarks (3× families)	$\mathbf{q}$	$\tilde{q} = (\tilde{u}_L,\, \tilde{d_L})$	$q_L = (u_L,\, d_L)$	-	$(\mathbf{3}, \mathbf{2})_{1/6}$
	$\mathbf{u^c}$	$\tilde{u}^*_R$	$u^\dagger_R$	-	$(\bar{\mathbf{3}}, \mathbf{1})_{-2/3}$
	$\mathbf{d^c}$	$\tilde{d^*_R}$	$d^\dagger_R$	-	$(\bar{\mathbf{3}}, \mathbf{1})_{1/3}$
sleptons, leptons (3× families)	$\mathbf{l}$	$\tilde{l} = (\tilde{\nu}_L,\, \tilde{e_L})$	$l = (\nu,\, e_L)$	-	$(\mathbf{1}, \mathbf{2})_{-1/2}$
	$\mathbf{e^c}$	$\tilde{e}^*_R$	$e^\dagger_R$	-	$(\mathbf{1}, \mathbf{1})_1$
Higgs, higgsinos	$\mathbf{h_u}$	$h_u = (h^+_u,\, h^0_u)$	$\tilde{h}_u = (\tilde{h}^+_u,\, \tilde{h}^0_u)$	-	$(\mathbf{1}, \mathbf{2})_{1/2}$
	$\mathbf{h_d}$	$h_d = (h^0_d,\, h^-_d)$	$\tilde{h}_d = (\tilde{h}^0_d,\, \tilde{h}^-_d)$	-	$(\mathbf{1}, \mathbf{2})_{1/2}$
Gauge supermultiplets					
gluino, gluon	$\mathbf{V_3}$	-	$\tilde{g}$	g	$(\bar{\mathbf{8}}, \mathbf{1})_0$
winos, W bosons	$\mathbf{V_2}$	-	$\tilde{W}^\pm,\, \tilde{W}^0$	$W^\pm,\, W^0$	$(\bar{\mathbf{1}}, \mathbf{3})_0$
bino, B boson	$\mathbf{V_1}$	-	$\tilde{B}$	B	$(\bar{\mathbf{1}}, \mathbf{1})_0$

5.2.1 The minimal supersymmetric standard model (MSSM)

A supersymmetry transformation relates bosonic and fermionic states. The superspace is spanned by fermionic Grassmann coordinates θ_α and the usual position 4-vector coordinates x^μ. Supersymmetric multiplets, or superfields, consist of one fermionic and one bosonic field, plus an auxiliary field which accounts for the difference in off-shell degrees of freedom. Chiral superfields $\mathbf{\Phi}$, also called matter superfields, consist of a scalar field ϕ , a Weyl spinor ψ, and an auxiliary field F. In Wess-Zumino gauge [133], the vector superfields $\mathbf{V}$ contain a vector field A_μ, a spin-1/2 Weyl field λ and its conjugate $\bar{\lambda}$, and an auxiliary field D. Superfield notation is clearer and more economical whenever supersymmetry is (approximately) conserved. Throughout this work, both the superfield language and component field language will be used. To distinguish them from component fields, we use bold type to denote superfields.

The MSSM with unbroken supersymmetry. The minimal supersymmetric standard model (MSSM) [63, 134, 135] is constructed by extending the Higgs sector of the standard model to contain two Higgs doublets h_u and h_d with hypercharge $Y = \pm\frac{1}{2}$ and promoting each field to a full supersymmetric multiplet. The second Higgs field h_d with hypercharge opposite to h_u is necessary to cancel the anomalies introduced by the fermionic partner to the Higgs boson, the higgsino. Also, since a consistent superpotential has to be *holomorphic*, the field h_u would not suffice to write down Yukawa couplings and generate masses after electroweak symmetry breaking for all the matter fields. The field content of the MSSM is summarized in Table 5.1.

The MSSM lagrangian with unbroken supersymmetry consists of three parts. The kinetic terms for the gauge bosons and their superpartners, the gauginos, arise from

$$\mathcal{L}_{\text{kin,gauge}} = \int d^2\theta \sum_{a=1,2,3} \left[\frac{1}{4g_a^2} \text{Tr}[\mathbf{W}^{a\alpha}\mathbf{W}^a_\alpha] + c.c. \right]. \tag{5.1}$$

where $\mathbf{W}_a$ are field strength chiral superfields defined by

$$\mathbf{W}_\alpha = -\frac{1}{4}\bar{D}\,\bar{D}\left(e^{-\mathbf{V}} D_\alpha e^{\mathbf{V}}\right) \qquad \text{and} \qquad \mathbf{W}_\alpha = T^a \mathbf{W}^a_\alpha \tag{5.2}$$

Here, D_α and $\bar{D}_{\dot{\alpha}}$ are chiral covariant derivatives. $\mathbf{V}$ are gauge supermultiplets containing the gauge boson fields A^μ and their superpartners the gauginos. For the matter fields in the supermultiplets $\phi_i = \mathbf{q}, \mathbf{u}^c, \mathbf{d^c}, \mathbf{l}, \mathbf{e^c}, \mathbf{h_u}, \mathbf{h_d}$, the kinetic terms and gauge interactions are encoded in:

$$\mathcal{L}_{\text{kin,matter}} = \int d^4\theta \sum_{i,j} \phi^{\dagger i} \left(e^{2T^a \mathbf{V}^a}\right)_i^{\ j} \phi_j. \tag{5.3}$$

Lastly, the Yukawa terms and the supersymmetric Higgs mass term are described by

$$\mathcal{L}_{\text{yuk}} = \int d^2\theta \underbrace{\left[\mu \mathbf{h_u}\mathbf{h_d} + \mathbf{h_u}\mathbf{q}_i (Y_u)_{ij} \mathbf{u^c}_j + \mathbf{h_d}\mathbf{q}_i (Y_d)_{ij} \mathbf{d^c}_j + \mathbf{h_d}\mathbf{l}_i (Y_l)_{ij} \mathbf{e^c}_j\right]}_{\mathcal{W}_{\text{MSSM}}} \tag{5.4}$$

where $\mathcal{W}_{\text{MSSM}}$ is the MSSM superpotential and $i, j = 1, 2, 3$ are flavor indices. Note that the MSSM with unbroken supersymmetry has only one additional parameter compared to the SM, namely the Higgs mass parameter μ.

In addition to the Yukawa terms above, which mirror the SM Yukawa interactions, it is possible to write down further couplings that are holomorphic and gauge invariant such as $\mathbf{l}\,\mathbf{l}\,\mathbf{e}^c$, $\mathbf{l}\,\mathbf{q}\,\mathbf{d}^c$, $\mathbf{l}\,\mathbf{h_u}$ and $\mathbf{u}^c\mathbf{d}^c\mathbf{d}^c$. These interactions are highly problematic since they violate either lepton or baryon number. To avoid them, usually a discrete symmetry like R-parity [63] or matter-parity [135–138] is imposed.

Soft supersymmetry-breaking terms. If supersymmetry was an exact symmetry, the superparticle masses would be degenerate with their SM counterparts. Since no superpartners have been detected yet, supersymmetry, if realized in nature at all, has to be a broken symmetry.

The mechanism and the resulting spectrum of superparticles can differ widely in different supersymmetric models. Generally, in order for supersymmetry to solve the hierarchy problem, SUSY breaking has to be *soft*, which means any supersymmetry-breaking operator should be relevant i.e. have a coefficient of positive mass dimension. Then, the dominant radiative corrections to the Higgs mass are of the form:

$$\Delta m_H^2 \sim \tilde{m}^2_{\text{soft}} \frac{\lambda}{16\pi^2} \ln\left(\frac{\Lambda_{UV}}{m_{\text{soft}}}\right) \tag{5.5}$$

where λ is a placeholder for whatever dimensionless couplings appear in the loop diagrams contributing to the Higgs mass term. In contrast, if SUSY were broken non-softly by an operator with dimensionless coefficient, one would obtain

$$\Delta m_H^2 \sim \frac{\lambda}{16\pi^2}\Lambda_{UV}^2, \tag{5.6}$$

resulting in naturalness constraints on a light Higgs mass just as severe as the original hierarchy problem without SUSY.

The most general soft supersymmetry breaking terms of the MSSM, expressed in component field notation, are [62]:

$$\begin{aligned}\mathcal{L}_{\text{soft}}^{\text{MSSM}} = &-\frac{1}{2}\Big(M_3\,\tilde{g}\tilde{g} + M_2\,\tilde{W}\tilde{W} + M_1\,\tilde{B}\tilde{B} + c.c\Big)\\ &-\Big(h_u\tilde{q}\mathbf{a_u}\tilde{u}^c + h_d\tilde{q}\mathbf{a_d}\tilde{d}^c + h_d\tilde{l}\mathbf{a_l}\tilde{e}^c + c.c.\Big)\\ &-\Big(\tilde{q}^\dagger\mathbf{\tilde{m}_q^2}\tilde{q} + \tilde{u}^{c\dagger}\mathbf{\tilde{m}_{u^c}^2}\tilde{u}^c + \tilde{d}^{c\dagger}\mathbf{\tilde{m}_{d^c}^2}\tilde{d}^c + \tilde{l}^\dagger\mathbf{\tilde{m}_l^2}\tilde{l} + \tilde{e}^{c\dagger}\mathbf{\tilde{m}_{e^c}^2}\tilde{e}^c + \tilde{m}_{\text{hu}}^2 h_u^\dagger h_u + \tilde{m}_{\text{hd}}^2 h_d^\dagger h_d\Big)\\ &-(b h_u h_d + c.c.)\end{aligned} \tag{5.7}$$

The first line of Eq. (5.7) contains the gaugino mass terms and the second line contains A-term couplings between three scalar fields. The scalar particles acquire masses through so-called scalar-squared soft terms in the third line. The last line of Eq. (5.7) contains a SUSY breaking soft off-diagonal Higgs mass term.

The soft SUSY breaking scalar-squared mass matrices $\mathbf{\tilde{m}_q^2}$, $\mathbf{\tilde{m}_{u^c}^2}$, $\mathbf{\tilde{m}_{d^c}^2}$, $\mathbf{\tilde{m}_l^2}$ and $\mathbf{\tilde{m}_{e^c}^2}$ as well as the A-terms $\mathbf{a_u}$, $\mathbf{a_d}$, $\mathbf{a_l}$ are 3×3 matrices in flavor space. After supersymmetry breaking, the higgsino, bino and wino states will mix, resulting in four neutralino $\tilde{\chi}^0$ and two chargino $\tilde{\chi}^\pm$ mass eigenstates.

The SUSY breaking Higgs mass parameter b is of dimension [mass]^2 and is interchangeably denoted as $b \equiv B\mu$. This notation emphasizes the fact that for a valid EWSB sector, the Higgs mass parameter μ should be of the same order of magnitude as the supersymmetry breaking soft masses, even though a μ-term by itself is compatible with unbroken supersymmetry. Unless otherwise specified, we assume that soft supersymmetry breaking terms as well as the higgsino mass parameter μ are generated at some more fundamental scale M_*. If nonzero, all these term are parametrically related to an overall amount of SUSY-breaking denoted by M_{SB}:

$$\mathbf{\tilde{m}_q^2}, \mathbf{\tilde{m}_{u^c}^2}, \mathbf{\tilde{m}_{d^c}^2}, \mathbf{\tilde{m}_l^2}, \mathbf{\tilde{m}_{e^c}^2}, \tilde{m}_{\text{hu}}^2, \tilde{m}_{\text{hd}}^2, b \sim M_{\text{SB}}^2 \tag{5.8a}$$

$$\mathbf{a_u}, \mathbf{a_d}, \mathbf{a_l}, M_1, M_2, M_3, \mu \sim M_{\text{SB}} \tag{5.8b}$$

A careful count [139] shows that the SUSY breaking lagrangian $\mathcal{L}_{\text{soft}}^{\text{MSSM}}$ introduces 105 new parameters. These are masses, phases and mixing angles of the MSSM lagrangian that cannot be eliminated by phase redefinitions or rotations in flavor space. Most of these 105 parameters however are severely restricted by experimental data, because they induce flavor violating processes. We will use the coming paragraph to discuss the flavor restrictions.

Flavor structure of the soft terms. The generic flavor scale suppressing new contributions to flavor-changing processes is $\Lambda_F \gtrsim 10^4$ TeV (see e.g. Ref. [140] for a comprehensive discussion), much larger than the scale at which the superparticles are generally expected to be found. Thus, in order to avoid conflicts with experimental constraints, the soft SUSY breaking terms need to display a quite specific structure dictated by the concept of minimal flavor violation (MFV) [103].

MFV is based on the observation that the SM in the absence of any Yukawa interactions has an additional flavor symmetry group

$$G_F \equiv \quad SU(3)_q \times SU(3)_u \times SU(3)_d \times SU(3)_l \times SU(3)_e \tag{5.9}$$

The Yukawa interactions break the G_F flavor symmetry. The flavor symmetry can be formally recovered by promoting the Yukawa coupling matrices $\mathbf{Y_u}$, $\mathbf{Y_d}$, $\mathbf{Y_e}$ to dimensionless spurion fields transforming as

$$\mathbf{Y_u} \sim (\bar{\mathbf{3}}, \mathbf{3}, \mathbf{1}, \mathbf{1}, \mathbf{1}) \qquad \mathbf{Y_d} \sim (\bar{\mathbf{3}}, \mathbf{1}, \mathbf{3}, \mathbf{1}, \mathbf{1}) \qquad \mathbf{Y_e} \sim (\mathbf{1}, \mathbf{1}, \mathbf{1}, \bar{\mathbf{3}}, \mathbf{3}) \tag{5.10}$$

under the G_F symmetry.[1] The principle of minimal flavor violation consists of letting the background values of the Yukawa coupling matrices $\mathbf{Y_u}$, $\mathbf{Y_d}$, $\mathbf{Y_e}$ be the sole source of G_F breaking in BSM scenarios. In that scenario, the exact amount of flavor violation depends on the respective model but is parametrically always of the same size as in the standard model and thus generally compatible with experimental bounds. It is convenient to choose the basis where the Yukawa matrices read

$$\begin{aligned}
\mathbf{Y_u} &= \begin{pmatrix} y_u & 0 & 0 \\ 0 & y_c & 0 \\ 0 & 0 & y_t \end{pmatrix} V_{\rm CKM}, \\
\mathbf{Y_d} &= \begin{pmatrix} y_d & 0 & 0 \\ 0 & y_s & 0 \\ 0 & 0 & y_b \end{pmatrix}, \\
\mathbf{Y_l} &= \begin{pmatrix} y_e & 0 & 0 \\ 0 & y_\mu & 0 \\ 0 & 0 & y_\tau \end{pmatrix},
\end{aligned} \tag{5.11}$$

where $V_{\rm CKM}$ is the Cabibbo-Kobayashi-Maskawa matrix and the y_i are the usual Yukawa couplings. Since the Yukawa couplings are very small except for the element y_t responsible for the top mass, the only relevant non-diagonal flavor structure is

$$(\mathbf{Y_u^\dagger Y_u})_{ij} \simeq y_t^2 V^*_{{\rm CKM},3i} V_{{\rm CKM},3j} \, .$$

[1] The spurion representations are chosen such that the MSSM Yukawa interactions in Eq. (5.4), with the matter superfields in the representation $\mathbf{q} \sim (\mathbf{3}, \mathbf{1}, \mathbf{1}, \mathbf{1}, \mathbf{1})$, $\mathbf{u^c} \sim (\mathbf{1}, \bar{\mathbf{3}}, \mathbf{1}, \mathbf{1}, \mathbf{1})$, $\mathbf{d^c} \sim (\mathbf{1}, \mathbf{1}, \bar{\mathbf{3}}, \mathbf{1}, \mathbf{1})$, $\mathbf{l} \sim (\mathbf{1}, \mathbf{1}, \mathbf{1}, \mathbf{3}, \mathbf{1})$ and $\mathbf{e^c} \sim (\mathbf{3}, \mathbf{1}, \mathbf{1}, \mathbf{1}, \bar{\mathbf{3}})$, are invariant under G_F. Note that this assignment is exactly opposite to the notation defined in [103] where the symmetry assignments for Y_u, Y_d and Y_l are chosen such that the SM Yukawa lagrangian $\mathcal{L} = H\bar{q}Y_u u_R + H_c\bar{q}_i(Y_d)_{ij}d_{Rj} + H_c\bar{l}_i(Y_l)_{ij}e_{Rj}$ is G_F-invariant, where $H_c = i\tau_2 H^*$.

Specifically for the MSSM, minimal flavor violation means that the supersymmetry-breaking squark mass terms and trilinear couplings are parameterized in a basis consisting of flavor-diagonal terms and flavor violating terms proportional to $\mathbf{Y_u^\dagger Y_u}$ only.

$$\tilde{\mathbf{m}}^{\mathbf{2}}_{\mathbf{q}} = \tilde{m}_q^2 \left(\mathbb{1} + b_q \mathbf{Y_u^\dagger Y_u}\right) \tag{5.12a}$$

$$\tilde{\mathbf{m}}^2_{\mathbf{u^c}} = \tilde{m}_u^2 \left(\mathbb{1} + b_u \mathbf{Y_u^\dagger Y_u}\right) \tag{5.12b}$$

$$\tilde{\mathbf{m}}^2_{\mathbf{d^c}} = \tilde{m}_d^2 \mathbb{1} \tag{5.12c}$$

$$\mathbf{a_u} = A_u \mathbf{Y_u} \tag{5.12d}$$

$$\mathbf{a_d} = A_d \left(\mathbb{1} + b_{Ad} \mathbf{Y_u^\dagger Y_u}\right) \mathbf{Y_d} \tag{5.12e}$$

Note that family-universal soft masses, as are often imposed in specific models, are a special case of MFV-compatible soft terms (5.12). The flavor structure of the A-terms implies that the $(3,3)$ entries of the matrices $a_{u_{ij}}$ and $a_{d_{ij}}$ dominate over all others. Often the notation $A_t \equiv a_{u33}/y_t$ is used.

So far, we have not yet discussed how the highly non-generic structure of soft terms can be generated. Clearly, an organizing principle needs to provide the appropriate flavor structure and reduce the 105 parameters in Eq. (5.7) to achieve SUSY models compatible with experiment i.e. with soft terms that obey the MFV structure Eq. (5.12). The mechanism employed to break supersymmetry should provide that principle and explain the non-generic structure of the soft terms.

5.2.2 The Higgs sector of the MSSM

The Higgs sector of the MSSM is of particular concern for SUSY phenomenology. In this section, its structure as well as the problems the LHC result of $m_h \sim 125\text{GeV}$ poses for the MSSM are discussed.

The Scalar Potential. The MSSM Higgs potential is necessarily more complicated than the standard model one, due to the presence of two Higgs doublets instead of only one in the standard model. Without loss of generality, the $SU(2)_L$ gauge transformations can be used to rotate into a basis with vanishing VEVs for the charged Higgs fields h_u^+ and h_d^-. In that basis, the MSSM Higgs potential reads

$$\begin{aligned} V = &(|\mu|^2 + \tilde{m}^2_{\text{hu}})|h_u^0|^2 + (|\mu|^2 + \tilde{m}^2_{\text{hd}})|h_d^0|^2 - (b\, h_u^0 h_d^0 + c.c.) \\ &+ \frac{1}{8}(g^2 + g'^2)(|h_u^0|^2 - |h_d^0|^2)^2 \end{aligned} \tag{5.13}$$

Note that in the absence of SUSY breaking, this potential reduces to

$$V = |\mu|^2(|h_u|^2 + |h_d^2|) + \frac{1}{8}(g^2 + g'^2)(|h_u^0|^2 - |h_d^0|^2)^2$$

such that $\langle h_u^0 \rangle = \langle h_d^0 \rangle = 0$ and the electroweak symmetry remains unbroken. This is one way to understand how supersymmetry protects the electroweak sector, as EWSB effects

are limited by the size of the SUSY breaking effects, i.e. $M_{\rm SB}$.

The scalar potential needs to be bounded from below. This is achieved automatically by the scalar quartic interaction in the last line of Eq. (5.13), except in the $|h_u| = |h_d|$ direction along which the quartic term vanishes. To stabilize the scalar potential in this direction, the b-term needs to fulfill

$$2b^2 \quad < 2|\mu|^2 + \tilde{m}^2_{\rm hu} + \tilde{m}^2_{\rm hd} \tag{5.14}$$

To provide W and Z boson masses the Higgs fields need to obtain a VEV and spontaneously break electroweak symmetry. Therefore, one linear combination of h_u and h_d has to have a negative mass term. This corresponds to a second condition

$$b^2 \quad > (|\mu|^2 + \tilde{m}^2_{\rm hu})(|\mu|^2 + \tilde{m}^2_{\rm hd})\,. \tag{5.15}$$

Since the parameters b, $\tilde{m}^2_{\rm hu}$, and $\tilde{m}^2_{\rm hd}$ all encode soft SUSY breaking terms, Eq. (5.15) implies that electroweak symmetry breaking requires supersymmetry breaking.

Together, the vacuum expectation values $v_u \equiv \langle h_u \rangle$ and $v_d \equiv \langle h_d \rangle$ generate the Z boson mass, specifically

$$v_u^2 + v_d^2 = v^2 = 2m_Z^2/(g^2 + g'^2) \sim (174\ \text{GeV})^2\,. \tag{5.16}$$

It is convenient to define

$$\tan\beta \equiv v_u/v_d \tag{5.17}$$

Using the conditions $\partial V/\partial h_u^0 = \partial V/\partial h_d^0 = 0$ at the minimum of the scalar potential, the parameters b and $|\mu|$ can be replaced by $\tan\beta$ and m_Z:

$$\sin(2\beta) = \frac{2\tan\beta}{1+\tan\beta^2} = \frac{2b}{\tilde{m}^2_{\rm hu} + \tilde{m}^2_{\rm hd} + 2|\mu|^2} \tag{5.18}$$

$$m_Z^2 = \frac{|\tilde{m}^2_{\rm hd} - \tilde{m}^2_{\rm hu}|}{\sqrt{1-\sin^2(2\beta)}} - \tilde{m}^2_{\rm hu} - \tilde{m}^2_{\rm hd} - 2|\mu|^2 \tag{5.19}$$

The expressions (5.18)-(5.19) are valid only at tree-level. For numerically stable results, one has to include one-loop corrections at least. This is customarily done by computing the corrections ΔV to the effective potential $V_{\rm eff}(v_u, v_d) = V + \Delta V$ as a function of v_u and v_d. ΔV is known up to two-loop order [141, 142]. Including those corrections amounts to replacing

$$\tilde{m}^2_{\rm hu} \to \tilde{m}^2_{\rm hu} + \frac{1}{2v_u}\frac{\partial(\Delta V)}{\partial v_u} \qquad\qquad \tilde{m}^2_{\rm hd} \to \tilde{m}^2_{\rm hd} + \frac{1}{2v_d}\frac{\partial(\Delta V)}{\partial v_d}\,. \tag{5.20}$$

To improve the convergence of the perturbative series, the renormalization scale is commonly chosen as the geometrical stop mass average

$$Q_{\rm SUSY} \equiv \sqrt{m_{\tilde{t}_1} m_{\tilde{t}_2}}\,. \tag{5.21}$$

where the physical stop masses $m_{\tilde{t}_1}$ and $m_{\tilde{t}_2}$ are obtained by diagonalizing the mass matrix of the gauge eigenstates $\tilde{q}_{u3}$ and $\tilde{u^c}_3$. For models with generic soft SUSY breaking terms c.f. Eq. (5.8), the evaluation scale coincides with the scale of SUSY breaking $Q_{\rm SUSY} \sim M_{\rm SB}$.

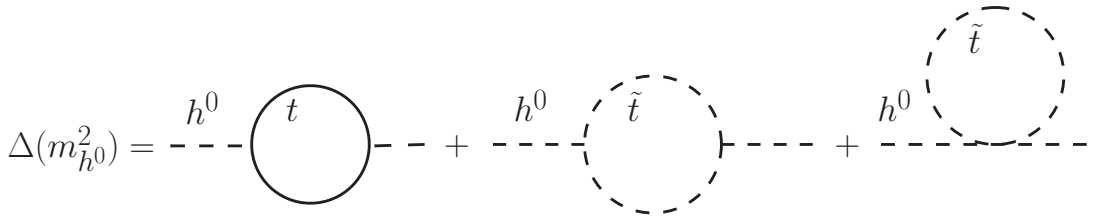

Figure 5.1: One-loop contributions to the h^0 mass in the MSSM

The SM-like Higgs. Of the eight degrees of freedom of the scalar Higgs doublets h_u and h_d, three are would-be Nambu-Goldstone bosons that become the longitudinal modes of the Z and W bosons after EWSB. There are five remaining degrees of freedom: two CP-even neutral scalars h and H^0, two charged Higgs fields $H^\pm$ and one CP-odd neutral scalar A^0. At tree-level, their masses are given by

$$m^2_{A^0} = 2b/\sin(2\beta) = 2|\mu|^2 + \tilde{m}^2_{\rm hu} + \tilde{m}^2_{\rm hd} \tag{5.22a}$$

$$m^2_{h,H^0} = \frac{1}{2}\left(m^2_{A^0} + m^2_Z \mp \sqrt{(m^2_{A^0} - m^2_Z)^2 + 4m^2_Z m^2_{A^0}\sin^2(2\beta)}\right) \tag{5.22b}$$

$$m^2_{H^\pm} = m^2_{A^0} + m^2_W \tag{5.22c}$$

The important observation at this point is that, at tree-level, m_h is bounded from above by the Z-mass

$$m_{h^0} \leq m_Z|\cos(2\beta)| \tag{5.23}$$

Of course, such a light Higgs has long been excluded [143] . The tree-level relation however is subject to rather large loop corrections, with the largest contributions typically coming from top and stop loops shown in Fig. 5.1.

A simple analytic approximation for the light Higgs mass taking into account one-loop and leading-log two-loop contributions from top and stop loops is found in [144]:

$$\begin{aligned} m^2_h = m^2_Z \cos^2 2\beta \left(1 - \frac{3}{\pi^2}\frac{m^2_t}{v^2}t\right) \\ + \frac{3}{4\pi^2}\frac{m^4_t}{v^2}\left[\frac{1}{2}X_t + t + \frac{1}{16\pi^2}\left(\frac{3}{2}\frac{m^2_t}{v^2} - 32\pi\alpha_3\right)(X_t t + t^2)\right] \end{aligned} \tag{5.24}$$

where

$$\begin{aligned} m_t &= M_t/(1 + \frac{4}{3\pi}\alpha_3) \quad \text{and } M_t \text{ is the pole top quark mass} \\ X_t &= \frac{2(A_t - \mu\cot\beta)^2}{Q^2_{\rm SUSY}}\left(1 - \frac{(A_t - \mu\cot\beta)^2}{12Q^2_{\rm SUSY}}\right) \\ t &= \ln\frac{Q^2_{\rm SUSY}}{M^2_t} \end{aligned}$$

The Higgs mass is maximized in the case of so-called *maximal mixing* where $|A_t| = \sqrt{6}\,Q_{\rm SUSY}$. The Higgs mass grows only logarithmically with $Q_{\rm SUSY}$. Therefore $Q_{\rm SUSY} \gg \Lambda_{\rm EWSB}$, i.e. very heavy stops, are necessary to achieve $m_h \sim 125\,\text{GeV}$.

5.2.3 Supersymmetry breaking

Next, we discuss some aspects of supersymmetry breaking. Contrasting the simplicity of unbroken supersymmetry with the intricacy of breaking SUSY, it is fair to say that SUSY phenomenology is SUSY breaking phenomenology [145]. The task is to explain how soft SUSY breaking terms are generated and why flavor symmetry is conserved. The aim is to find models where SUSY is broken spontaneously and the multitude of soft terms can be related to a small number of fundamental parameters in a simpler underlying theory.

Mechanisms of supersymmetry breaking. It is possible to show that direct supersymmetry breaking in the MSSM sector itself would require some of the superparticles to be lighter than their SM counterparts, which is incompatible with experimental non-observation. This is the reason for the paradigm of *hidden sector SUSY breaking* which states that there is a new sector separate from the visible sector containing the SM field and their superpartners. In this hidden sector supersymmetry is broken by a scale much larger than the weak scale. This large primordial sector SUSY breaking is subsequently communicated to the SM fields through messenger interactions, where all fields that couple to both the hidden as well as the visible sector are messengers. Common SUSY breaking mechanisms include gravity mediated SUSY breaking [146, 147] and gauge mediated SUSY breaking (GMSB) [148, 149].

In gravity mediation, supersymmetry breaking in the hidden sector is communicated to the visible sector dominantly through gravitational interactions. Since gravity couples to all forms of energy, the primordial SUSY breaking sector and the visible sector are necessarily connected by gravitational interactions. Thus, unless a different and stronger interaction is at work, supersymmetry breaking is necessarily gravity mediated. The problematic aspect of gravity mediation is that it does not explain the flavor structure of the soft terms. One way to avoid the flavor problem would be to impose a global flavor symmetry at the Planck scale. However, while our understanding of possible UV completions of gravity is very limited, there are hints that a fundamental theory of gravity is unlikely to respect global symmetries like such a flavor symmetry. Thus, gravity mediation typically does not provide a satisfying explanation for why SUSY breaking does not introduce significant flavor violation.[2]

In gauge mediated supersymmetry breaking (GMSB), messengers charged under the SM gauge group $SU(3)_c \times SU(2)_L \times U(1)_Y$ are assumed to be present at a scale M_{m} some orders of magnitude below M_{Pl}. In that case gauge mediated SUSY breaking terms dominate over the unavoidable gravity mediated ones. Gauge mediation is the SUSY breaking mechanism we employ in our approach to building MSSM models with reduced fine-tuning in the next chapter. A huge advantage of gauge mediation is that only flavor diagonal soft terms will be generated, since gauge interactions are flavor blind. Furthermore, it is a very predictive framework: Even in the most general implementation, there are at most six parameters describing all the supersymmetry breaking soft masses $\tilde{\mathbf{m}}_{\mathbf{i}}$ and A-terms. The predictiveness

[2] For an implementation of gravity mediation addressing the flavor problem of gravity mediation, see e.g. [150].

of gauge mediated SUSY breaking comes at a cost however: In models with GMSB, it is generally difficult to generate the Higgs parameters μ and $b \equiv B\mu$ of appropriate size. This is known as the $\mu/B\mu$-problem [151].

Another supersymmetry breaking mechanisms is anomaly mediated SUSY breaking [152, 153]. We forego a discussion of this mechanism since it is not relevant for this work.

MSSM models with reduced parameter space. As discussed before, the number of parameters in models of supersymmetry is far too high to allow for a controlled parameter scan, already at the level of the MSSM with its 105 parameters.

Therefore, phenomenological studies are always performed in models with a reduced set of parameters. The derived limits consequently depend on the choice of underlying model constraining the parameter space. Bounds obtained using a specific model assumption have to be analyzed very carefully in order to decide whether or not they are applicable to another model of interest.

The most widely used MSSM benchmark model is called interchangeably mSUGRA (for *minimal supergravity*) or cMSSM (for *constrained MSSM*). It is based on gravity mediated supersymmetry breaking and is defined at the fundamental scale of $M_* = M_{\mathrm{GUT}}$. At that scale, the following soft term structure is imposed:

- The soft scalar-squared mass terms are completely universal:

$$\tilde{\mathbf{m}}_{\mathbf{q}} = \tilde{\mathbf{m}}_{\mathbf{u^c}} = \tilde{\mathbf{m}}_{\mathbf{d^c}} = \tilde{\mathbf{m}}_{\mathbf{l}} = \tilde{\mathbf{m}}_{\mathbf{e^c}} = \tilde{m}_{\mathrm{hu}} = \tilde{m}_{\mathrm{hd}} = m_0^2 \mathbb{1} \tag{5.25}$$

- The gaugino masses unify:

$$M_3 = M_2 = M_1 = m_{1/2} \tag{5.26}$$

- The A-terms are universal in the sense that

$$\mathbf{a_u} = A_0 \mathbf{Y_u} \qquad \mathbf{a_d} = A_0 \mathbf{Y_d} \qquad \mathbf{a_l} = A_0 \mathbf{Y_l} \tag{5.27}$$

  where $\mathbf{Y_u}$, $\mathbf{Y_d}$ and $\mathbf{Y_l}$ are the Yukawa matrices defined in Eq. (5.11).

The assumptions (5.25)-(5.27) are not theoretically motivated, they simply represent one very simple parametrization of a MSSM model compatible with the concepts of gravity mediation. With these assumptions, the cMSSM is fully described in terms of just five parameters $\{a_i\} = \{m_0^2, m_{1/2}, A_0, b, \mu\}$.[3] Using Eq. (5.18), b is often traded for the parameter $\tan\beta$, and similarly applying the condition $m_Z = 91.2\,\mathrm{GeV}$ determines $|\mu|$ via Eq. (5.19).

Another widely used benchmark model is called mGMSB (for *minimal gauge mediated supersymmetry breaking*). It is based on the scenario of gauge mediated SUSY breaking and assumes that the gauge messengers form one complete $SU(5)$ multiplet. This assumption

[3] As a matter of fact, there is one additional parameter, the gravitino mass $m_{\tilde{G}}$, which is however mostly irrelevant for phenomenology.

determines the soft terms generated at the input scale which is set by the messenger mass, $M_* = M_{\rm m}$. The mGMSB is described in terms of the parameters $\{a_i\} = \{M_{\rm m}, \Lambda, \mu, b\}$, where Λ is the parameter defining the overall scale of the soft supersymmetry breaking terms.

The cMSSM as well as the mGMSB are both useful benchmark points but in their simplicity fail to reflect much of the possible phenomenology. In a strive towards more model independence, the so-called phenomenological MSSM (or pMSSM) [154,155] has been introduced. The pMSSM only makes minimal assumptions beyond those already dictated by the absence of experimental signals of large flavor and CP violation. The 19 parameters of the pMSSM represent a significant simplification compared to the unconstrained MSSM, but typical analyses still require huge computing efforts and scans over discretely generated points in the parameter space in which crucial features can easily be missed.

In light of the start of LHC operations, a bottom-up effective field theory approach to obtain SUSY limits has also been proposed. The idea is to analyze data in the context of simplified effective models [156–159] that contain only the lightest LHC accessible particles. This approach is aimed at obtaining limits that can easily be applied to any given top-down model.

RG Evolution of soft terms and radiative electroweak symmetry breaking. Independent of the specific scheme of generating the soft terms as well as the μ term, the scale M_* where those terms are generated is typically much higher than the electroweak scale $\Lambda_{\rm EWSB}$. Therefore, RG effects crucially affect the resulting mass spectrum.

The form of the RG equations for supersymmetric theories, including the MSSM, is governed by the *supersymmetric non-renormalization theorem* [160, 161]. This theorem states that in models with unbroken supersymmetry all radiative contributions can be written in terms of wave-function renormalization only, while the superpotential itself does not receive corrections at any order in the loop-expansion.

A consequence of the non-renormalization theorem is that the β-function of each supersymmetric parameter, such as μ or the Yukawa couplings, is proportional to itself. Specifically, the 1-loop RG equations for the top Yukawa coupling and μ read

$$\beta_{y_t} \equiv \frac{\partial}{\partial t} y_t = \frac{y_t}{16\pi^2}\left[6|y_t|^2 + |y_b|^2 - \frac{16}{3}g_3^2 - 3g_2^2 - \frac{13}{15}g_1^2\right] \tag{5.28}$$

and

$$\beta_{\mu} \equiv \frac{\partial}{\partial t} \mu = \frac{\mu}{16\pi^2}\left[3|y_t|^2 + 3|y_b|^2 + |y_\tau|^2 - 3g_2^2 - \frac{3}{5}g_1^2\right]. \tag{5.29}$$

Here t denotes the logarithm of the running scale $t = \ln(\mu_{RG}/M_*)$. Since the corrections to μ are proportional only to μ itself and there is no dependence on the soft masses, μ is typically very stable throughout its RG evolution.

In contrast, the soft mass terms can change substantially between the high scale M_* and the weak scale. The evolution of the gaugino masses M_a is independent of the other soft

masses and driven solely by the running of the gauge couplings α_a which evolve according to

$$\frac{\partial}{\partial t}\alpha_a^{-1} = -\frac{b_a}{2\pi} \qquad \text{where } (b_1, b_2, b_3) = \left(\frac{33}{5}, 1, -3\right) \text{ in the MSSM.} \tag{5.30}$$

The gaugino masses are strictly proportional to the gauge couplings, i.e.

$$\frac{M_a}{\alpha_a} = \text{const.} \tag{5.31}$$

Since in the MSSM the gauge couplings unify at the scale M_{GUT}, it is a popular assumption that gaugino masses also unify at a value $m_{1/2}$. In that case, the gaugino mass ratios at the weak scale are approximately $M_1 : M_2 : M_3 = 1 : 2 : 7$.

The RG equations of the soft scalar-squared masses $\tilde{m}^2$ are a complicated set of interdependent differential equations. The complete set of 1-loop RG equations can be found e.g. in [62]. To be able to make reliable statements about the resulting physical spectrum of superparticle masses, the use of computer programs implementing the RGEs including threshold and some 2-loop effects is advisable. Various such SUSY spectrum calculators such as e.g. `Softsusy` [162], `Spheno` [163, 164] and `Suspect` [154] are publicly available.

Of particular interest is the RGE evolution of the up-type soft mass term $\tilde{m}^2_{\text{hu}}$. The most important terms driving its RGE evolution are proportional to the large Yukawa coupling y_t. (For high values of $\tan\beta$ (i.e. $\tan\beta \gtrsim 40$), effects proportional to y_b will be similarly sizable.) Therefore, the third generation squark masses, in particular those of the stops and the left-handed sbottom, dominate the running of $\tilde{m}^2_{\text{hu}}$. Neglecting effects proportional to y_b, y_τ and g_1^2, the system of differential equations to solve is:

$$\begin{aligned} 16\pi^2 \frac{\partial}{\partial t} \begin{pmatrix} \tilde{m}^2_{\text{hu}} \\ \tilde{m}^2_{\text{q3}} \\ \tilde{m}^2_{\text{u3}} \end{pmatrix} &= \begin{pmatrix} 6 \\ 4 \\ 2 \end{pmatrix} y_t^2 [\tilde{m}^2_{\text{hu}} + \tilde{m}^2_{\text{q3}} + \tilde{m}^2_{\text{u3}}] \\ &\quad - \frac{32}{3} g_3^2 \begin{pmatrix} 0 \\ 1 \\ 1 \end{pmatrix} |M_3|^2 - 6 g_2^2 \begin{pmatrix} 1 \\ 1 \\ 0 \end{pmatrix} |M_2^2| \end{aligned} \tag{5.32}$$

Note that the dominant effects proportional to y_t^2 strictly reduce $\tilde{m}^2_{\text{hu}}$. In many model configurations this leads to negative negative values of $\tilde{m}^2_{\text{hu}}$ at low energy scales. This feature is known as *radiative electroweak symmetry breaking* (rEWSB). rEWSB provides a way of understanding how –with a generic set of soft masses at the input scale M_*– only the $\tilde{m}^2_{\text{hu}}$ soft term becomes negative at low energy scales. This provokes a Higgs VEV while the other soft scalar mass parameters remain positive thus avoiding vacuum expectation values that would spontaneously break electric charge Q or color charge. In that sense, not only is SUSY-breaking a necessary condition for EWSB to occur, but once SUSY is broken radiative effects provide a simple mechanism to break electroweak symmetry while keeping the symmetries of the SM intact.

Also note that since the RG evolution is homogeneous in the soft masses, the scale Q_{c^*} where $\tilde{m}^2_{\rm hu}$ crosses zero depends only on M_* and dimensionless ratios between the soft masses, but is parametrically unrelated to the size $M_{\rm SB}$ of those soft terms.

5.3 Searches for supersymmetry

The earliest searches for supersymmetry were performed at the LEP experiment at CERN, which operated between 1989 and 2000 with maximal center-of-mass energies of $\sqrt{s} = 209\,\text{GeV}$. Being an e^+e^- collider, LEP provided a particularly clean experimental environment for new physics searches and could obtain an almost completely model-independent bound on the lightest chargino mass of $m_{\tilde{\chi}^\pm} \gtrsim 103.5\,\text{GeV}$ [165], as well as lower bounds on the masses of the lepton superpartners that are relevant to this day. The Higgs mass limit of $m_h \geq 114.4\,\text{GeV}$ [143] established by LEP first spurred the discussion of SUSY naturalness.

Since the beginning of its operation, the Large Hadron Collider has already produced significant new direct exclusion limits. The advantages of the LHC for supersymmetry searches are on one hand its high center-of-mass energy and on the other hand that, being a hadron collider, the LHC can take advantage of the large cross-sections of QCD-mediated processes, resulting in the production of a large number of SUSY particles.

The main production mechanism for superparticles at hadron colliders are squark-squark, squark-gluino and gluino-gluino production. The direct LHC searches for SUSY are conducted by the experiments CMS [166] and ATLAS [167]. The copious analysis output is documented in [168] and [169]. A compact recent overview can be found e.g. in Ref. [170].

Typical SUSY search signatures are characterized by several high-p_T jets, which are produced in the decay chains of heavy colored superparticles, and a significant amount of missing momentum. The latter is expected as a result of two stable neutral LSPs produced at the end of the decay chain which escape undetected. LSP is a consequence of R-parity conservation commonly imposed to forbid proton decay in supersymmetric

We are mainly concerned with the limits relevant to SUSY naturalness. As will be discussed in more detail in the following Sec. 5.4, the lower mass bounds on gluino and third generation squarks are of particular significance for the discussion of the naturalness of EWSB in supersymmetric models.

We begin by describing the experimental situation in generic SUSY models before discussing some specific scenarios in which the generic SUSY bounds may not apply.

The lack of any SUSY signal so far translates into lower gluino mass bounds which depend on the size of the masses of the first and second generation squarks $m_{\tilde{q}}$. If the squarks are in the same mass range as the gluino, the limit is roughly $m_{\tilde{g}} \gtrsim 1.4\,\text{TeV}$. This is relaxed to $m_{\tilde{g}} \gtrsim 0.9\,\text{TeV}$ for the case of $m_{\tilde{g}} \ll m_{\tilde{q}}$ [171, 172]. Stops ($\tilde{t}$) and sbottoms ($\tilde{b}$) are produced at the LHC in gluino decays or via direct pair-production. The production via gluino decays dominates, provided the gluinos are not too heavy and the gluinos branching ratio to stops and sbottoms is sizeable. Direct stop and sbottom pair production

is expected to be more than an order of magnitude smaller than the pair-production cross-section of first and second generation squarks and moreover subject to large backgrounds from top-quark pair production. The CMS collaboration determined that sbottom pair production is excluded for sbottom masses below 500 GeV (assuming LSP masses below 150 GeV and a 100% branching fraction into a bottom quark and a neutralino) [173, 174]. The ATLAS collaboration has recently set limits in direct stop production. Specifically, for the case of a massless LSP, the direct lower limits on the stop mass as determined by ATLAS reach 500 GeV but leave a open window around the top quark mass. The ATLAS analyses [175–179] assume specific stop decay modes, namely $\tilde{t} \to b\tilde{\chi}^{\pm}$ for light stops and $\tilde{t} \to t\tilde{\chi}^{0}$ for heavy stops.

The bounds on superparticles can be relaxed for certain non-standard SUSY spectra. In a scenario called *compressed supersymmetry* [180], limits from standard searches are avoided as the visible energy of the events is too small to pass the selection criteria and events with large missing transverse energy are excluded from the analysis. In the compressed SUSY scenarios, the gluino mass has been constrained to $m_{\tilde{g}} \gtrsim 500\,(600)$ GeV in the 7 (8) TeV run [181, 182]. The 14 TeV run will be able to probe gluino masses higher than 1 TeV.

Another approach to avoid the standard SUSY limits is called *stealth supersymmetry* Ref. [183, 184]: Additional particles with masses of order of the electroweak scale are introduced to modify the decay patterns of the MSSM particles. In stealth SUSY, the gluino is already constrained to $m_{\tilde{g}} \gtrsim 1$ TeV [185] in cases when an isolated photon is produced in the decay chain.

SUSY bounds can also be relaxed if R-parity is violated. To limit this scenario, CMS is performing searches for multi-lepton final states [186] and 3-jet resonances to be expected from R-parity violating gluino decays [187]. ATLAS complements these searches by looking for non-resonant $e + \mu$ production, mediated by t-channel squark exchange [188] as well as for neutralino decay signalled by displaced, massive vertices with high track multiplicity and accompanied by a high-p_T muon [189].

Supersymmetry is also subject to indirect constraints. For instance, the LHCb experiment has measured the $B_s \to \mu\mu$ decay rate [190] with increased precision and determined that any new contribution to this process needs to be smaller than the SM decay rate. $B_s \to \mu\mu$ decays are low energy processes best described by effective 4-fermion operators. In supersymmetric models, new contributions to these effective operators arise from exchange of the heavy and pseudo-scalar Higgs particles. The corresponding bounds, determined in [191], are of concern in particular if $\tan\beta$ is large $\tan\beta \gtrsim 30$. It has also further been found that models with light stops are often at odds with the $b \to s\gamma$ branching fraction [192].

Finally, the recent discovery of the Higgs boson with mass $m_h \sim 125$ GeV [32, 33] poses a challenge for supersymmetric models, in particular the MSSM. The consequences of the Higgs boson discovery for SUSY naturalness will be discussed in more detail in the next section. It is worth mentioning however that the fact that the determined Higgs boson mass m_h is still relatively close the Z boson mass m_Z can be interpreted as a hint in favor of supersymmetry.

5.4 The naturalness problem of supersymmetry

As mentioned in the beginning of this chapter, naturalness is *la raison d'être* for supersymmetry. Hence in the absence of any signals for the existence of superparticles, it is decisive to quantify how problematic the existing experimental bounds are in terms of fine-tuning (FT).

While supersymmetry solves the original hierarchy problem of the SM model, i.e. a fine-tuning in the Higgs mass of more than 30 orders of magnitude, it suffers from its own naturalness problem. Generally speaking, the remaining fine-tuning in supersymmetry is the result of a hierarchy between Λ_{EWSB} and the amount of supersymmetry breaking characterized by M_{SB}.

While the direct limits on M_{SB} are becoming more constraining and begin to pose a challenge for SUSY naturalness, the main concern regarding naturalness in the MSSM stems from the need to realize the observed Higgs mass of $m_h \sim 125\,\mathrm{GeV}$. As discussed in Sec. 5.2.2, in order to obtain a value of m_h above the Z boson mass m_Z, loop corrections need to be of a size comparable to the tree-level contribution itself. To realize this, the stop masses need to be very large. Heavy stops induce even larger loop corrections to the $\tilde{m}_{\mathrm{hu}}$ parameter: these corrections grow quadratically with the stop masses, while the corrections to m_h only grow logarithmically. Raising the Higgs mass in the MSSM therefore comes with the prize of a very large soft mass term for h_u. This is problematic because $\tilde{m}_{\mathrm{hu}}$ is directly related to the amount of electroweak symmetry breaking and more specifically to the Z boson mass. For $\tan\beta \gtrsim 5$, Eq. (5.19) is approximated by

$$\frac{m_Z^2}{2} = \frac{\tilde{m}_{\mathrm{hd}}^2 - \tilde{m}_{\mathrm{hu}}^2 \cdot \tan^2\beta}{\tan^2\beta - 1} - \mu^2 \simeq -\tilde{m}_{\mathrm{hu}}^2 - \mu^2. \tag{5.33}$$

For very large $\tilde{m}_{\mathrm{hu}}^2 \gg (1\,\mathrm{TeV})^2$, the observed Z boson mass can only be achieved via an unnatural cancellation between $\tilde{m}_{\mathrm{hu}}^2$ and μ^2.

To naturally obtain the correct Z mass from Eq. (5.33), values for $|\tilde{m}_{\mathrm{hu}}^2|$ and μ^2 of $\sim (100\,\mathrm{GeV})^2$ are preferred. Because various superparticles, most importantly the stops, contribute quadratically to $\tilde{m}_{\mathrm{hu}}^2$, this means that naturalness requires those superparticles to be light. How to quantify naturalness and how fine-tuning limits translate into upper bounds on superparticle masses has been discussed first in [193], and has since been a primary concern of MSSM phenomenology. Naturalness in supersymmetry has been under siege for a long time. The LHC Higgs discovery, locating m_h at around 125 GeV and thus significantly above the LEP limit of $m_h > 114.4\,\mathrm{GeV}$, has made the naturalness concerns even more pressing.

It should be emphasized that the Higgs mass limits SUSY naturalness in an indirect way: In supersymmetric models beyond the MSSM, like the next-to-minimal supersymmetric standard model (NMSSM), the Higgs sector can be modified such that $m_h \sim 125\,\mathrm{GeV}$ is obtained with lighter stops. Naturalness in supersymmetric models with such extended Higgs sectors is probed by direct LHC searches placing lower mass boundss on the individual superparticles that contribute radiatively to $\tilde{m}_{\mathrm{hu}}^2$.

5.4.1 How to measure fine-tuning

There are various approaches to quantify fine-tuning. Fine-tuning is not a physical quantity in the strictest sense, but rather a measure of how convincing a certain model is given our current understanding of physics. Prescriptions to quantify fine-tuning therefore necessarily have a certain degree of ambivalence.

As a general rule, any statement such as *"model a is fine-tuned by 1 part in 500"* does not have much meaning in isolation. Quantifying fine-tuning rather serves to compare different models by their respective degree of fine-tuning quantified by the same prescription. An extensive discussion on various measures of fine-tuning the inherent model-dependence of the subject can be found in section VII of [194].

The analysis of fine-tuning limits on superparticle masses differs from most other phenomenological studies, in which the setup with completely uncorrelated parameters always contains more restricted models as a subset. In contrast for the issue of fine-tuning, correlations can dictate the result. A model-independent fine-tuning analysis is —even in principle— impossible.

High scale prescription. A widely used fine-tuning measure is based on the general concept that SUSY breaking is mediated to the visible sector at some rather high scale M_*. At this scale the soft mass terms defining the ultimate superparticle spectrum are defined in terms of few fundamental parameters a_i.

A model is considered to be fine-tuned if the m_Z mass is extremely sensitive to even tiny changes in the fundamental parameters. Specifically, fine-tuning is quantified using a prescription defined in [193, 195]:

(i) Define the set of fundamental parameters $\{a_i\}$.

(ii) For each fundamental parameter a_i of the SUSY model define a sensitivity coefficient

$$c_i \equiv \frac{\partial \ln m_Z^2}{\partial \ln a_i} \tag{5.34}$$

For the cMSSM for instance, calculate the sensitivity coefficients with respect to $\{a_i\} = \{m_0^2, m_{1/2}^2, A_0^2, b, \mu^2\}$.

(iii) Measure FT by the size of the maximum absolute value of the c_i

$$\Delta \equiv \max(|c_i|) \tag{5.35}$$

Several comments concerning this measure are in order: There is no stringent reason to prefer the maximum of the individual sensitivity coefficients as in (5.35) over e.g $\Delta \equiv \sqrt{\sum_i c_i^2}$ to quantify the overall fine-tuning. The main source of arbitrariness however stems from choosing the "fundamental parameters" in step (i). An important question is for example whether to only include MSSM specific model parameters or whether all parameters in the lagrangian should be included into $\{a_i\}$, including the Yukawa and the gauge couplings [196].

Individual fine-tuning contributions from uncorrelated soft masses. Alternatively to the top-down approach just described, the subject of fine-tuning is also often investigated from a low scale perspective. In this approach, defined in [197], physical soft masses at the weak scale are assumed to be fully independent parameters. For each soft term the contribution to the quadratic coefficient of the scalar potential $m_{\tilde{h}}^2$ is calculated. For moderate $\tan\beta \gtrsim 5$, this coefficient is approximated by

$$m_{\tilde{h}}^2 = \mu^2 + \tilde{m}_{\rm hu}^2\big|_{\rm tree} + \delta\tilde{m}_{\rm hu}^2 \tag{5.36}$$

where $\tilde{m}_{\rm hu}^2\big|_{\rm tree}$ and $\delta\tilde{m}_{\rm hu}^2$ represent the tree-level and radiative contributions to $\tilde{m}_{\rm hu}^2$, respectively. The fine-tuning measure for the soft masses is defined as

$$\Delta \equiv \frac{\delta\tilde{m}_{\rm hu}^2}{m_h^2}. \tag{5.37}$$

This fine-tuning measure translates into direct bounds on superparticle masses:

For the stops, the relevant contributions to $\delta\tilde{m}_{\rm hu}^2$ in the leading-log approximation are:

$$\delta\tilde{m}_{\rm hu}^2\big|_{\rm stop} = \frac{3}{8\pi^2} y_t^2 (\tilde{m}_{\rm q3}^2 + \tilde{m}_{\rm u3}^2 + |A_t|^2) \ln\left(\frac{M_*}{\rm TeV}\right) \tag{5.38}$$

where $\tilde{m}_{\rm q3}^2$ and $\tilde{m}_{\rm u3}^2$ are the left- and right-handed stop soft mass terms and M_* denotes the scale at which SUSY breaking effects are mediated to the MSSM.

Demanding that fine-tuning does not exceed a fixed value $\Delta_{\rm max}$ leads to an upper bound on the physical stop masses of

$$\sqrt{m_{\tilde{t}_1}^2 + m_{\tilde{t}_2}^2} \lesssim 600\,{\rm GeV} \frac{\sin\beta}{\sqrt{1+x_t^2}} \left(\frac{\ln(M_*/{\rm TeV})}{3}\right)^{-1/2} \left(\frac{m_{\tilde{h}}}{120\,{\rm GeV}}\right) \left(\frac{\Delta_{\rm max}}{20\%}\right) \tag{5.39}$$

where $x_t \equiv A_t \left(m_{\tilde{t}_1}^2 + m_{\tilde{t}_2}^2\right)^{-1/2}$.

For gluinos, the contributions to $\delta\tilde{m}_{\rm hu}^2$ are:

$$\delta\tilde{m}_{\rm hu}^2\big|_{\rm gluino} = -\frac{2}{\pi^2} y_t^2 \left(\frac{\alpha_s}{\pi}\right) |M_3|^2 \ln^2\left(\frac{M_*}{\rm TeV}\right) \tag{5.40}$$

(For very large A-terms, an additional mixed $A_t M_3$ contribution can also be relevant.) Eq. (5.40) translates into a naturalness bound on the gluino mass of

$$M_3 \lesssim 900\,{\rm GeV} \sin\beta \left(\frac{\ln(M_*/TeV)}{3}\right)^{-1} \left(\frac{m_{\tilde{h}}}{120\,{\rm GeV}}\right) \left(\frac{\Delta_{\rm max}}{20\%}\right). \tag{5.41}$$

Following an analysis analogous to the one performed for the gluino, the following naturalness bounds on wino and bino mass terms M_2 and M_1 are obtained:

$$M_{2,1} \lesssim S_{2,1} \left(\frac{\ln(M_*/TeV)}{3}\right)^{-1/2} \left(\frac{m_{\tilde{h}}}{120\,{\rm GeV}}\right) \left(\frac{\Delta_{\rm max}}{20\%}\right) \tag{5.42}$$

$$\tag{5.43}$$

with $S_2 = 900\,\text{GeV}$ and $S_1 = 3\,\text{TeV}$, respectively. The wino is almost as constrained as the gluino, while the bino is much less constrained by naturalness.

Note that in this approach, all soft masses are assumed to be completely independent, even though the existence of some higher, more fundamental scale M_* is implicitly assumed as can be gathered from the logarithms in the equations above. If there exist correlations at that high scale, the above analysis does in principle not hold.

5.4.2 The *natural supersymmetry* paradigm

Based on a fine-tuning analyses similar the one performed in the previous Sec. 5.4.1 a rough picture of a SUSY spectrum that optimally balances fine-tuning and at the same time avoids LHC bounds has emerged, see e.g. [198–200]. This schematic spectrum has received the designation *natural supersymmetry*. The main idea is to separate sparticles into two categories: Those giving rise to large contributions to $\delta\tilde{m}^2_{\text{hu}}$ and those whose impact on $\delta\tilde{m}^2_{\text{hu}}$, and hence naturalness, is comparatively small. The optimal spectrum is obtained by keeping the sparticles in the first category as light as possible, while the sparticles in the second category are allowed to be heavy which can help to alleviate direct exclusion limits. A *natural supersymmetry* spectrum requires:

- both stop and lefthanded sbottom are rather light $m_{\tilde{t},\tilde{b}} \lesssim 600\,\text{GeV}$
- moderately heavy gluino mass of $m_{\tilde{g}} \lesssim 0.9 - 1.5\,\text{TeV}$
- light higgsinos $\mu \lesssim 200 - 300\,\text{GeV}$

The first and second generation squarks, in contrast to those of the third generation, can have masses as high as 20 TeV.

Since the beginning of the LHC operation, much effort has been dedicated to identify credible models that feature such a spectrum. Model building to embed *natural supersymmetry* spectra into complete models has proven to be a difficult undertaking, in particular regarding the conservation of flavor bounds. No convincing picture has emerged so far, despite the existence of some interesting new approaches such as e.g. [201, 202].

We want to conclude this chapter by pointing out potentially problematic aspects of the *natural SUSY* approach to fine-tuning, in order to motivate an alternative approach presented in the next chapter.

Models featuring a *natural supersymmetry* spectrum are by design at the brink of exclusion. Limits on direct stop and sbottom pair production, interpreted in the context of simplified models, have started and will continue to directly constrain the natural SUSY parameter space [176]. Of concern are also frequent conflicts with the experimentally determined $b \to s\gamma$ branching ratio [203, 204]. Lastly, with the light stops characteristic for *natural supersymmetry* spectra, the Higgs mass of $m_h \sim 125\,\text{GeV}$ cannot be realized. The *natural supersymmetry* approach thus necessarily requires to extend the MSSM Higgs sector.

CHAPTER 6

REDUCING FINE-TUNING IN THE MSSM VIA STABLE NEAR-CRITICALITY

For decades, supersymmetry with superpartner masses predicted to be of the order of 100 GeV has been the widely accepted standard scenario for beyond-the-SM physics. However, the fact that no evidence for the existence of superparticles has been found during the first years of LHC operation has put supersymmetry, if it exists in nature, at a crossroads:

It is possible that even if supersymmetry is realized, electroweak symmetry is still broken by an unnaturally small amount. In this case, supersymmetry only reduces the hierarchy problem to the SUSY naturalness problem but does not solve it entirely. While this means discarding the original and arguably strongest motivation for SUSY, other promising features of supersymmetry, such as gauge coupling unification and the existence of a compelling dark matter candidate, can still be realized. Examples for this approach of abandoning the concept of SUSY naturalness are *split supersymmetry* [64, 65] or more recently *simply unnatural SUSY* [205].

In contrast, if supersymmetry *does* address the naturalness problem of EWSB, very non-generic models are required.[1] Following the *natural supersymmetry* approach, model building efforts are made to implement tailored spectra with light stops, left-handed sbottoms and gluinos. In these models usually an extended Higgs sector beyond the MSSM is required to explain the Higgs mass of $m_h \sim 125\,\text{GeV}$. Furthermore direct exclusion limits on the gluino mass and stop masses are beginning to constrain this scenario. Via additional model building it is possible to evade many of the existing limits. Examples for those strategies are *compressed SUSY* spectra [180], *stealth supersymmetry* [183, 184] or models with R-parity violation such as e.g. in [206]. Model building following this line of reasoning often predicts interesting signatures since by definition supersymmetry signals are 'just around the corner', but it also faces increasing difficulties to be in compliance with direct and indirect exclusion limits.

An alternative approach to preserve naturalness in supersymmetry is based on the observation that quantifying fine-tuning by assessing the fine-tuning contributions of the individual superparticles, treating each soft mass as a free and uncorrelated parameter, might

[1] This fact is has been called "fine-tuning in model space" [205] and used as argument against supersymmetry as a solution to the naturalness problem.

not be applicable. If robust correlations in the underlying model lead to fine-tuning constraints on the superparticle spectrum that differ from those specified in Sec. 5.4.1, models with a spectrum quite unlike the typical natural spectra can unexpectedly turn out to be natural.

In this work, we will concentrate on this last possibility. This option requires a careful analysis of the actual principles behind the notion of fine-tuning. The aim of this chapter is to identify a mechanism that robustly predicts small values of the Higgs mass parameter at the weak scale, even in the presence of heavy superfields including stops.

6.1 An alternative view of the SUSY naturalness problem

To set the stage for our approach to reduce fine-tuning, we want to describe and alternative view of the SUSY naturalness problem that has been introduced in Ref. [207]. The authors demonstrate that the naturalness problem of supersymmetry can be illustrated by contemplating the RG evolution of the Higgs mass parameter $m_2^2 \equiv \tilde{m}_{\rm hu}^2 + \mu^2$, which is schematically depicted in Fig. 6.1.

The argument on Ref. [207] is as follows. In supersymmetric models, typically the soft terms as well as the Higgsino mass term μ are roughly of the same order which we denote by $M_{\rm SB}$ (c.f. Eq. (5.8)). The scalar potential is evaluated at the scale $Q_{\rm SUSY}$, which is itself of the same order as $M_{\rm SB}$ since it is defined by the stop masses (see Eq. (5.21) and Eq. (5.8)). As is illustrated in Fig. 6.1a, the Higgs mass term $m_2^2 = \tilde{m}_{\rm hu}^2 + \mu^2$ at the scale $Q_{\rm SUSY}$ is expected to be of the order of $M_{\rm SB}^2$. However, since exclusion limits are pushing $M_{\rm SB}$ to values closer to the several-TeV regime than to the EWSB scale of $\mathcal{O}(100\,\text{GeV})$, how can a small value of m_2^2 be explained? The answer is that EWSB in the SUSY model needs to be very close to criticality, i.e. the scale where electroweak symmetry is broken radiatively is very close to the scale where the spectrum is evaluated. In other words, electroweak symmetry is just barely broken. Defining Q_c as the scale where m_2^2 crosses zero, near-criticality amounts to requiring that Q_c closely coincides with $Q_{\rm SUSY}$. The scenario of near-criticality is depicted in Fig. 6.1b. This coincidence is precisely what constitutes fine-tuning. Why would nature pick a specific value for Q_c, which is parametrically unrelated to $M_{\rm SB}$, when the allowed range is the entire interval between $Q_{\rm SUSY}$ and the scale M_* where SUSY breaking is mediated to the visible sector?

This view of the SUSY naturalness problem is generally equivalent to the naturalness problem of supersymmetry as it is usually formulated, namely as the problem of fine-tuned cancellations between $\tilde{m}_{\rm hu}^2$ and μ^2. This can be observed in Fig. 6.1b: A SUSY model can always be forced to exhibit $Q_c \sim Q_{\rm SUSY}$ and to reproduce the correct, comparatively small value of $m_Z^2 \simeq -\frac{1}{2}m_2^2$, by choosing $|\mu|^2$ such that it precisely cancels the large negative $\tilde{m}_{\rm hu}^2$ term. The SUSY model would thus be near-critical (in the sense that the EWSB is just barely broken) only at the cost of a fine-tuning cancellation between μ^2 and $\tilde{m}_{\rm hu}^2$.

Contrasting the usual case of near-criticality of coming at the cost of fine-tuning, in the next section we introduce a setup we call *stable near-criticality* (SNC) [40]. We argue that near-criticality can be a robust feature in certain supersymmetric models and that no fine-tuned cancellations between unrelated terms are necessary. To realize SNC, very

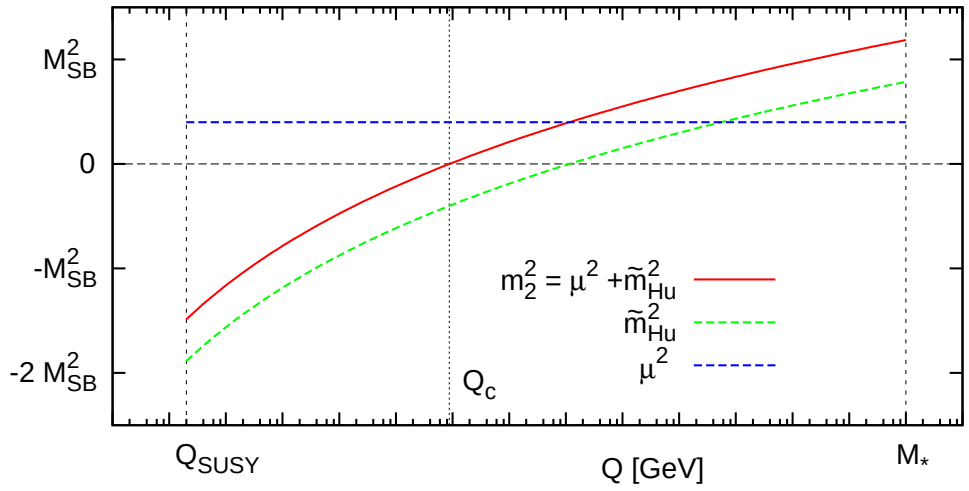

(a) RG evolution of the Higgs mass parameter m_2^2. Q_c can be located at any position in the interval $[Q_{\rm SUSY}, M_*]$ which generically results in a Higgs mass parameter at the low scale that is of the order of SUSY breaking, $(-m_2^2) \sim M_{\rm SB}^2$.

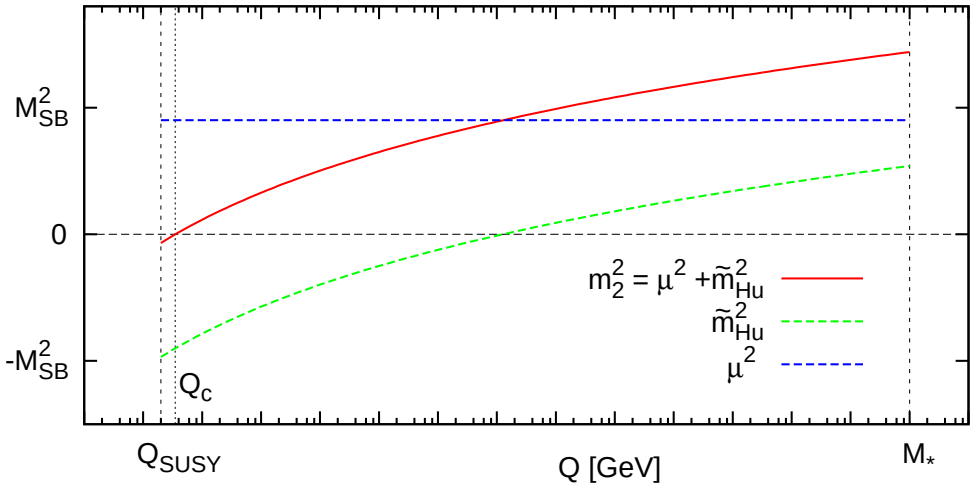

(b) The special case of near-criticality where Q_c is very close to $Q_{\rm SUSY}$. In this case, m_2^2 is much smaller than the overall size of SUSY breaking $M_{\rm SB}$. Usually, fine-tuning between the (unrelated) parameters $\tilde{m}_{\rm hu}^2$ and μ^2 is necessary to achieve near-criticality.

Figure 6.1: Schematic view of the RG evolution of the Higgs mass parameter $m_2^2 = \tilde{m}_{\rm hu}^2 + \mu^2$. The soft SUSY breaking parameters as well as μ are generated with values of order $M_{\rm SB}$ at the input scale M_* where SUSY breaking is mediated to the visible sector. Q_c is defined as the scale where m_2 crosses zero and electroweak symmetry is broken radiatively.

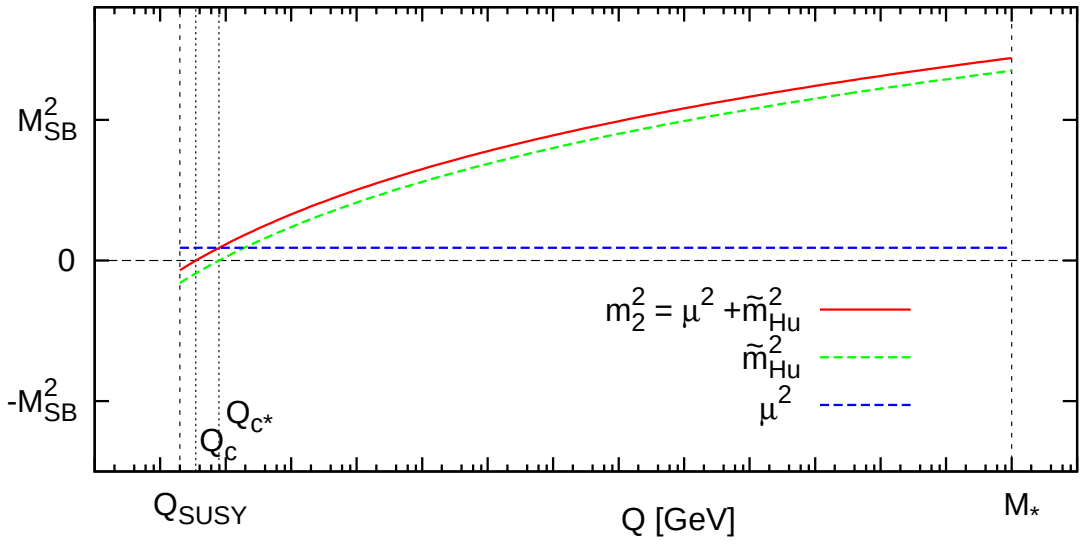

Figure 6.2: Setup of stable near-criticality: If it can be realized that $\tilde{m}^2_{\rm hu}$ is driven automatically to zero near $Q_{\rm SUSY}$ through correlation among the soft masses at the input scale M_*, no fine-tuning is necessary to obtain small $m_2^2(Q_{\rm SUSY})$.

specific correlations between the soft terms contributing to the RGE running are required. These correlations need to arise from the underlying model of SUSY breaking. We discuss in detail which types of correlations are required in a supersymmetric model in order to achieve SNC.

6.2 The concept of stable near-criticality

If the underlying model of SUSY breaking relates the soft terms among each other in a way that near-criticality is a generic feature rather than a special case, this would provide an explanation for the hierarchy between $\Lambda_{\rm EWSB}$ and the scale of the soft terms $M_{\rm SB}$. We dub this scenario stable near-criticality (SNC). SNC leads to a significant reduction in the fine-tuning even in the presence of large stop masses. In this section we will discuss precisely how we define SNC and which conditions that need to be satisfied by a MSSM model to display SNC.

Near-criticality means that electroweak symmetry is radiatively broken at a scale close to $Q_{\rm SUSY}$, i.e. $Q_c \sim Q_{\rm SUSY}$. As discussed in the previous Sec. 6.1, this usually requires a fine-tuned cancellation between $\tilde{m}^2_{\rm hu}$ and μ^2 at the scale $Q_{\rm SUSY}$.

To avoid this fine-tuning, ideally one would try to build a model that *predicts* such a cancellation between $\tilde{m}^2_{\rm hu}$ and μ^2 at the scale $Q = Q_{\rm SUSY}$. This would require an implementation of SUSY breaking mediation to the visible sector that constrains the $\tilde{m}^2_{\rm hu}(M_*)$-$\mu^2(M_*)$ input parameter plane to precisely the line for which the low scale values $\tilde{m}^2_{\rm hu}(Q_{\rm SUSY})$ and $\mu^2(Q_{\rm SUSY})$ cancel. However, it appears unlikely that any model can be constructed to dis-

play this behavior. Achieving cancellation between $\tilde{m}^2_{\rm hu}$ and μ^2 at $Q_{\rm SUSY}$ requires a very complicated connection between μ^2 and $\tilde{m}^2_{\rm hu}$ at the input scale M_*. The reason is that the two terms RG evolve very differently due to their different symmetry structure: the higgsino mass term μ by itself is compatible with unbroken supersymmetry while $\tilde{m}^2_{\rm hu}$ is not. Therefore, $\tilde{m}^2_{\rm hu}(Q_{\rm SUSY})$ is subject to large RGE effects which depend on the sizes of the other soft masses, while $\mu^2(Q_{\rm SUSY}) \simeq \mu^2(M_*)$ remains almost constant throughout scale evolution and is independent from the soft mass spectrum.

The question arises whether correlations among other parameters exist that are useful to achieve near-criticality and that can actually be realized through simple correlations at the input scale. To address this question we define, analogously to Q_c, the scale Q_{c^*} as the scale where $\tilde{m}^2_{\rm hu}$ changes sign. Since $\tilde{m}^2_{\rm hu}$ is independent of the Higgsino mass term μ, so is Q_{c^*}. Note that if $Q_{c^*} \sim Q_{\rm SUSY}$ can be arranged, near-criticality merely requires μ^2 to be of the order of $\Lambda_{\rm EWSB}$ but not to be fine-tuned to any specific value. The setup is illustrated in Fig. 6.2. Even more important is the observation that correlations leading to $Q_{c^*} \sim Q_{\rm SUSY}$ are straightforward to implement: Since the RG evolution is homogeneous in the soft terms, the scale Q_{c^*} depends only on $M_{\rm Pl}$ and on the dimensionless ratios among the soft masses but not on the overall size of the soft masses $M_{\rm SB}$. This observation is well-known in the literature, and it is in fact at the core of the *Focus Point* mechanism [194, 208–211] to reduce fine-tuning.

Our approach however differs from the *Focus Point* approach by the strict requirement that $Q_{c^*} \sim Q_{\rm SUSY}$ should be a truly robust feature of the SUSY model. Fine-tuning has to be avoided with respect to *all* lagrangian parameters. This extends to the dimensionfull model parameters, such as μ and the soft masses, as well as to the dimensionless ratios between the soft masses or the SM gauge and Yukawa couplings. Specifically, we put forward the following requirements for an SNC model:

(A) Fine-tuning with respect to the dimensionfull parameters is can be avoided if

(AI) at the input scale all soft masses are given in terms of a single SUSY breaking parameter Λ

$$\begin{aligned} \tilde{m}_i^2(M_*) &= f_i\,\Lambda^2 && \text{for } i = q, u^c, d^c, l, e^c, h_u, h_d \\ M_a(M_*) &= f_{M_a}\,\Lambda && \text{for } a = 1,2,3 \\ A_F(M_*) &= f_F\,\Lambda && \text{for } F = t, b, l \end{aligned}$$

where the ratios among the soft masses f_i, f_{M_a}, f_F are predicted by the mechanism of SUSY breaking mediation to the visible sector and not free parameters

(AII) and

The ratios among the soft masses f_i, f_{M_a}, f_F are such that $Q_{c^*} \simeq Q_{\rm SUSY}$.

Note that condition (AI) implies that the scale of SUSY breaking $M_{\rm SB}$ is determined by Λ alone, $M_{\rm SB} \equiv \Lambda$. This is a stricter requirement than the assumption that that all the soft terms are of the same order of magnitude as e.g. in Eq. (5.8). The requirements (AI) and (AII) resemble those leading to the *Focus Point* effect, however we go beyond *Focus Point* scenario by strictly requiring that the dimensionsless ratios

f_i, f_{M_a} and f_F should be predicted by the model itself and not be dependent on other continuous parameters of the SUSY breaking mechanism.

(B) Fine-tuning with respect to the gauge and Yukawa couplings is also a concern, as was first pointed out in Ref. [196]. Usually, these fine-tunings are not taken into account when analyzing the naturalness of a specific SUSY model, as it is silently assumed that they are subdominant to fine-tuning with respect to the parameters connected to the SUSY breaking itself. If the latter tunings however can be held small, the fine-tuning of the EWSB sector with regard to the gauge and Yukawa and can no longer be ignored. Of particular importance here are the sensitivities w.r.t. the SM couplings g_3 and y_t. The theory needs to be modified in a way that EWSB becomes less fine-tuned with regard to the input values of these couplings.

In the following, we first consider requirement (A) in more detail and give two simple explicit model examples in Sec. 6.3. In Sec. 6.4, a possible realization of condition (B) will be discussed. Finally, in Sec. 6.6, we demonstrate the reduction of fine-tuning through Stable near-criticality in a complete model implementation.

6.3 SNC in gauge mediated MSSM models

In the following we want to show that simple models can be built that exhibit the necessary properties worked out in the previous section.

Requirement (A) implies that the underlying supersymmetric model may only have a small number of model parameters. As discussed in Sec. 5.2.1, reducing the number of model parameters is always necessary in SUSY models for reasons of flavor and CP conservation. Further reducing the parameter space thus does not per se have to be an unreasonable restriction, any such reduction however needs to be justified by the underlying model. Ad hoc assumptions relating the soft masses, such as imposing universal scalar-squared soft masses in the cMSSM (see Eq. (5.25)-(5.27)), are not valid for our purposes as they is no justification of the correlation by the model of SUSY breaking itself.

We select the mechanism of gauge mediation to break supersymmetry in our setup. This choice has two reasons. First, in addition to elegantly solving the SUSY flavor problem, GMSB is a quite predictive scenario since the soft terms are a direct consequence of the gauge quantum numbers of the messenger fields. Second, the messenger scale $M_{\rm m}$ can be substantially lower than $M_{\rm GUT}$, which turns out to be key to suppress fine-tuning with respect to g_3 and y_t in our mechanism.

Achieving $\tilde{m}^2_{\rm hu}(Q_{\rm SUSY}) \simeq 0$ in the context of models of gauge mediated SUSY breaking has first been discussed, in the terminology of the *Focus Point* approach in Ref. [212]. The simplest and most restricted model with GMSB is minimal gauge mediation (mGMSB). We proceed to demonstrate that the mGMSB can be modified to achieve SNC.

In minimal gauge mediation (mGMSB), supersymmetry is broken by a single gauge singlet spurion field X acquiring a vacuum expectation value $X \to \langle X \rangle = M + \theta\theta F$. SUSY

breaking is then communicated to the MSSM via gauge interactions with messengers in a complete SU(5) multiplet $\mathbf{5} \oplus \bar{\mathbf{5}} = L, \bar{L}, D, \bar{D}$ coupling to the SUSY breaking spurion X as described by the superpotential

$$\mathcal{W}_{\mathrm{SB}} = \lambda_L X L \bar{L} + \lambda_D X D \bar{D}. \tag{6.1}$$

Usually $\lambda_L = \lambda_D$ is implied in order to make this superpotential explicitly $SU(5)$-invariant. Irregardless, the size of the MSSM soft masses only depends on the parameter

$$\Lambda = \frac{\lambda_{L,D} F}{\lambda_{L,D} M} = \frac{F}{M} \tag{6.2}$$

because the λ_i drop out in the ratio. The input scale M_* is defined as the scale where the messengers are integrated out, $M_* = M_{\mathrm{m}} = \lambda_{L,D} M$. At this scale, the soft masses generated are given by

$$\tilde{m}_i^2(M_{\mathrm{m}}) = 2\frac{\Lambda^2}{(4\pi)^2} \sum_a c_{ia} \alpha_a^2(M_{\mathrm{m}}) \tag{6.3a}$$

$$M_a(M_{\mathrm{m}}) = \frac{\Lambda}{4\pi} \alpha_a(M_{\mathrm{m}}) \tag{6.3b}$$

$$A_a(M_{\mathrm{m}}) = 0 \tag{6.3c}$$

where c_{ia} denote the quadratic Casimir invariants of the respective scalar.[2]

From the above expressions, it is obvious that the model of minimal gauge mediation satisfies the requirement (AI) which requires all soft terms to originate from a single scale. However mGMSB does not exhibit a cancellation in the running of $\tilde{m}_{\mathrm{hu}}^2$, i.e. condition (AII) is not fulfilled. In order to actually achieve this cancellation and hence small values of $\tilde{m}_{\mathrm{hu}}^2(Q_{\mathrm{SUSY}})$, we have to change minimal gauge mediation in a way that condition (AII) can be satisfied without forfeiting condition (AI). In particular, we do not introduce new continuous parameters which affect the relative sizes of the soft masses.

In [212], various modifications of mGMSB to fulfill (AII) are discussed. However the author focused on models in which the gaugino masses are negligible compared to the soft scalar mass terms. This assumption traces back to the original formulation of the *Focus Point*. As the RG equations become very simple in the case when gaugino masses can be neglected, the cancellation in the running of $\tilde{m}_{\mathrm{hu}}^2$ can be demonstrated semi-analytically. Subleading gaugino masses are however not strictly necessary. The crucial requirement is that the gaugino masses do not introduce a new independent scale, as made manifest in condition (AI). In fact, in light of new LHC bounds on the gluino mass limiting $m_{\tilde{g}} \gtrsim 1\mathrm{TeV}$, small gaugino masses are not phenomenologically viable. In the presence of non-negligible gaugino masses, the requirements on the dimensionless ratios of soft mass as specified in (AII) are quite different from what is discussed in [212].

[2] In our convention, the quadratic Casimir invariants of a particle i in the fundamental representation of $SU(N)$ are $c_{i,N} = (N^2-1)/(2N)$. The Casimir invariant corresponding to the $U(1)_Y$ charge of the particle i is $c_{i,1} = 3/5 Y_i^2$ in the hypercharge normalization where the H_u has $Y = 1/2$.

In the following we introduce two MSSM models which fulfill conditions (AI) and (AII), and are almost as minimal as the mGMSB model. In fact, these models have the same set of fundamental continuous parameters determining the spectrum generated at $M_{\rm m}$, namely $\{a_i\} = \{\Lambda, \mu, b, M_{\rm m}\}$. For a quantitative analysis, we implement our models into `softsusy` [162]. The `softsusy` program calculates the resulting low scale MSSM spectrum from the high scale input, taking into account threshold and higher-loop effects. Conveniently, `softsusy` also provides an option to calculate the fine-tuning. We use this feature to explicitly show the reduction of fine-tuning in the exemplary models compared to models with mGMSB.

6.3.1 Model I: messengers in incomplete GUT multiplets

One simple modification of mGMSB that can satisfy both conditions (AI) and (AII) is to allow for multiple gauge messengers in incomplete GUT multiplets. Examples for such models can be found e.g. in [213]. Note that this implies giving up on (apparent) gauge unification.

In our setup, we allow arbitrary combinations of messengers fields Φ_i and $\bar{\Phi}_i$ with different gauge quantum numbers. However we will require that different Φ_i carry different gauge charges, or alternatively introduce new messenger quantum numbers such as an explicit *messenger parity* [214], to forbid mixing terms among the messengers. This ensures that the superpotential connecting the messengers and the SUSY breaking spurion X is diagonal:

$$\mathcal{W}_{\rm SB} = X \sum_i \lambda_i \Phi_i \bar{\Phi}_i. \tag{6.4}$$

Diagonality is a crucial requirement of models containing several gauge messengers, since otherwise hypercharge D-terms can large induce scalar mass contributions at the one-loop level that would lead to tachyonic superparticle masses. For our purpose a further important fact is that diagonality, together with the restriction to a single SUSY breaking spurion X, implies that the precise values of the couplings λ_i are irrelevant for the size of soft masses. This is easily verified by checking that these couplings cancel out in the ratio

$$\Lambda = \frac{\lambda_i F}{\lambda_i M}$$

which determines the size of the soft MSSM terms, c.f. Eq. (6.1) and Eq. (6.2). Hence, no new continuous parameter affecting the soft mass spectrum are introduced. [3]

With messengers in incomplete GUT multiplets, the soft masses depend on the Dynkin-invariants $n_{i,a}$ corresponding to the gauge quantum numbers of the messengers Φ_i. Defining

$$N_3 = \sum_i n_{i,3} \qquad N_2 = \sum_i n_{i,2} \qquad N_1 = \sum_i n_{i,1}, \tag{6.5}$$

[3] There is one caveat though: The spectrum does depend on the scale where the soft terms are generated and different λ_i in principle do translate into i different messenger scales $M_{{\rm m},i} = \lambda_i M$. However, since the dependence is only logarithmic, it is valid to work with just one common messenger scale $M_{\rm m}$ as long as the λ_i do not exhibit a rather extreme hierarchy.

Table 6.1: Potential messenger particles in simple $SU(5)$ multiplets, with their respective gauge quantum number and corresponding Dynkin-invariants.

SU(5)	$\mathrm{SU}(3)_C \otimes \mathrm{SU}(2)_L \otimes \mathrm{U}(1)_Y$	n_3	n_2	n_1
5	D=$(3,1)_{-1/3}$	1	0	2/5
	L=$(1,2)_{1/2}$	0	1	3/5
10	U=$(3,1)_{-2/3}$	1	0	8/5
	Q=$(3,2)_{1/6}$	2	3	1/5
	E=$(1,1)_1$	0	0	6/5
15	S=$(6,1)_{-2/3}$	5	0	16/5
	Q=$(3,2)_{1/6}$	2	3	1/5
	T=$(1,3)_1$	0	4	18/5
24	X=$(3,2)_{5/6}$	2	3	5
	V=$(1,3)_0$	0	2	0
	G=$(8,1)_0$	3	0	0

Table 6.2: Benchmark choices for models with a single SUSY breaking spurion X and gauge messengers in incomplete GUT multiplets that fulfill requirement (A) of SNC. The choice of gauge messengers corresponding to a triple $\{N_1, N_2, N_3\}$ is not necessarily unique.

Name	N_1	N_2	N_3	Messengers
model I (a)	1.4	5	2	Q,V,E
model I (b)	10.2	7	3	U,T,X
model I (c)	10.4	12	5	U, Q, T, X, V

the soft masses generated at the scale M_{m} read

$$\tilde{m}_i^2(M_{\mathrm{m}}) = 2\frac{\Lambda^2}{(4\pi)^2}\sum_{a=1}^{3} c_{ia} N_a \alpha_a^2(M_{\mathrm{m}}) \tag{6.6a}$$

$$M_a(M_{\mathrm{m}}) = \frac{\Lambda}{(4\pi)} N_a \alpha_a(M_{\mathrm{m}}) \tag{6.6b}$$

$$A_F(M_{\mathrm{m}}) = 0 \tag{6.6c}$$

We have listed possible messengers from simple $SU(5)$ multiplets and their respective Dynkin-invariants in Table 6.1. The discussed models with messengers in incomplete GUT multiplets are almost as simple as minimal gauge mediation. In fact, the mGMSB corresponds to the special case of $N_1 = N_2 = N_3 = 1$. The only additional degrees of freedom affecting the spectrum are the discrete parameters of N_1, N_2 and N_3.

Therefore, the first requirement (AI) that all the soft mass terms are given by a single scale Λ, is fulfilled. Specifically, the $\tilde{m}_{\mathrm{hu}}^2(Q)$ can be factored into Λ^2 and a function of dimensionless parameters f_{N_1,N_2,N_3}:

$$\tilde{m}_{\mathrm{hu}}^2(Q) = \frac{\Lambda^2}{(4\pi)^2} \cdot f_{N_1,N_2,N_3}[y_t, \alpha_a](\ln Q/M_{\mathrm{m}}), \tag{6.7}$$

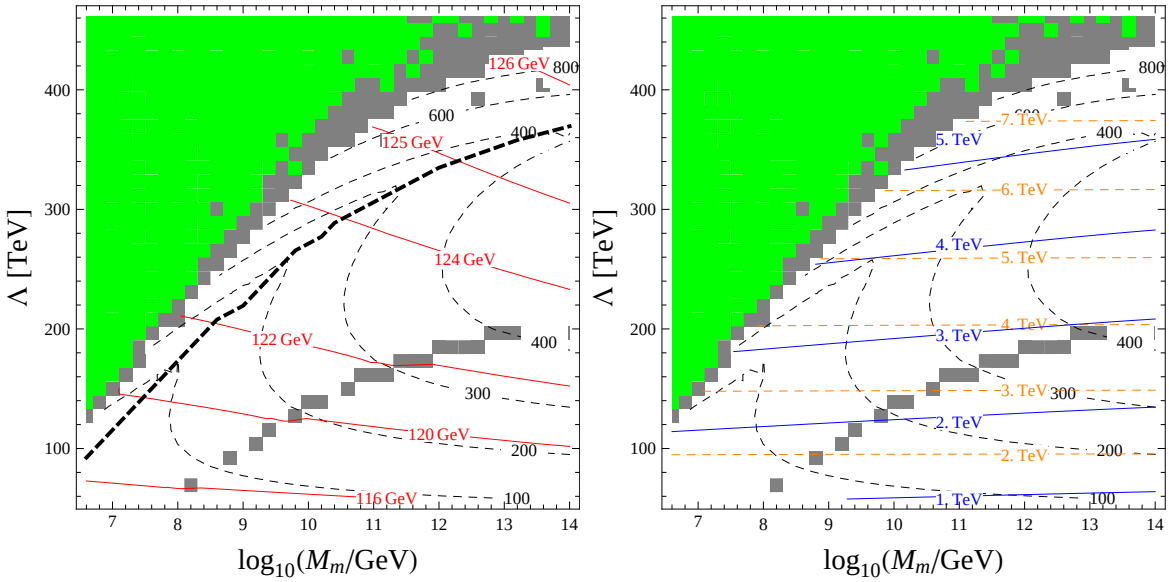

Figure 6.3: Contours in the $(M_{\rm m}, \Lambda)$-plane for fixed $\tan\beta = 30$ and negative $\mathrm{sgn}(\mu)$ to characterize the benchmark model I (b) with $\{N_1, N_2, N_3\} = \{10.2, 7, 3\}$. *Left:* Contours of m_h (red) and the fine-tuning $\max(|c_\mu|, |c_\Lambda|)$ (black-dashed). The thick black-dashed line connects points with optimal $M_{\rm m}$ (minimal fine-tuning) for a given Λ. *Right:* Contours of the lightest stop mass $m_{\tilde{t}_1}$ (blue), the gluino mass $m_{\tilde{g}}$ (orange-dashed) and the fine-tuning (black-dashed). The green shaded areas are excluded because electroweak symmetry is unbroken. The grey shaded areas cannot be evaluated because `softsusy` fails to converge.

where

$$f_{N_1,N_2,N_3}[y_t, \alpha_a](0) = 2\left(\frac{3}{4}N_2\alpha_2^2(M_{\rm m}) + \frac{3}{20}N_1\alpha_1^2(M_{\rm m})\right). \tag{6.8}$$

Condition (AII) is fulfilled if a triple $\{N_1, N_2, N_3\}$ can be found such that $\tilde{m}^2_{\rm hu}(Q_{\rm SUSY})$ is driven to zero in the RG running, i.e.

$$f_{N_1,N_2,N_3}[y_t, \alpha_a](\ln Q_{\rm SUSY}/M_{\rm m}) \simeq 0. \tag{6.9}$$

Obviously, there exist many different possible messenger combinations and corresponding triples $\{N_1, N_2, N_3\}$. In order to find combinations that lead to $\tilde{m}^2_{\rm hu}(Q_{\rm SUSY}) \simeq 0$, we identify the soft masses that contribute negatively ($\tilde{m}^2_{\rm q3}$, $\tilde{m}^2_{\rm u3}$, M_3^2) and positively ($\tilde{m}^2_{\rm hu}$, M_2^2, M_1^2) to the running of $\tilde{m}^2_{\rm hu}$.

With the help of (6.6), we can infer how different choices for N_1, N_2 and N_3 qualitatively affect f_{N_1,N_2,N_3}. Keep in mind that, because the messenger scale $M_{\rm m}$ is lower than $M_{\rm GUT}$, the gauge couplings obey the hierarchy $\alpha_3^2(M_{\rm m}) > \alpha_2^2(M_{\rm m}) > \alpha_1^2(M_{\rm m})$. The squark masses at the messenger scale are thus dominated by effects proportional to $N_3\alpha_3^2$. It becomes clear that increasing N_3 lowers $f_{N_1,N_2,N_3}(\ln Q_{\rm SUSY}/M_{\rm m})$, while increasing N_1 and N_2 has the opposite effect. The influence of N_1 is generally quite weak.

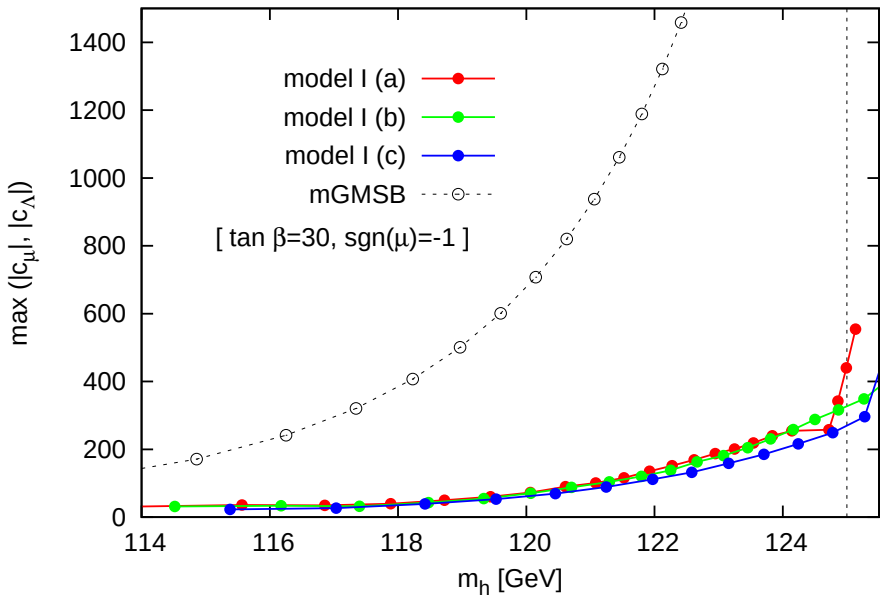

Figure 6.4: Contrasting fine-tuning as function of m_h in the mGMSB and the SNC models I (a)-(c) listed in Table 6.2 with messengers in incomplete GUT multiplets. For each input parameter value Λ, the value of $M_{\rm m}$ is optimized within a range of $M_{\rm m} \in [10^{6.5}, 10^{14}]\,\text{GeV}$ in order to minimize fine-tuning. Clearly, fine-tuning with respect to the fundamental parameters μ and Λ is reduced significantly in the models I (a)-(c) compared to mGMSB through SNC effects.

These rough arguments can be refined and made more quantitative by an analysis similar to the one performed in [212] (which however does not yet take into account the gaugino contributions).

Without going into a prolonged discussion of the details of assessing which messenger combinations reduce $f_{N_1,N_2,N_3}(\ln Q_{\rm SUSY}/Mm)$ most effectively, it is plausible that there is enough freedom in choosing N_1, N_2 and N_3 to find combinations that realize requirement (A) for stable near-criticality. In Table 6.2 we provide three examples of combinations of $\{N_1, N_2, N_3\}$ that exhibit SNC.

We have implemented these models into the `softsusy` software in order to calculate the resulting spectra in a reliable way. As announced before these models, defined by Eq. (6.6), have new discrete parameters N_1, N_2, N_3, but the same continous parameter space spanned by $\{a_i\} = \{\Lambda, \mu, b, M_{\rm m}\}$ as mGMSB. In the practical spectrum calculation, b is traded for $\tan\beta$ and $|\mu|$ is obtained by requiring $m_Z = 91.2\,\text{GeV}$. For each model and various choices of $\tan\beta$ and $\text{sgn}(\mu)$, we performed scans in the $(\Lambda, M_{\rm m})$-plane.

The fine-tuning is also calculated in `softsusy` following to the usual prescription defined in [193,195]. In this prescription, fine-tuning is calculated by first evaluating the coefficients

c_{a_i} and then taking the maximum of the absolute values:

$$c_{a_i} = \frac{\partial \ln m_Z^2}{\partial \ln a_i(M_{\rm m})} \qquad \text{for } \{a_i\} = \{\Lambda, \mu, b, M_{\rm m}\}$$
$$\Delta \equiv \max(|c_{a_i}|) \tag{6.10}$$

For any given value of Δ, the model under consideration is then said to be fine-tuned to a degree of 1:Δ.

In practice, the absolute values of the fine-tuning coefficients c_Λ and c_μ exceed those of c_B, $c_{M_{\rm m}}$ by far.

In Fig. 6.3, we show the results of the `softsusy` scan for model I (b), with $\tan\beta = 30$ and negative $\mathrm{sgn}(\mu)$. Observe that $m_h \sim 125\,\mathrm{GeV}$ is compatible with fine-tuning of less than $\Delta = \max(|c_\mu|, |c_\Lambda|) < 400$. In the right panel of Fig. 6.3, the contours of the lighter stop mass $m_{\tilde{t}_1}$ and the gluino mass $m_{\tilde{g}}$ for the same scan are shown. We again display the contours of fine-tuning, so as to show that stop masses of up to $m_{\tilde{t}_1} \sim 5\,\mathrm{TeV}$ can be compatible with fine-tuning of $\Delta < 400$ which is an excellently low value given the general sitatuon of naturalness in supersymmetry.

To illustrate the reduction of fine-tuning in the models I (a)-(c) as compared to mGMSB, in Fig. 6.4 we show for each model a function minimal fine-tuning versus m_h mass for m_h ranging from the LEP bound of $m_h > 114.4\,\mathrm{GeV}$ up to the actual Higgs mass value of $m_h \sim 125\,\mathrm{GeV}$. In determining the fine-tuning values depicted in Fig. 6.4, we optimized $M_{\rm m}$ for each input parameter value Λ within a range $M_{\rm m} \in [10^{6.5}, 10^{14}]\,\mathrm{GeV}$. This corresponds to moving across the $(\Lambda, M_{\rm m})$-plane along the line of minimal fine-tuning for each given Λ. For the example of model I (b), this line is shown (thick black-dashed) in Fig. 6.3. The models I (a)-(c) exhibit significantly reduced fine-tuning as compared to the mGMSB.

While successfully reducing fine-tuning, these simple models with messengers in incomplete GUT multiplets do not exhibit gauge coupling unification since by definition $N_1 = N_2 = N_3$ is not satisfied. While it is always possible to force the gauge couplings to unify by adding so-called unifons (new particles that serve the sole purpose of changing the RGE evolution of the gauge couplings), this appears to be a very artificial approach to preserve unification.

6.3.2 Model II: SUSY breaking spurion in the adjoint representation

We introduce another model that displays SNC and in addition explicitly preserves unification. In this setup, inspired by a model introduced in the appendix of [215], the SUSY breaking spurion X is chosen to be the $SU(3) \times SU(2)_L \times SU(1)_Y$ singlet component of the SU(5) adjoint rather than a $SU(5)$ singlet. SUSY breaking does not lead to breaking of the SM gauge group if only the singlet component of the **24** adjoint representation acquires a SUSY-breaking VEV. For models with X in other non-trivial representations of $SU(5)$, see e.g. [216]. The messengers are assumed to form a complete $\mathbf{5} + \bar{\mathbf{5}} = L, D, \bar{L}, \bar{D}$ multiplets. The superpotential giving rise to SUSY-breaking is

$$\mathcal{W}_{\rm SB} = X[\lambda_L L\bar{L} + \lambda_D D\bar{D}] + \lambda_s S[L\bar{L} + D\bar{D}]. \tag{6.11}$$

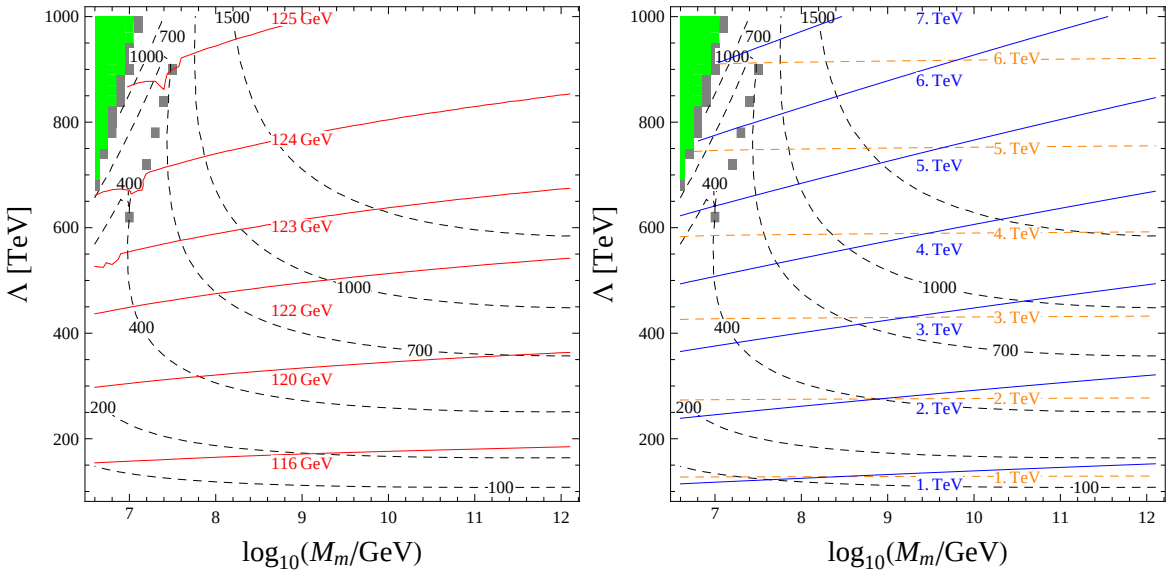

Figure 6.5: Contours in the $(M_{\rm m}, \Lambda)$-plane for fixed $\tan\beta = 30$ and $\mathrm{sgn}(\mu) = -1$ to characterize the model II. *Left:* Contours of m_h (red) and the fine-tuning $\max(|c_\mu|, |c_\Lambda|)$ (black-dashed). *Right:* Contours of the lightest stop mass $m_{\tilde{t}_1}$ (blue), the gluino mass $m_{\tilde{g}}$ (orange-dashed) and the fine-tuning (black-dashed). The green shaded areas are excluded because electroweak symmetry is unbroken. The grey shaded areas cannot be evaluated because `softsusy` does not converge.

The Yukawa couplings of the messengers to X are $SU(5)$-invariant, but not $SU(5)$ singlets. Instead, $SU(5)$ invariance requires $3\lambda_D = -2\lambda_L$.

While model I with messengers in incomplete $SU(5)$ multiplets relied on the fact that SUSY breaking and messenger mass originated from the $\theta\theta$ and scalar component VEV of a single spurion X, in this model we assume that the messengers obtain their dominant mass contribution from a singlet spurion field S that acquires a scalar VEV $\langle S\rangle$ but does not break supersymmetry.

The soft masses generated at the messenger scale $M_{\rm m} = \lambda_s\langle S\rangle$ in this setup are:

$$\tilde{m}_i^2(M_{\rm m}) = 2\frac{\Lambda^2}{(4\pi)^2}\left[c_{i3}\,\alpha_3^2(M_{\rm m}) + \frac{9}{4}c_{i,2}\,\alpha_2^2(M_{\rm m}) + \frac{7}{4}c_{i1}\,\alpha_1^2(M_{\rm m})\right] \tag{6.12a}$$

$$M_3(M_{\rm m}) = \frac{\Lambda}{4\pi}\alpha_3(M_{\rm m}) \tag{6.12b}$$

$$|M_2(M_{\rm m})| = \frac{3}{2}\frac{\Lambda}{4\pi}\alpha_2(M_{\rm m}) \tag{6.12c}$$

$$|M_1(M_{\rm m})| = \frac{1}{2}\frac{\Lambda}{4\pi}\alpha_1(M_{\rm m}) \tag{6.12d}$$

$$A_F(M_{\rm m}) = 0 \tag{6.12e}$$

Here we defined $\Lambda = \frac{\lambda_D F_x}{\lambda_s\langle S\rangle}$. Again, $c_{i,a}$ are the quadratic Casimir invariants corresponding to the gauge representations of the particles i. Note that the spectrum generated in this

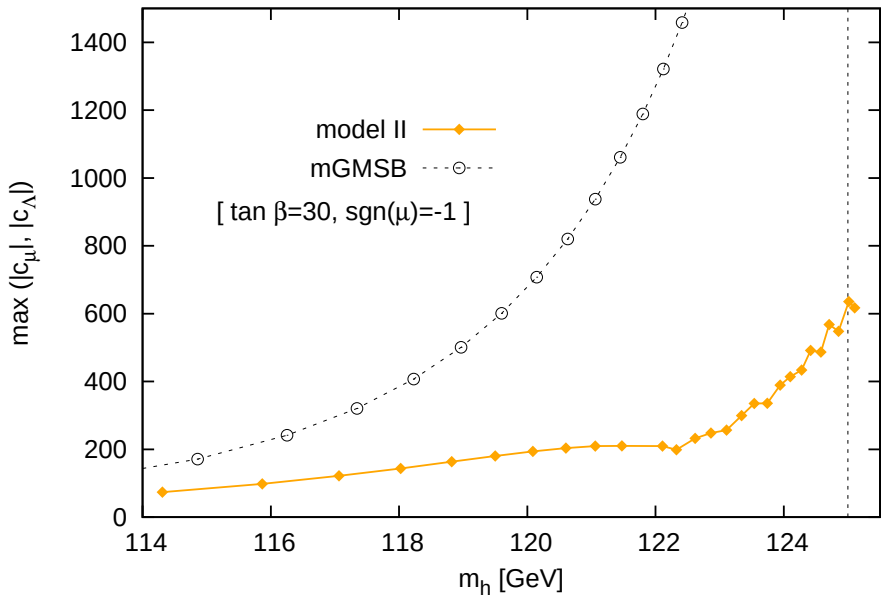

Figure 6.6: Contrasting fine-tuning as a function of m_h in the mGMSB with SNC model II. For each input parameter value Λ, the value of $M_{\rm m}$ is optimized within a range of $M_{\rm m} \in [10^{6.5}, 10^{14}]$ GeV to minimize fine-tuning. Clearly, fine-tuning with respect to the fundamental parameters μ and Λ is reduced significantly by SNC effects as compared to the mGMSB.

model depends on the same fundamental parameters as the mGMSB.

This model clearly satisfies condition (AI), and since the ratios among the individual soft masses are modified as compared to mGMSB, it can potentially also satisfy condition (AII). To numerically check whether condition (AII) is in fact fulfilled, we again perform scans over the input $(M_{\rm m}, \Lambda)$-plane using the program `softsusy`.

In Fig. 6.5, we show the results of one exemplary scan for which we set chose $\tan\beta = 30$ and $\mathrm{sgn}(\mu) = -1$. Observe that the Higgs mass value of $m_h \sim 125\,\mathrm{GeV}$ is compatible with fine-tuning of $\Delta = \max(|c_\mu|, |c_\Lambda|) < 700$. In the right panel of Fig. 6.5, the contours of the lighter stop mass $m_{\tilde{t}_1}$ and the gluino mass $m_{\tilde{g}}$ for the same scan are shown. We again display the contours of fine-tuning, and find that stop masses of up to $m_{\tilde{t}_1} \sim 5\,\mathrm{TeV}$ can be compatible with fine-tuning of less than 1:700.

To directly show the reduction of fine-tuning in model II as compared to mGMSB, in Fig. 6.6 we show the line of minimal fine-tuning versus the Higgs mass m_h. Again, the points shown correspond to moving across the $(\Lambda, M_{\rm m})$-plane along the line of minimal fine-tuning for each given Λ. The fine-tuning is reduced significantly as compared to the mGMSB, although slightly less so than in the models I (a)-(c) with messengers in incomplete GUT multiplets which were shown in Fig. 6.4.

6.4 Stabilizing near-criticality with respect to gauge and Yukawa couplings

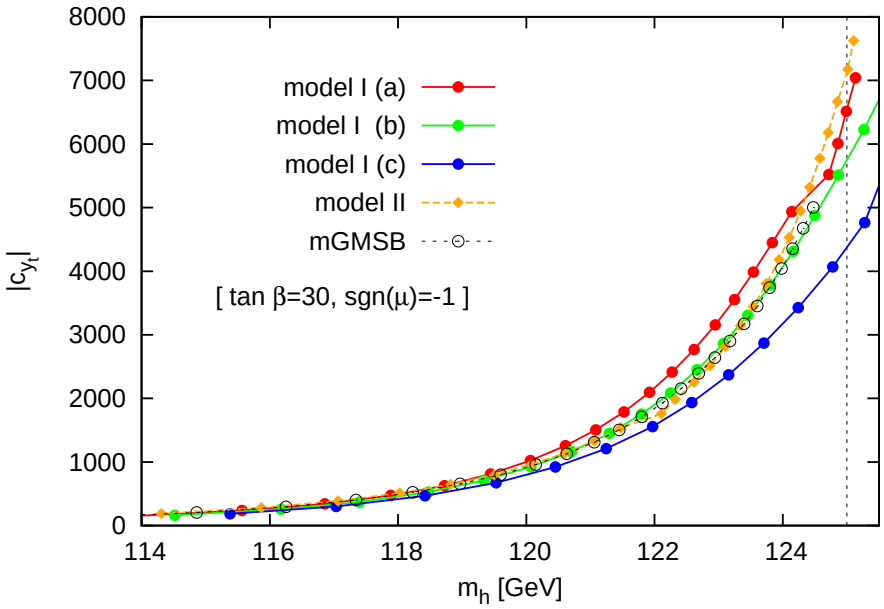

Figure 6.7: Fine-tuning with respect to the top Yukawa coupling, characterized by the fine-tuning coefficients c_{y_t} for the models I (a), (b), (c), model II and the mGMSB for comparison. The points lie on the respective lines of minimal $\max(|c_\mu|, |c_\Lambda|)$ fine-tuning in the $(\Lambda, M_{\rm m})$-plane.

So far, we have not considered fine-tuning with respect to to the dimensionless couplings. These are almost never taken into account throughout the literature on fine-tuning in SUSY models. This omission appears to be based on the implicit assumption that these effects are subleading or at most comparable to the other fine-tuning coefficients, but is not justified by any physical principle.

In fact, by arguing that fine-tuning with respect to the top Yukawa coupling ought to be considered in a complete analysis, the authors of [196] dispute the validity of the central claim of the *Focus Point* literature [194, 208–210, 212], namely that heavy stops can be natural. By that same argument the naturalness of the SNC models I and II is doubtful at best, unless we show that large fine-tuning coefficients with respect to y_t can be avoided. Hence it is imperative to demonstrate that this problem can be solved.

To assess the severity of this issue, we modify `softsusy` to automatically determine the fine-tuning coefficients c_{g_3} and c_{y_t}. We define these coefficients, in analogy to the other fine-tuning coefficients Eq. (6.10), as

$$c_{g_a} \equiv \frac{\partial \ln m_Z^2}{\partial \ln g_a(M_{\rm m})} \qquad\qquad c_{y_t} \equiv \frac{\partial \ln m_Z^2}{\partial \ln y_t(M_{\rm m})}. \tag{6.13}$$

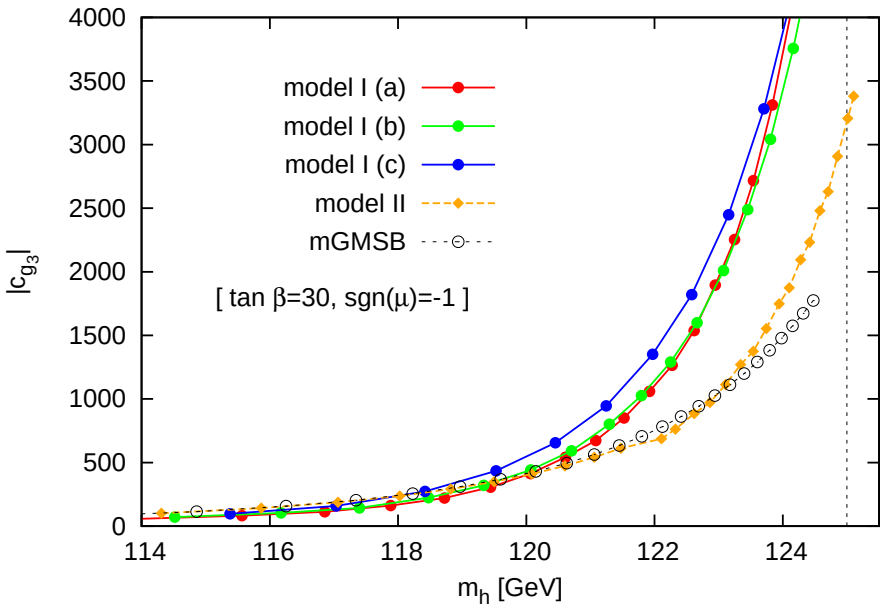

Figure 6.8: Fine-tuning with respect to g_3, characterized by the fine-tuning coefficients c_{g_3} for the models I (a), (b), (c), model II and the mGMSB for comparison. The points lie on the respective lines of minimal $\max(|c_\mu|, |c_\Lambda|)$ fine-tuning in the $(\Lambda, M_{\rm m})$-plane.

In Fig. 6.7, a plot of c_{y_t} for the SNC models I (a)-(c) and model II is shown. The selected points are the same as those in Fig. 6.4 and Fig. 6.6, i.e. lie on line of minimal $\Delta = \max(|c_\mu|, |c_\Lambda|)$ fine-tuning in the $(\Lambda, M_{\rm m})$-plane. While c_μ and c_Λ are reduced significantly in the SNC models as compared to mGMSB, the fine-tuning coefficient c_{y_t} is large, of order $\mathcal{O}(1000)$, and of comparable size in all models including the mGMSB.

In Fig. 6.8, we present the c_{g_3} dependence. The g_3 sensitivity is also unacceptably large, and even stronger in the SNC models than in the mGMSB. This is in particular true for the SNC models of type I, where effects proportional to $\alpha_3 M_3^2$ contribute strongly to the cancellation in the running of $\tilde{m}^2_{\rm hu}$. We also quantified the fine-tuning coefficients c_{g_2} and c_{g_1}, but found them to be orders of magnitude smaller than c_{g_3} and hence not of immediate concern.

Considering the size of the fine-tuning coefficients c_{g_3} and c_{y_t} it is clear that without a mechanism to suppress these fine-tunings, the SNC models do not offer a convincing solution to the problematic issues of SUSY fine-tuning.

Having assessed the impact of the problem, we want to pause to elaborate on the discussion of why the fine-tuning evaluation should include c_{g_3} and c_{y_t} at all.

One argument given against considering the fine-tuning with respect to the gauge and Yukawa couplings is that, since the objective is to quantify naturalness of the supersymmetric solution to the hierarchy problem, only the parameters connected to SUSY breaking should be included into the naturalness solution [209]. In our opinion, however, it is more

appropriate to think of the naturalness of the MSSM lagrangian in its entirety, instead of categorizing different types of fine-tuning and addressing only some but not others. Another argument is that y_t can be fixed by a separate new flavor sector [194] and its analysis should be put on hold in the hope that this theory of flavor flat-out predicts the correct value of the top Yukawa coupling. However even if this were to be the case, the problem with fine-tuning with respect to g_3 would still remain.

If the fine-tuning coefficients c_{g_3} and c_{y_t} are to be included in the fine-tuning evaluation, what are mechanisms that could dampen their impact?

Until now, we have taken the messenger scale $M_{\rm m}$ to play the rôle of the fundamental scale M_* where all the parameters of the model are defined. However, this does not necessarily need to be the appropriate fundamental scale for the dimensionless couplings. There could be a more fundamental scale above $M_{\rm m}$. The obvious candidate for such a more fundamental scale is the gauge coupling unification scale $M_{\rm GUT}$. It appears to be more appropriate to quantify fine-tuning by determining the sensitivity coefficients with respect to the input parameters at the GUT scale $M_{\rm GUT}$ rather than at the messenger scale $M_{\rm m}$.

Effectively, this means that the fine-tuning coefficients c_{a_i} as defined in Eq. (6.13) have to be replaced by coefficients $\tilde{c}_{a_i}$ defined as

$$\begin{aligned}\tilde{c}_{a_i} &= \frac{\partial \ln m_z^2}{\partial \ln a_i(M_{\rm GUT})} = \sum_j \frac{\partial \ln m_z^2}{\partial \ln a_j(M_{\rm m})} \underbrace{\frac{\partial \ln a_j(M_{\rm m})}{\partial \ln a_i(M_{\rm GUT})}}_{\equiv r_{[j,i]}} \\ &= \sum_j c_{a_j} \cdot r_{[j,i]} \end{aligned} \tag{6.14}$$

where a_i are the fundamental parameters of the model including gauge and Yukawa couplings, and the reweighting factors $r_{[j,i]}$ provide the mapping between the fine-tuning coefficients c_{a_i} and $\tilde{c}_{a_i}$, defined at the messenger scale $M_{\rm m}$ and the GUT scale $M_{\rm GUT}$, respectively.

Specifically, just considering the leading 1-loop level relations among the gauge and Yukawa couplings, expressions Eq. (6.14) imply

$$\tilde{c}_{g_U} = c_{g_3} \cdot r_{[g_3,g_U]} + c_{g_2} \cdot r_{[g_2,g_U]} + c_{g_2} \cdot r_{[g_2,g_u]} + c_{y_t} \cdot r_{[y_t,g_U]} \tag{6.15}$$

$$\tilde{c}_{y_t} = c_{y_t} \cdot r_{[y_t,y_t]} \tag{6.16}$$

where g_U is the unified coupling at the GUT scale

$$g_U \equiv g_3(M_{\rm GUT}) = g_2(M_{\rm GUT}) = g_1(M_{\rm GUT}).$$

If the relevant reweighting factors $r_{[i,j]}$ are small, the coefficients $\tilde{c}_{y_t}$ and $\tilde{c}_{g_U}$ can be significantly lower than the coefficients c_{y_t} and c_{g_3} shown in Fig. 6.7 and Fig. 6.8. We spend the next two subsections discussing how the running of the gauge and Yukawa couplings between $M_{\rm m}$ and $M_{\rm GUT}$ gives rise to these small reweighting factors.

Of course, changing from the c_{a_i} basis into the $\tilde{c}_{a_i}$ basis is only justified if the underlying model is explicitly compatible with grand unification. This means, our approach is applicable to model II, but not to the models I (a)-(c).

6.4.1 Achieving small reweighting factors $r_{[g_a,g_U]}$

In gauge mediated SUSY breaking, the messenger particles modify the RGE running above the messenger threshold $M_{\rm m}$. If the messengers form complete SU(5) multiplets with universal quadratic Casimir invariants $N_1 = N_2 = N_3 = N$ as in model II, then the running of all three gauge couplings is modified uniformly and unification still takes places at $M_{\rm GUT}$. The unified coupling $\alpha_{U,N}$ larger than the usual MSSM unified coupling $\alpha_U \equiv \alpha_{U,0} \simeq 1/24$ due to the presence of the messenger fields above $M_{\rm m}$. At 1-loop level $\alpha_{U,N}$ is given by

$$\alpha_{U,N}^{-1} = \alpha_{U,0}^{-1} - \frac{N}{2\pi} \ln\left(\frac{M_{\rm GUT}}{M_{\rm m}}\right). \tag{6.17}$$

The relation between the gauge couplings $\alpha_a(M_{\rm m})$ at the messenger scale and $\alpha_{U,N}$ is

$$\alpha_a^{-1}(M_{\rm m}) = \alpha_{U,N}^{-1} + \frac{b_a + N}{2\pi} \ln\left(\frac{M_{\rm GUT}}{M_{\rm m}}\right). \tag{6.18}$$

From that relation, we obtain

$$r_{[g_a,g_U]} \equiv \frac{\partial \ln g_a(M_{\rm m})}{\partial \ln g_a(M_{\rm GUT})} = \frac{\alpha_a(M_{\rm m})}{\alpha_{U,N}} \tag{6.19}$$

Small values of $r_{[g_a,g_U]}$ are obtained if the unified coupling $\alpha_{U,N}$ is larger than $\alpha_a(M_{\rm m})$. This can always be arranged by adding more particles in complete $SU(5)$ multiplets at the messenger scale. Concretely, we extend the superpotential of model II, given by (6.11), to

$$\mathcal{W}_{\rm SB} = X[\lambda_L L\bar{L} + \lambda_D D\bar{D}] + \lambda_s S[L\bar{L} + D\bar{D}] + S\sum_k^{N_k} \lambda_k^\rho \rho_k \bar{\rho}_k \tag{6.20}$$

Because the new fields ρ_k do not couple to the SUSY breaking spurion X, they do not act as messengers and do not contribute to the soft masses given by (6.12a). If the ρ_k particles form complete SU(5) multiplets, unification is preserved. Consider for example ρ_k being in the fundamental **5** representation,

$$\rho_k = (\rho_k^L, \rho_k^D) \qquad \text{with} \quad \rho_k^L \sim (1,2)_{1/2} \text{ and } \rho_k^D \sim (3,1)_{-1/3}\,. \tag{6.21}$$

Then the N_k generations of new particles ρ_k, $\bar{\rho}_k$ contribute to the running of the gauge couplings according to Eq. (6.17), where N is the sum of N_k and the messenger contribution $N_m = 1$.

The unified coupling strength $\alpha_{U,N}$ (with $N = N_k + N_m$) can thus be increased at will by raising N_k, and therefore the reweighting coefficients $r_{[g_a,g_U]}$ can be made small according to Eq. (6.19).

The only limitation on the maximally achievable suppression of the reweighting factors stems from the requirement to ensure perturbativity up to $M_{\rm GUT}$. Namely $\alpha_{U,N}$ should not exceed $\alpha_{U,N} \leq 1$. According to Eq. (6.19), this translates into a lower bound on $r_{[g_3,g_U]}$ given by the value of $\alpha_3(M_{\rm m})$ itself. This bound is not so strong as to prevent sufficient suppression of c_{g_3} however. Even for messenger scales as low as $M_{\rm m} = 10^6\,\text{GeV}$, the lower bound is smaller than $\simeq 0.075$ and thus leaves enough room for sufficiently small $r_{[g_3,g_U]}$.

6.4.2 Achieving small reweighting factors $r_{[y_t,i]}$

A similar approach can be used to generate small reweighting factors $r_{[y_t,i]}$ where i is a placeholder for the couplings y_t, g_U as well as any new Yukawa couplings contributing to the RGE evolution of y_t above the messenger scale $M_{\rm m}$. In analogy to the way we achieve small reweighting factors $r_{[g_3,g_U]}$, the factors $r_{[y_t,j]}$ such as for example

$$r_{[y_t,y_t]} = \frac{\partial \ln(M_{\rm m})}{\partial \ln y_t(M_{\rm GUT})}$$

can be suppressed by altering running of y_t above $M_{\rm m}$. For that purpose, we can use the same additional fields ρ_k, $\bar{\rho}_k$ introduced previously to modify the gauge coupling running.

Any Yukawa coupling involving the new fields ρ_k, $\bar{\rho}_k$ and at least one of the MSSM fields h_u, q or u^c will affect the RG evolution of y_t.

If we choose for example ρ_k to be in the fundamental representation of $SU(5)$, c.f. Eq. (6.21), the following Yukawa terms can be added to the superpotential (6.20) of the extended model II:

$$y_k^A \rho_k^D u^c e^c \qquad y_k^B \bar{\rho}_k^D h_d q \qquad y_k^C \rho_k^L q u^c \qquad y_k^D \bar{\rho}_k^L q d^c \qquad y_k^E \bar{\rho}_k^L l e^c \tag{6.22}$$

Any of these new Yukawa couplings y_k^i with $i = \{A, B, C, D, E\}$ contributes positively to the β-function of y_t and vice versa. This is encouraging since we already found that raising the value of $g_a(M_{\rm m})$ leads to small $r_{[g_a,g_U]}$. We might hope that raising the value of $y_t(M_{\rm GUT})$ similarly leads to reduced reweighting factors $r_{[y_t,j]}$. The fact that we have new, otherwise unconstrained couplings at our disposal can only be helpful for this task.

At this point, we want to emphasize that none of the new Yukawa couplings in Eq. (6.22) affect the MSSM spectrum below $M_{\rm m}$. Hence, the new fine-tuning coefficients $\tilde{c}_{y_k^i}$ corresponding to these additional Yukawa couplings stem from the influence of y_k^i on the value of $y_t(M_{\rm m})$ and are proportional to c_{y_t}:

$$\tilde{c}_{y_k^i} = c_{y_t} r_{[y_t,y_k^i]} \tag{6.23}$$

The coupled β-functions describing the RG evolution of the Yukawa couplings are too complicated to be solved and analyzed on in a closed form, but can easily be implemented and solved numerically, provided the values of $y_t(M_{\rm m})$ and $g_a(M_{\rm m})$ as boundary condition. We will discuss a specific example in Sec. 6.6, and we will explicitly demonstrate that $r_{[y_t,y_t]}$, $r_{[y_t,g_U]}$ and $r_{[y_t,y_k^A]}$ can easily be smaller than 0.1, sufficient to suppress the fine-tuning coefficients $\tilde{c}_{g_U}$, $\tilde{c}_{y_t}$ and $\tilde{c}_{y_k^i}$ (compare to Eqs. (6.15), (6.16) and (6.23)).

6.5 A Solution to the μ-$B\mu$ Problem in gauge mediation compatible with SNC

Now we introduce a final aspect which is relevant to building a fully valid model of SNC.

So far, we have only emphasized the advantages of adopting gauge mediation instead of gravity mediation for building models with reduced fine-tuning via the SNC principle. Besides the customary motivation that gauge mediation explains why SUSY breaking does not

lead to flavor violation beyond the amount that is already contained within the SM Yukawa couplings, in the context of SNC there are additional useful properties of gauge mediation. In particular, gauge mediation predicts strongly correlated soft terms and simple models exist that plausibly relate all soft masses to one single scale Λ. Further, gauge mediation not only allows for unification, thus justifying substituting $M_{\rm m}$ but $M_{\rm GUT}$ as fundamental input scale for the dimensionless couplings, but also offers enough room between $M_{\rm GUT}$ and $M_{\rm m}$ to mitigate the sensitivity to gauge couplings g_a and the top Yukawa coupling y_t.

Gauge mediated models of supersymmetry however face difficulties to generate appropriate values for the higgsino mass μ and the Higgs mass mixing term called b which is also interchangeably denoted by $B\mu$. To be more specific, while $B\mu \sim \mu^2$ is required for a viable MSSM Higgs sector, in models of gauge mediation typically a B term is generated which is two orders of magnitude too large [151]. This issue is widely known as the μ-$B\mu$ problem of gauge mediation. Without a mechanism to generate a suitable μ and $B\mu$ terms, no model of gauge mediated SUSY breaking can be considered complete.

The issue becomes particularly pressing in the context of SNC: Since we rely on robust correlations among the soft terms at the input scale, we require a mechanism that not only generates suitable μ and $B\mu$ terms, but also does not generate new contributions to $\tilde{m}^2_{\rm hu}$ that could potentially alter these correlations.

Therefore, we want to demonstrate explicitly that at least one solution the to μ-$B\mu$ problem compatible with SNC correlations exists. The mechanism we will use to generate appropriate μ and $B\mu$ terms solution has been introduced in [217] and will be discussed shortly in the remainder of this section.

In [217], the following superpotential is introduced:

$$\mathcal{W}_{\rm SB} = N\left(\lambda h_u h_d + \frac{\lambda_1}{2}S^2 - M_S^2\right) + \xi S\bar{\Phi}_1\Phi_2 + X(\bar{\Phi}_1\Phi_1 + \bar{\Phi}_2\Phi_2) \tag{6.24}$$

Supersymmetry breaking originates as usual from a SUSY breaking spurion $X \to \langle X\rangle = M_{\rm m}(1+\theta\theta\Lambda)$. This superpotential has the most general form compatible with the following symmetry assignments

	X	Φ_1	$\bar{\Phi}_1$	Φ_2	$\bar{\Phi}_2$	N	S
$U(1)_X$ symmetry	1	1	0	0	-1	0	0
R symmetry	0	1	1	1	1	2	0
$\mathbb{Z}_2$ parity	+	-	-	+	+	+	-

(6.25)

Imposing the $\mathbb{Z}_2$ symmetry is optional: it only serves to forbid bilinear terms NS and $\bar{\Phi}_1\Phi_2$, which are inconsequential for the mechanism. Since $h_u h_d$ does not carry R-charge, a bare superpotential μ-term is forbidden. In the Kähler potential, the appearance of $h_u h_d$ is not constrained and thus μ will be generated once supersymmetry is broken. Using the technique of *analytic continuation into superspace* [218, 219], the scalar potential obtained after integrating out the messengers is calculated. The interaction $\xi S\bar{\Phi}_1\Phi_2$ leads to a potential for S below the messenger scale that reads:

$$V_{\rm soft} = \tilde{m}_S^2|S|^2 + (A_S\lambda_1 NS^2 + h.c) \tag{6.26}$$

$$\tag{6.27}$$

with the the soft terms

$$\tilde{m}_S^2(M_{\rm m}) = \frac{\Lambda^2}{(4\pi)^2}\alpha_\xi(M_{\rm m})\left(35\alpha_\xi(M_{\rm m}) - 16\alpha_3(M_{\rm m}) - 6\alpha_2(M_{\rm m}) - 2\alpha_1(M_{\rm m})\right) \tag{6.28}$$

$$A_s(M_{\rm m}) = -5\frac{\Lambda}{4\pi}\alpha_x i(M_{\rm m}) \tag{6.29}$$

In the above expressions we used $\alpha_\xi = \xi^2/(4\pi)$. This potential leads to vacuum expectation values for N and S. The dynamic N and S fields then obtain masses of the order of $\langle S\rangle \sim M_S/\lambda_1$, which can easily be of the order of the messenger scale. Hence, this model has precisely the MSSM particle spectrum below $M_{\rm m}$. The μ and $B\mu$ terms are obtained from the scalar and F-term component of the VEV of N. In terms of the lagrangian parameters, the μ and B terms generated at the scale $M_{\rm m}$ read:

$$\mu(M_{\rm m}) = -\frac{\lambda}{\lambda_1}A_S^\dagger = \frac{5\lambda\alpha_\xi(M_{\rm m})}{\lambda_1}\left(\frac{\Lambda^\dagger}{4\pi}\right) \tag{6.30}$$

$$B(M_{\rm m}) = \frac{\tilde{m}_S^2 - |A_S|^2}{A_S^\dagger} = \left(\frac{\Lambda}{4\pi}\right)\left(\frac{16}{5}\alpha_3(M_{\rm m}) + \frac{6}{5}\alpha_2(M_{\rm m}) + \frac{2}{5}\alpha_1(M_{\rm m}) - 2\alpha_\xi(M_{\rm m})\right) \tag{6.31}$$

This mechanism presented in [217] does not lead to any new contributions to $\tilde{m}_{\rm hu}^2$, $\tilde{m}_{\rm hd}^2$ or to A-terms. This is a feature crucial for SNC models as it ensures that the solution to the μ-$B\mu$ problem is not in conflict with requirement (A) for SNC as specified in Sec. 6.3.

6.6 Proof of principle: A complete MSSM model with stable near-criticality

Now we are ready to describe one exemplary complete model implementation that combines all the features necessary for a successful SNC model discussed so far: fine-tuning with respect to the soft SUSY-breaking parameters can be reduced via SNC correlations as described in Sec. 6.3. Moreover, to avoid excessive fine-tuning with respect to the Yukawa and gauge couplings, we invoke the GUT scale as fundamental scale for the gauge and Yukawa couplings and modify the RG evolution of the SM couplings between $M_{\rm m}$ and $M_{\rm GUT}$ as described in Sec. 6.4. Finally a convincing mechanism, similar to the one presented in the previous section Sec. 6.5, for generating μ and $B\mu$ terms while not altering the SNC features will be embedded in the model.

6.6.1 Superpotential

We specify the superpotential of our complete model of SNC as

$$\begin{aligned}\mathcal{W}_{\rm SB} =& X[\lambda_L(L_1\bar{L}_1 + L_2\bar{L}_2) + \lambda_D(D_1\bar{D}_1 + D_2\bar{D}_2)] + \lambda_s S_M[(L_1\bar{L}_1 + L_2\bar{L}_2 + D_1\bar{D}_1 + D_2\bar{D}_2)] \\ &+ N(\lambda h_u h_d + \frac{\lambda_1}{2}S^2 - M_S^2) + \xi_L S\bar{L}_1 L_2 + \xi_D S\bar{D}_1 D_2 \\ &+ \sum_k^{N_k}\lambda_{\rho,k}S_{M\rho}[(\rho_k^L\bar{\rho}_k^L + \rho_k^D\bar{\rho}_k^D] + y_k\bar{\rho}_k^D h_d q\end{aligned} \tag{6.32}$$

Eq. (6.32) is the most general superpotential consistent with a simultaneous exchange symmetry

$$\begin{aligned} L_1 &\leftrightarrow \bar{L}_2 \quad \text{and } L_2 \leftrightarrow \bar{L}_1 \\ D_1 &\leftrightarrow \bar{D}_2 \quad \text{and } D_2 \leftrightarrow \bar{D}_1 \end{aligned} \tag{6.33}$$

as well as an assignment of $U(1)_X$, R and optionally $\mathbb{Z}_2$ charges similar to those in (6.25):

	X	S_M	$\begin{pmatrix} L_1 \\ D_1 \end{pmatrix}$	$\begin{pmatrix} \bar{L}_1 \\ \bar{D}_1 \end{pmatrix}$	$\begin{pmatrix} L_2 \\ D_2 \end{pmatrix}$	$\begin{pmatrix} \bar{L}_2 \\ \bar{D}_2 \end{pmatrix}$	N	S	$S_{M\rho}$	$\begin{pmatrix} \rho_k^L \\ \rho_k^D \end{pmatrix}$	$\begin{pmatrix} \bar{\rho}_k^L \\ \bar{\rho}_k^D \end{pmatrix}$
$U(1)_X$	1	1	-1	0	0	-1	0	0	-1	1	0
R	0	0	1	1	1	1	2	0	0	1	1
$\mathbb{Z}_2$	+	+	-	-	+	+	+	-	+	+	+

(6.34)

X, S_M and $S_{m\rho}$ are spurion fields. $X \to \theta\theta F$ breaks supersymmetry, while $\langle S_M \rangle$ and $\langle S_{M\rho} \rangle$ provide mass terms for the messengers $L_{1,2}$, $\bar{L}_{1,2}$, $D_{1,2}$, and $\bar{D}_{1,2}$ and the additional fields ρ_k, respectively. The ρ_k fields are in the fundamental representation **5** of $SU(5)$, c.f. Eq. (6.21). $SU(5)$ is broken only by the Yukawa interactions ξ_L, ξ_D and y_ρ, and hence the approximate gauge unification of the MSSM is preserved.

Since an explicit R symmetry is introduced to justify the form of the superpotential (6.32), this same R symmetry can be used to forbid dangerous MSSM interactions, such as lle^c or $u^c d^c d^c$, that violate baryon or lepton number. These terms are usually forbidden by imposing an R-parity. Assigning R-charge = 1 to the MSSM superfields q, u^c, d^c, l, e^c and R-charge = 0 to h_u and h_d fulfills the same purpose. With these assignments, no new Yukawa couplings other than the interaction $y_k \bar{\rho}_k^D h_d q$ are allowed.

The first line of the superpotential (6.32) is a generalization of the superpotential (6.11) of model II to contain two messengers. Again, we assume X to be the singlet of the adjoint representation **24** of $SU(5)$ and hence $\lambda_L = -3/2\lambda_D$. Defining $M_{\rm m} = \lambda_S \langle S_M \rangle$ and $\Lambda = \lambda_D F / M_{\rm m}$, the following soft masses, very similar to the terms in model II defined in Sec. 6.3.2, are generated at the messenger scale:

$$\tilde{m}_i^2(M_{\rm m}) = 4\frac{\Lambda^2}{(4\pi)^2}\left[c_3^i \alpha_3^2(M_{\rm m}) + \frac{9}{4} c_2^i \alpha_2^2(M_{\rm m}) + \frac{7}{4} c_1^i \alpha_1^2(M_{\rm m})\right] \tag{6.35a}$$

$$M_3(M_{\rm m}) = 2\frac{\Lambda}{4\pi}\alpha_3(M_{\rm m}) \tag{6.35b}$$

$$|M_2(M_{\rm m})| = 2\frac{3}{2}\frac{\Lambda}{4\pi}\alpha_2(M_{\rm m}) \tag{6.35c}$$

$$|M_1(M_{\rm m})| = 2\frac{1}{2}\frac{\Lambda}{4\pi}\alpha_1(M_{\rm m}) \tag{6.35d}$$

The superpotential terms in the second line of Eq. (6.32) are responsible for the generation of μ and $B\mu$ terms in a way very similar to the one introduced in [217] and described in Sec. 6.5. For simplicity, we assume that one coupling of S to the messengers dominates the

other[4], $\alpha_{\xi_L} \gg \alpha_{\xi_D}$. In this case, we obtain the following μ and B terms at the messenger scale:

$$\mu(M_{\rm m}) = -\frac{\lambda}{\lambda_1} A_S^\dagger = \frac{2\lambda\alpha_{\xi_L}(M_{\rm m})}{\lambda_1}\left(\frac{\Lambda^\dagger}{4\pi}\right) \tag{6.36}$$

$$B(M_{\rm m}) = \frac{\tilde{m}_S^2 - |A_S|^2}{A_S^\dagger} = \left(\frac{\Lambda}{4\pi}\right)\left(2\alpha_2(M_{\rm m}) + \frac{3}{5}\alpha_1(M_{\rm m}) - 2\alpha_{\xi_L}(M_{\rm m})\right) \tag{6.37}$$

Using these expressions, for every choice of Λ and $M_{\rm m}$ determining the scalar-squared and gaugino soft masses, the $b = B\mu$ and μ parameters can be adjusted by choosing appropriate values of α_{ξ_L} and λ/λ_1, respectively.

Finally, in the third line of the superpotential (6.32) we have added N_k generations of additional particles ρ_k, $\bar{\rho}_k$ to modify the RGE running of the gauge couplings and y_t and mitigate the fine-tuning with respect to g_3 and y_t as described in section Sec. 6.4. We take the masses of these new particles,given by $\lambda_{\rho,k}\langle S_{M\rho}\rangle$, to be roughly equal to the messenger scale $M_{\rm m}$. This assumption is not necessary for the mechanism to work, it is just convenient to reduce the number of scales.

The RG evolution of y_t above $M_{\rm m}$ is modified due to the presence of the $y_k\bar{\rho}_k^D h_d q$ Yukawa terms. The 1-loop RGE equations, neglecting y_b and y_τ, read

$$16\pi^2\frac{\partial y_t}{\partial t} = y_t\left(6y_t^2 + \sum_k^{N_k} y_k^2 - \frac{16}{3}g_3^2 - 3g_2^2 - \frac{13}{15}g_1^2\right) \tag{6.38a}$$

$$16\pi^2\frac{\partial y_k}{\partial t} = y_k\left(6y_k^2 + y_t^2 - \frac{16}{3}g_3^2 - 3g_2^2 - \frac{7}{15}g_1^2\right). \tag{6.38b}$$

We use `Mathematica` to implement the RG running between $M_{\rm m}$ and $M_{\rm GUT}$ and to calculate the reweighting factors $r_{[y_t,\alpha_3]}$, $r_{[y_t,y_t]}$ and $r_{[y_t,y_k]}$.

6.6.2 Fine-tuning analysis at a benchmark point

We start the analysis of the model specified in Eq. (6.32), by implementing the soft-masses Eq. (6.35) in `softsusy`. We performed scans in the $(M_{\rm m}, \Lambda)$-plane for several fixed values of $\tan\beta$ and $\mathrm{sgn}(\mu) = \pm 1$. Fig. 6.9 shows the result of one such scan with $\tan\beta = 25$ and positive $\mathrm{sgn}(\mu)$. From Fig. 6.9, it can be read off that $m_h = 125\,\mathrm{GeV}$ is compatible with fine-tuning of $\Delta = \max(|c_\mu|, |c_\Lambda|) < 660$.

For further discussion of the fine-tuning with respect to all parameters of the fundamental model Eq. (6.32), we specify a benchmark point P1, corresponding to

$$\underline{\text{P1:}} \qquad \Lambda = 623\,\mathrm{TeV} \qquad M_{\rm m} = 2.24\cdot 10^4\,\mathrm{TeV} \qquad \tan\beta = 25 \qquad \mathrm{sgn}(\mu) = +1 \tag{6.39}$$

[4]It is not phenomenologically relevant which coupling is chosen to be larger. However it is crucial that S does not couple to the messengers in a $SU(5)$ symmetric way. In that case, the contributions to A_S from $S\bar{L}_1 L_2$ and $S\bar{D}_1 D_2$ cancel each other because of $\lambda_L = -3/2\lambda_D$, and no μ term is generated.

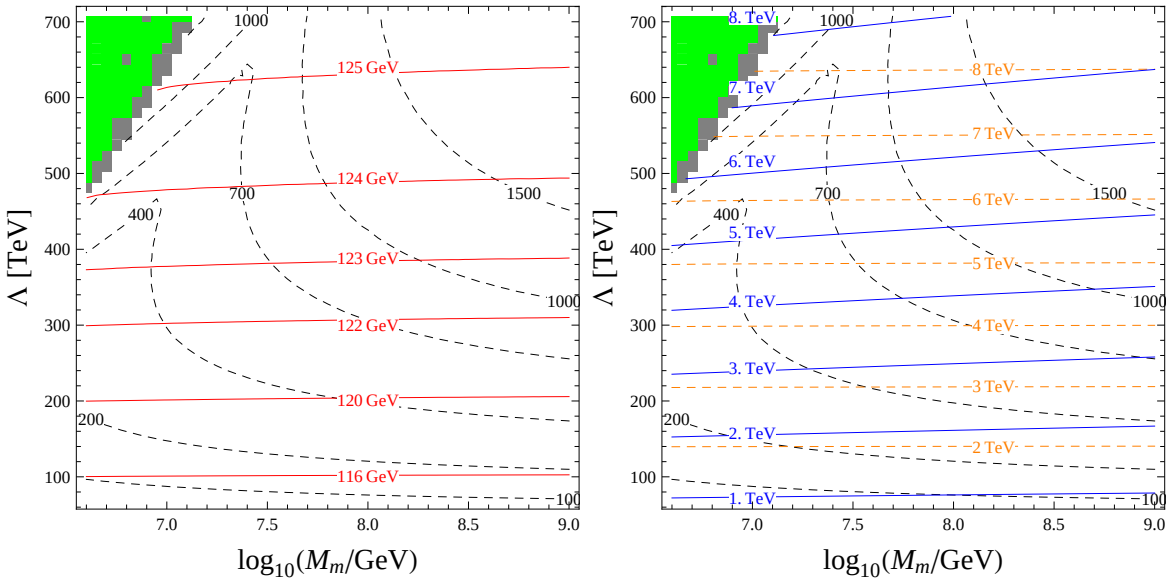

Figure 6.9: Results of a scan of the full SNC model, for fixed $\tan\beta = 25$ and positive $\mathrm{sgn}(\mu)$. The relevant contours obtained in the $(M_{\rm m}, \Lambda)$-plane are shown. *Left:* Contours of m_h (red) and fine-tuning $\max(|c_\mu|, |c_\Lambda|)$ (black-dashed). *Right:* Contours of the lightest stop mass $m_{\tilde{t}_1}$ (blue), the gluino mass $m_{\tilde{g}}$ (orange-dashed) and the fine-tuning (black-dashed). The green shaded areas are excluded because electroweak symmetry is unbroken. The grey shaded areas cannot be evaluated because `softsusy` does not converge.

P1 is chosen such that $m_h = 125.0\,\mathrm{GeV}$. The gluino, lightest stop and lightest neutralino masses of our benchmark point are all very large and safely above all current exclusion limits

$$m_{\tilde{g}} = 7.86\,\mathrm{TeV} \qquad m_{\tilde{t}_1} = 7.27\,\mathrm{TeV} \qquad m_{\tilde{\chi}_1^0} = 883\,\mathrm{GeV} \tag{6.40}$$

and above the current sensitivity of the LHC SUSY searches. The dimensionfull parameters $\{a_i\}$ at the messenger scale are:

$$\Lambda = 623.0\,\mathrm{TeV} \quad M_{\rm m} = 2.240 \cdot 10^4\,\mathrm{TeV} \quad \mu = 1179\,\mathrm{GeV} \quad b = -184157\,\mathrm{GeV}^2, \tag{6.41}$$

were the values of μ and b have been calculated from the requirements of $\tan\beta = 25$ and $m_Z = 91.2\,\mathrm{GeV}$.

The fine-tuning coefficients corresponding to these parameters, calculated by `softsusy`, are

$$c_\Lambda = -657 \qquad c_{M_{\rm m}} = -0.047 \qquad c_\mu = -612 \qquad c_b = -3.62 \tag{6.42}$$

Clearly, of these fine-tuning coefficients only c_Λ and c_μ arerelevant for the fine-tuning analysis. If we were not concerned about the fine-tuning with respect to the gauge and Yukawa couplings, at this point we could conclude that the fine-tuning in this model at the benchmark point P1 is $\Delta = \max(|c_\Lambda|, |c_\mu|) = 657$.

However, the fine-tuning coefficients calculated for to the dimensionless couplings y_t and g_3 by `softsusy` are, as discussed in Sec. 6.4, also of concern. Specifically for the benchmark point P1, we confirm that these fine-tuning coefficients are certainly of troubling sizes:

$$c_{y_t} = 7809 \qquad c_{g_3} = 4372 \qquad c_{g_2} = -558.5 \qquad c_{g_1} = 88.0 \tag{6.43}$$

We will now address how these fine-tunings are mitigated when we consider $M_{\rm GUT}$ to be the full fundamental scale for the gauge and Yukawa couplings, i.e. switch from the c_i basis into the $\tilde{c}_i$ basis. We take as input the values of the couplings at the messenger scale as determined by `softsusy`. This ensures that the leading 2-loop and threshold corrections in the evolution between the low scales and $M_{\rm m}$ are correctly taken into account. For the benchmark point P1 the values of these couplings are

$$y_t(M_{\rm m}) = 0.7109 \quad \alpha_3(M_{\rm m}) = 0.05829 \quad \alpha_2(M_{\rm m}) = 0.03346 \quad \alpha_2(M_{\rm m}) = 0.02112 \tag{6.44}$$

Then, in order to calculate the reweighting coefficients $r_{[i,j]}$, we implement and evaluate the one-loop running, determined by Eq. (6.38) and

$$\frac{\partial \alpha_a}{\partial t} = \frac{1}{2\pi}(b_a + 2 + N_k) \quad \text{where } (b_3, b_2, b_1) = \left(-3, 1, \frac{33}{5}\right) \tag{6.45}$$

numerically in `Mathematica`. The values of the couplings at the $M_{\rm GUT} = 8.79 \cdot 10^{15}$GeV scale and the reweighting coefficients $r_{[i,j]}$ then depend on N_k and the choice of the hitherto unconstrained Yukawa couplings y_k. We find that for $N_k = 6$ and a common value $y_k(M_{\rm m}) = 1.154$ for all k generations of $\bar{\rho}_k^D$, we obtain

$$\begin{aligned} \alpha_a(M_{\rm GUT}) &= \frac{g_U^2}{4\pi} = 0.696 \\ \alpha_{y_t}(M_{\rm GUT}) &= \frac{y_t^2(M_{\rm GUT})}{4\pi} = 0.948 \qquad \alpha_{y_k}(M_{\rm GUT}) = \frac{y_k^2(M_{\rm GUT})}{4\pi} = 0.107 \end{aligned} \tag{6.46}$$

as well as the following reweigthing coefficients

$$r_{[g_3,g_U]} = 0.084 \qquad r_{[g_2,g_U]} = 0.048 \qquad r_{[g_1,g_U]} = 0.030 \tag{6.47}$$

$$r_{[y_t,y_t]} = 0.074 \qquad r_{[y_t,g_U]} = -0.099 \qquad r_{[y_t,y_k]} = -0.048. \tag{6.48}$$

Hence, the fine-tunings with respect to the couplings at the GUT scale, for this particular choice of N_k and $y_k(M_{\rm m})$, are substantially reduced

$$\tilde{c}_{g_U} = c_{g_3} \cdot r_{[g_3,g_U]} + c_{g_2} \cdot r_{[g_2,g_U]} + c_{g_1} \cdot r_{[g_1,g_U]} + c_{y_t} \cdot r_{[y_t,g_U]} = -427 \tag{6.49}$$

$$\tilde{c}_{y_t} = c_{y_t} \cdot r_{[y_t,y_t]} = 574 \tag{6.50}$$

$$\tilde{c}_{y_k} = c_{y_t} \cdot r_{[y_t,y_k]} = -371 \tag{6.51}$$

Since those fine-tuning coefficients all have absolute values smaller than $|c_\Lambda|$ and $|c_\mu|$, the latter ultimatively determine the overall fine-tuning of among the model parameters at the benchmark point P1.

We can thus conclude that in our model Eq. (6.32), $m_h = 125\,\text{GeV}$ is compatible with an overall fine-tuning of 1:657. This is a small value given the current state of SUSY naturalness

and competitive with the minimal fine-tunings in models of *natural supersymmetry* which typically are not below 1:1000 using the same Giudice-Barbieri prescription Eq. (6.10) to quantify fine-tuning. An advantage of the SNC approach as compared is that we know its concrete high scale implementation Eq. (6.32). In contrast, typical *natural supersymmetry* models are only specified in terms of their low energy spectrum without demonstrating that a model implementation leading to that spectrum actually exists.

6.6.3 Discussion

We want to stress that the model specified in Eq. (6.32) is only intended to be one concrete example illustrating the possibility of finding complete models that display stable near-criticality. Similarly, the parameters specified for the benchmark point are just one particular choice demonstrating that the values of the fine-tuning coefficients can be kept relatively small in models displaying SNC correlations. A full analysis of the available parameter space of Eq. (6.32) and determination of the maximally achievable reduction of fine-tuning is beyond the scope of this work.

Several comments are in order before we conclude.

- It has been argued, e.g. in Ref. [220], in the prescription to quantify fine-tuning should compare m_Z^2 to parameters that also have quadratic mass dimensions, i.e. substituting $\{a_i\} = \{\Lambda, \mu, \ldots\}$ by $\{a_i\} = \{\Lambda^2, \mu^2, \ldots\}$. This choice would halve the respective fine-tuning coefficients.

- Similarly, one could advocate that the dimensionless couplings' fine-tuning should be measured with respect to α_a and α_{y_t} instead of y_t and g_a which would also reduce the corresponding fine-tuning coefficients by a factor 2. This is just another instance of the inherent arbitrariness of of quantifying fine-tuning. There is no objectively correct choice, and it is important to make statements about SUSY naturalness only in terms of comparing two models using the same prescription. We therefore stick to the prescription based on Ref. [193,195] which is the most widely used one throughout the literature on the subject.

- Another comment pertains quantifying fine-tuning with respect to μ. If we commit to the mechanism described above to generate μ and $B\mu$, in particular to

$$\mu = \frac{2\lambda\alpha_{\xi_L}}{\lambda_1}\frac{\Lambda}{4\pi}, \tag{6.52}$$

  then μ is not an independent parameter at the messenger scale anymore. In that case, the basis choice of fine-tuning coefficients

$$\bar{c}_\Lambda = c_\Lambda + c_\mu \frac{\partial \ln \mu}{\partial \ln \Lambda} = c_\Lambda + c_\mu \tag{6.53}$$

$$\bar{c}_\lambda = \bar{c}_{\lambda_1} = c_\mu \tag{6.54}$$

  appears more appropriate to quantify fine-tuning. In this basis, the fine-tuning of the benchmark point P1 would be roughly doubled.

Again, however, our point of selecting a mechanism to generate μ and $B\mu$ was not to promote this specific implementation but rather demonstrate that mechanisms exist that neither upset the correlations among the soft masses nor change the RG running below $M_{\rm m}$. By sticking to the original definition of fine-tuning coefficients c_Λ and c_μ, it is easier to compare our results with other values in the literature.

6.7 Conclusion: a strategy towards minimally tuned gauge mediated MSSM models

The LHC data collected thus far puts supersymmetry as a solution to the gauge hierarchy problem on the spot. Model building to realize so-called "natural spectra" in supersymmetric models with light stops and gauginos but heavy first and second generation squarks is becoming increasingly difficult.

In an alternative approach, we want to point out that constraints from fine-tuning considerations on superparticle masses can deviate significantly from those obtained in an naïve analysis assuming completely unrelated soft mass parameters. This can be the case if the fundamental model imposes correlations among the soft terms. Correlations among the soft masses are necessary at any rate since the flavor structure of soft terms already needs to be highly non-generic to phenomenologically viable.

The aim of this work is to identify models in which the value of the soft mass term for the up-type Higgs at the scale $Q_{\rm SUSY}$ where the Higgs scalar potential is evaluated, $\tilde{m}^2_{\rm hu}(Q_{\rm SUSY})$, is robustly small even for large input values for $\tilde{m}^2_{\rm hu}(M_{\rm m})$ and other soft masses at the messenger scale $M_{\rm m}$. Such models require that the various contributions in the RGE running of $\tilde{m}^2_{\rm hu}$ are correlated in the correct way, described by the requirements (AI) and (AII) specified in Sec. 6.2.

Of course, to argue convincingly that fine-tuning can be reduced by correlating various contributions to the $\tilde{m}^2_{\rm hu}(Q_{\rm SUSY})$, the correlations have to be a truly robust feature of the underlying model parameterizing how SUSY breaking is communicated to the visible sector. This is the main weakness of the argument in *Focus Point* models [194, 208–211] as well as recently suggested models of *radiative natural supersymmetry* [203, 204]. In those models a cancellation takes place but hinges on unjustified assumptions such as universal soft masses or new continuous parameters are introduced which themselves need to be fine-tuned.

We demonstrate that models exist with necessary robust cancellations to reduce fine-tuning. We call this *stable near-criticality*. The upside to having to impose strict correlations among the soft parameters without dependence on new continuous parameters is that the model implementations are particularly simple. Because of its high degree of predictiveness, we identify gauge mediation as promising underlying SUSY breaking mechanism for potential SNC models.

An important issue questioning the validity of all approaches to reduce fine-tuning via cancellations among the soft parameters, including SNC, was raised in [196]. The authors point out that, as the RGE trajectories of the soft mass terms depend sensitively on the values of the SM gauge and Yukawa couplings, the fine-tuning with respect to those dimen-

sionless couplings is considerable. Thus reducing fine-tuning with respect to the relevant parameters describing the superparticle masses, eg. Λ and μ in gauge mediation, is not sufficient to reduce overall fine-tuning. It has been argued before that the apparent fine-tuning with respect to y_t and g_3 could be mitigated by introducing a more fundamental scale above $M_{\rm m}$ [194]. But to our knowledge we are the first to provide an explicit mechanism to demonstrate the feasibility of our approach. For our implementation it is crucial that the apparent gauge coupling unification of the MSSM is preserved. We achieve that by only adding particles in complete GUT multiplets at the messenger scale. Furthermore, several orders of magnitude are needed between the scales $M_{\rm m}$ and $M_{\rm GUT}$ to allow for sizable RGE effects. This is readily realized in gauge mediation as the messenger scale $M_{\rm m}$ is essentially a free parameter.

Finally, as we commit to gauge mediation as mechanism to softly break supersymmetry, we have to address the μ-$B\mu$ problem. A mechanism is needed which not only makes sure that the appropriate terms can be generated, but also that in doing so no additional contributions to $\tilde{m}^2_{\rm hu}$ and A_t arise since these would alter the correlations necessary to reduce fine-tuning in SNC models. We adapted the mechanism proposed in [217] to demonstrate explicitly that at least one compatible solution exists.

In conclusion, we have demonstrated that fully consistent models exist that exhibit stable near-criticality and have relatively small fine-tunings in spite of multi-TeV stop masses. In particular we demonstrate that $m_h = 125\,\text{GeV}$ and stop masses above 7 TeV can be compatible with fine-tuning of $\Delta < 660$ quantified according to the prescription [193, 195]. While that amount of fine-tuning implies that EWSB in our MSSM models is not entirely natural, it is a very low value considering the current state of SUSY naturalness constraints. We have discussed at length the requirements for consistent stable near-criticality.

On a final note, we want to point out that it is certainly possible that models exist that reduce fine-tuning even more efficiently than the example we provided in Sec. 6.6. However there will always be an amount of irreducible fine-tuning. Even though $\tilde{m}^2_{\rm hu}(M_{\rm SB})$ in leading loop order can in principle vanish entirely if the conditions (A) and (B) specified in Sec. 6.2 are satisfied perfectly, there are always remaining contributions from integrating out the superparticles at $Q_{\rm SUSY}$. The largest contribution is of order $\mathcal{O}\left(\frac{6}{8\pi^2} y_t^2 m^2_{\tilde{t}}\right)$ and stems from integrating out the stop fields. Note that these irreducible contributions are scheme-dependent. An explicit prescription to quantify the irreducible fine-tuning, taking into account solely effects from integrating out superparticles at the scale $Q_{\rm SUSY}$, has been introduced in [221]. The authors evaluate electroweak fine-tuning by examining the minimization condition from the Higgs sector scalar potential. Therefore, even in the most optimal scenario, SNC can at best reduce fine-tuning to an irreducible amount of about 1:10 to 1:100 for $Q_{\rm SUSY}$ of in the range of $1 - 10\,\text{TeV}$. The SUSY naturalness problem still arises in principle from the mismatch between $\Lambda_{\rm EWSB}$ and $Q_{\rm SUSY} \sim M_{\rm SB}$, but the naturalness constrains can be weakened by several orders of magnitude by certain correlations defined in the setup of stable near-criticality.

CHAPTER 7

CONCLUSIONS

The Large Hadron Collider has the potential to extensively probe scenarios of beyond the standard model physics. It is the task of the theory community to derive testable predictions that will allow experimentally distinguishing new physics contributions from standard model signatures and the various beyond-the-standard-model scenarios from each other. Given on the one hand the resilience of the SM, which despite definite evidence that it cannot be the ultimate theory of fundamental particles and interactions has so far passed all direct tests, and on the other hand the vast landscape of new physics possibilities, the search for physics beyond the standard model is a formidable task.

The concept of effective field theories provides a powerful organizing scheme and calculational toolbox to obtain predictions in arbitrary theories. In this work, we derived an effective theory for heavy Majorana fermions, which appear in many extensions of the standard model. The effective theory is particularly useful for the description of bound states of long-lived colored Majorana particles, in close analogy to the well-known heavy quark effective theory, which can be applied to describe the dynamics of heavy B and D mesons.

We further demonstrated how a combination of the concepts of WIMP dark matter and grand unification provides strong motivation for novel models with colored particles at the TeV scale. We investigated the LHC implications of this scenario for the two complementary cases where the new colored particles either are stable and form R-hadrons or else decay promptly to final states including a Higgs boson. Although the original benchmark points provided to illustrate our findings have already been rendered obsolete by newer LHC data, the central claims of our work remain valid.

A primary objective of the LHC is to search for supersymmetry. Certain exclusion bounds on superparticles already reach beyond 1 TeV. Since the expectation of superparticles being rather light with masses comparable to the weak scale is based on naturalness requirements (or equivalently, on the absence of fine-tuning), it is reasonable that the new LHC limits have initiated renewed efforts to investigate the link between naturalness in supersymmetric models and the existence of LHC-accessible superparticles. The recent discovery of the Higgs boson with $m_h \sim 125\,\text{GeV}$ provides an additional motivation to re-evaluate the status of SUSY naturalness. In this work, we devised a framework called

stable near-criticality (SNC), in which the usual fine-tuning upper bounds on superparticle masses are avoided in certain supersymmetric models. The models in question have to exhibit specific and robust correlations between the individual soft masses and are therefore by definition rather minimal. An important finding of our work is that the soft Higgs mass term at the low energy scale, $\tilde{m}^2_{\mathrm{hu}}(Q_{\mathrm{SUSY}})$, can be stabilized at small values even if the gauge and Yukawa couplings are considered variable parameters. Our analysis shows that in models fulfilling the requirements of stable near-criticality, fine-tuning is comparatively low even as stop masses extend to multi-TeV values. From a fine-tuning perspective, SNC is competitive with models with spectra tailored to the requirements of *natural supersymmetry*. At the same time, since superparticle masses in the scenario of SNC are of the order of several TeV, stable near-criticality is not affected by the direct and indirect limits resulting from the various, all hitherto negative, SUSY searches at the LHC.

APPENDIX A

FORBIDDING PROTON DECAY

In Sec. 4.4 of chapter 3, we did not require the unification scale to be high enough to suppress proton decay. For example, in the benchmark $V + 2X$ model, the unification scale is $M_{\rm GUT} \sim 10^{11}$GeV, significantly lower than the standard GUT scale $\sim 10^{16}$GeV. Therefore, it is essential to discuss how proton decay can be avoided in principle, even though it has no phenomenological relevance at the TeV scale.

A robust way to avoid the proton decay problem is simply to forbid it by a symmetry. For example, we can consider "baryon triality" [222], $\phi \to \mathrm{e}^{\mathrm{i}\frac{2\pi}{3}(B_\phi - 2Y_\phi)}\phi$, where B_ϕ and Y_ϕ are the baryon number and hypercharge of a field ϕ, respectively. Baryon triality implies that the baryon number can only be violated in units of 3. Thus, it will absolutely forbid not only proton decay but also neutron-antineutron oscillation [223]. Alternatively, for forbidden proton decay only, one could impose "quark parity", $q, d^c, u^c \to -q, -d^c, -u^c$.

Clearly, such symmetries necessarily treat quarks and leptons differently, so the simplest possibility of embedding quarks and leptons into unified GUT multiplets (e.g. $\bar{\mathbf{5}} \oplus \mathbf{10}$ for $SU(5)$) does not work. Instead, quarks and leptons must come from separate multiplets, e.g.:

$$\bar{\mathbf{5}}_{d^c} = \begin{pmatrix} d^c \\ 0 \end{pmatrix}, \quad \bar{\mathbf{5}}_l = \begin{pmatrix} 0 \\ l \end{pmatrix}, \tag{A.1}$$

where $\bar{\mathbf{5}}_{d^c}$ and $\bar{\mathbf{5}}_l$ carry the same baryon triality (or quark parity) quantum numbers as d^c and l, respectively. Before discussing how to promote such incomplete multiplets to fully GUT-invariant multiplets, we would like to point out that splitting SM matter fields from their heavy "GUT partners" is plausible in the sense that there is already a split multiplet, i.e. the Higgs doublet, and whatever mechanism that splits the Higgs from its GUT partner could also work for the SM matter fields. Moreover, separating quarks and leptons allows us to trivially incorporate non-unified mass relations for the 1st and 2nd generations (i.e. $m_e/m_d, m_\mu/m_s \neq 1$ at the unification scale).

Now, let us discuss how the above "incomplete" multiplets can be compatible with a GUT symmetry. A simple and plausible way to do so is to copy the mechanism [224–226] of "incomplete" multiplets nature already has in the low-energy QCD. QCD undergoes a symmetry breaking from $G \equiv SU(3)_L \otimes SU(3)_R$ down to $H \equiv SU(3)_{L\oplus R}$. Here, the low-mass hadrons form "incomplete" multiplets", i.e. multiplets of the unbroken subgroup H, not those of the full group G. Of course, the theory must be invariant under G, which is

accomplished by nonlinear realization [227, 228] in terms of the Nambu-Goldstone boson field Σ transforming as $\Sigma \to g\Sigma h^{-1}$ with $g \in G$ and $h \in H$. This permits us to promote any multiplet of H, ϕ_H, to a full multiplet of G, ϕ_H, as $\phi_G \equiv \Sigma\phi_H$.

By analogy, let us consider the following GUT scenario. Imagine a new confining strong dynamics with a "flavor symmetry" $G = SU(5)$ which undergoes "chiral symmetry breaking" $G \to H$ with $H = SU(3) \otimes SU(2) \otimes \mathrm{U}(1)$. G is also weakly gauged, providing the SM gauge group with a single unified coupling at the G confinement scale (which therefore can be called the GUT scale). We then imagine that the split quark and lepton multiplets as well as the Higgs doublet are "hadrons" of the new strong dynamics which form multiplets of H, with appropriate quark parity or baryon triality, etc. They can be promoted to full G multiplets by nonlinear realization. (If we further integrate in the "ρ mesons" into this picture by employing "hidden local symmetry" [229], then we essentially obtain the 2-site moose model considered in Ref. [230].)

Constructing an explicit, UV-complete 4D gauge theory that realizes this scenario is beyond the scope of this paper, but it is straightforward to construct a 5D realization via the AdS/CFT correspondence (For reviews, see [231, 232]), as is done in Ref. [233]. The simplest setup would be the Randall-Sundrum framework [234], i.e., where we take the UV boundary and the bulk to be G-symmetric while the IR boundary to be only H-symmetric, by putting a G gauge field in the bulk with the boundary condition that the G/H gauge bosons vanish at the IR boundary. The split matter and Higgs multiplets can then be put either in the bulk with the appropriate boundary conditions to project out the unwanted "G-partner" states, or simply at the IR boundary as multiplets of H. With an appropriate symmetry such as quark parity or baryon triality, this setup solves the proton decay problem, but since the scale associated with the IR boundary is the GUT scale, there are no observable consequences of the Kaluza-Klein excitations. (There are, however, RS GUT models with the TeV-scale IR brane, with split multiplets and a discrete symmetry to forbid proton decay, which do have experimental consequences at the TeV scale [235, 236]. The main difference between those models and ours is that their physics above the TeV scale is a strong conformal dynamics (or a 5D theory via AdS/CFT) while we assume a perturbative 4D physics up to the GUT scale.)

BIBLIOGRAPHY

[1] Manuel Drees and Gilles Gerbier. Mini-Review of Dark Matter: 2012. 2012.

[2] Marco Cirelli, Nicolao Fornengo, and Alessandro Strumia. Minimal dark matter. *Nucl.Phys.*, B753:178–194, 2006.

[3] Marco Cirelli, Alessandro Strumia, and Matteo Tamburini. Cosmology and Astrophysics of Minimal Dark Matter. *Nucl.Phys.*, B787:152–175, 2007.

[4] S.L. Glashow. Partial Symmetries of Weak Interactions. *Nucl.Phys.*, 22:579–588, 1961.

[5] Steven Weinberg. A Model of Leptons. *Phys.Rev.Lett.*, 19:1264–1266, 1967.

[6] Murray Gell-Mann. A Schematic Model of Baryons and Mesons. *Phys.Lett.*, 8:214–215, 1964.

[7] H. Fritzsch, Murray Gell-Mann, and H. Leutwyler. Advantages of the Color Octet Gluon Picture. *Phys.Lett.*, B47:365–368, 1973.

[8] D.J. Gross and Frank Wilczek. Ultraviolet Behavior of Nonabelian Gauge Theories. *Phys.Rev.Lett.*, 30:1343–1346, 1973.

[9] H. David Politzer. Reliable Perturbative Results for Strong Interactions? *Phys.Rev.Lett.*, 30:1346–1349, 1973.

[10] Peter W. Higgs. Broken Symmetries and the Masses of Gauge Bosons. *Phys.Rev.Lett.*, 13:508–509, 1964.

[11] Peter W. Higgs. Broken symmetries, massless particles and gauge fields. *Phys.Lett.*, 12:132–133, 1964.

[12] G.S. Guralnik, C.R. Hagen, and T.W.B. Kibble. Global Conservation Laws and Massless Particles. *Phys.Rev.Lett.*, 13:585–587, 1964.

[13] F. Englert and R. Brout. Broken Symmetry and the Mass of Gauge Vector Mesons. *Phys.Rev.Lett.*, 13:321–323, 1964.

[14] Peter W. Higgs. Spontaneous Symmetry Breakdown without Massless Bosons. *Phys.Rev.*, 145:1156–1163, 1966.

[15] T.W.B. Kibble. Symmetry breaking in nonAbelian gauge theories. *Phys.Rev.*, 155:1554–1561, 1967.

[16] F.J. Hasert, H. Faissner, W. Krenz, J. Von Krogh, D. Lanske, et al. SEARCH FOR ELASTIC MUON-NEUTRINO ELECTRON SCATTERING. *Phys.Lett.*, B46:121–124, 1973.

[17] F.J. Hasert et al. Observation of Neutrino Like Interactions Without Muon Or Electron in the Gargamelle Neutrino Experiment. *Phys.Lett.*, B46:138–140, 1973.

[18] T. Eichten, H. Faissner, F.J. Hasert, S. Kabe, W. Krenz, et al. MEASUREMENT OF THE NEUTRINO - NUCLEON ANTI-NEUTRINO - NUCLEON TOTAL CROSS-SECTIONS. *Phys.Lett.*, B46:274–280, 1973.

[19] G. Arnison et al. Experimental Observation of Isolated Large Transverse Energy Electrons with Associated Missing Energy at s**(1/2) = 540-GeV. *Phys.Lett.*, B122:103–116, 1983.

[20] G. Arnison et al. Experimental Observation of Lepton Pairs of Invariant Mass Around 95-GeV/c**2 at the CERN SPS Collider. *Phys.Lett.*, B126:398–410, 1983.

[21] M. Banner et al. Observation of Single Isolated Electrons of High Transverse Momentum in Events with Missing Transverse Energy at the CERN anti-p p Collider. *Phys.Lett.*, B122:476–485, 1983.

[22] P. Bagnaia et al. Evidence for Z0 $\rightarrow$ e+ e- at the CERN anti-p p Collider. *Phys.Lett.*, B129:130–140, 1983.

[23] the SLD Electroweak. A Combination of preliminary electroweak measurements and constraints on the standard model. 2003.

[24] A. Czarnecki. Muon g-2: A theoretical review. *Nucl.Phys.Proc.Suppl.*, 144:201–205, 2005.

[25] J. van der Bij and M.J.G. Veltman. Two Loop Large Higgs Mass Correction to the rho Parameter. *Nucl.Phys.*, B231:205, 1984.

[26] J.J. van der Bij, K.G. Chetyrkin, M. Faisst, G. Jikia, and T. Seidensticker. Three loop leading top mass contributions to the rho parameter. *Phys.Lett.*, B498:156–162, 2001.

[27] Giuseppe Degrassi and Paolo Gambino. Two loop heavy top corrections to the Z0 boson partial widths. *Nucl.Phys.*, B567:3–31, 2000.

[28] R. Boughezal, J.B. Tausk, and J.J. van der Bij. Three-loop electroweak correction to the Rho parameter in the large Higgs mass limit. *Nucl.Phys.*, B713:278–290, 2005.

[29] F. Abe et al. Observation of top quark production in $\bar{p}p$ collisions. *Phys.Rev.Lett.*, 74:2626–2631, 1995.

[30] S. Abachi et al. Observation of the top quark. *Phys.Rev.Lett.*, 74:2632–2637, 1995.

[31] K. Kodama et al. Observation of tau neutrino interactions. *Phys.Lett.*, B504:218–224, 2001.

[32] Serguei Chatrchyan et al. Observation of a new boson at a mass of 125 GeV with the CMS experiment at the LHC. *Phys.Lett.*, B716:30–61, 2012.

[33] Georges Aad et al. Observation of a new particle in the search for the Standard Model Higgs boson with the ATLAS detector at the LHC. *Phys.Lett.*, B716:1–29, 2012.

[34] F. Zwicky. On the Masses of Nebulae and of Clusters of Nebulae. *Astrophys.J.*, 86:217–246, 1937.

[35] G. Hinshaw, D. Larson, E. Komatsu, D.N. Spergel, C.L. Bennett, et al. Nine-Year Wilkinson Microwave Anisotropy Probe (WMAP) Observations: Cosmological Parameter Results. 2012.

[36] M.J.G. Veltman. The Infrared - Ultraviolet Connection. *Acta Phys.Polon.*, B12:437, 1981.

[37] Steven Weinberg. Gauge Hierarchies. *Phys.Lett.*, B82:387, 1979.

[38] Can Kilic, Karoline Kopp, and Takemichi Okui. LHC Implications of the WIMP Miracle and Grand Unification. *Phys.Rev.*, D83:015006, 2011.

[39] Karoline Kopp and Takemichi Okui. Effective Field Theory for a Heavy Majorana Fermion. *Phys.Rev.*, D84:093007, 2011.

[40] Prerit Jaiswal, Karoline Kopp, and Takemichi Okui. Minimally tuned gauge mediation. To appear.

[41] Gerard 't Hooft. Renormalization of Massless Yang-Mills Fields. *Nucl.Phys.*, B33:173–199, 1971.

[42] Ira Z. Rothstein. TASI lectures on effective field theories. 2003.

[43] Aneesh V. Manohar. Effective field theories. 1996.

[44] H. Georgi. Effective field theory. *Ann.Rev.Nucl.Part.Sci.*, 43:209–252, 1993.

[45] Matthias Neubert. Effective field theory and heavy quark physics. pages 149–194, 2005.

[46] David B. Kaplan. Effective field theories. 1995.

[47] David B. Kaplan. Five lectures on effective field theory. 2005.

[48] Raman Sundrum. Effective field theory for a three-brane universe. *Phys.Rev.*, D59:085009, 1999.

[49] Mikhail A. Shifman and M.B. Voloshin. On Annihilation of Mesons Built from Heavy and Light Quark and anti-B0 – B0 Oscillations. *Sov.J.Nucl.Phys.*, 45:292, 1987.

[50] Mikhail A. Shifman and M.B. Voloshin. On Production of d and D* Mesons in B Meson Decays. *Sov.J.Nucl.Phys.*, 47:511, 1988.

[51] Nathan Isgur and Mark B. Wise. Weak Decays of Heavy Mesons in the Static Quark Approximation. *Phys.Lett.*, B232:113, 1989.

[52] Nathan Isgur and Mark B. Wise. WEAK TRANSITION FORM-FACTORS BETWEEN HEAVY MESONS. *Phys.Lett.*, B237:527, 1990.

[53] Howard Georgi. Heavy quark effective field theory. 1991.

[54] Mark B. Wise. Heavy quark physics: Course. pages 1051–1089, 1997.

[55] T. Mannel. Heavy quark effective field theory. *Rept.Prog.Phys.*, 60:1113–1172, 1997.

[56] A.G. Grozin. Heavy quark effective theory. *Springer Tracts Mod.Phys.*, 201:1–213, 2004.

[57] Michael E. Luke and Aneesh V. Manohar. Reparametrization invariance constraints on heavy particle effective field theories. *Phys.Lett.*, B286:348–354, 1992.

[58] Yu-Qi Chen. On the reparametrization invariance in heavy quark effective theory. *Phys.Lett.*, B317:421–427, 1993.

[59] Wolfgang Kilian and Thorsten Ohl. Renormalization of heavy quark effective field theory: Quantum action principles and equations of motion. *Phys.Rev.*, D50:4649–4656, 1994.

[60] Raman Sundrum. Reparameterization invariance to all orders in heavy quark effective theory. *Phys.Rev.*, D57:331–336, 1998.

[61] Shmuel Nussinov and Werner Wetzel. Comparison of Exclusive Decay Rates for b —¿ u and b —¿ c Transitions. *Phys.Rev.*, D36:130, 1987.

[62] Stephen P. Martin. A Supersymmetry primer. 1997.

[63] Glennys R. Farrar and Pierre Fayet. Phenomenology of the Production, Decay, and Detection of New Hadronic States Associated with Supersymmetry. *Phys.Lett.*, B76:575–579, 1978.

[64] Nima Arkani-Hamed and Savas Dimopoulos. Supersymmetric unification without low energy supersymmetry and signatures for fine-tuning at the LHC. *JHEP*, 0506:073, 2005.

[65] G.F. Giudice and A. Romanino. Split supersymmetry. *Nucl.Phys.*, B699:65–89, 2004.

[66] Georges Aad et al. Search for Heavy Long-Lived Charged Particles with the ATLAS detector in pp collisions at sqrt(s) = 7 TeV. *Phys.Lett.*, B703:428–446, 2011.

[67] Vardan Khachatryan et al. Search for Heavy Stable Charged Particles in pp collisions at sqrt(s)=7 TeV. *JHEP*, 1103:024, 2011.

[68] Debrupa Chakraverty, Triptesh De, Binayak Dutta-Roy, and Anirban Kundu. Effective theory approach to SUSY hadron spectroscopy. *Phys.Rev.*, D53:5293–5297, 1996.

[69] Richard J. Hill and Mikhail P. Solon. Universal behavior in the scattering of heavy, weakly interacting dark matter on nuclear targets. *Phys.Lett.*, B707:539–545, 2012.

[70] J. Beringer et al. Review of Particle Physics (RPP). *Phys.Rev.*, D86:010001, 2012.

[71] Edward W. Kolb and Michael W. Turner. *The early universe*. Addison-Wesley, 1990.

[72] H. Goldberg. Constraint on the Photino Mass from Cosmology. *Phys.Rev.Lett.*, 50:1419, 1983.

[73] John R. Ellis, J.S. Hagelin, Dimitri V. Nanopoulos, Keith A. Olive, and M. Srednicki. Supersymmetric Relics from the Big Bang. *Nucl.Phys.*, B238:453–476, 1984.

[74] R. Bernabei et al. First results from DAMA/LIBRA and the combined results with DAMA/NaI. *Eur.Phys.J.*, C56:333–355, 2008.

[75] R. Bernabei et al. New results from DAMA/LIBRA. *Eur.Phys.J.*, C67:39–49, 2010.

[76] http://cogent.pnnl.gov/. Also see the CoGeNT collaboration webpages.

[77] C.E. Aalseth, P.S. Barbeau, J. Colaresi, J.I. Collar, J. Diaz Leon, et al. Search for an Annual Modulation in a P-type Point Contact Germanium Dark Matter Detector. *Phys.Rev.Lett.*, 107:141301, 2011.

[78] Z. Ahmed et al. Dark Matter Search Results from the CDMS II Experiment. *Science*, 327:1619–1621, 2010.

[79] Z. Ahmed et al. Results from a Low-Energy Analysis of the CDMS II Germanium Data. *Phys.Rev.Lett.*, 106:131302, 2011.

[80] E. Armengaud et al. Final results of the EDELWEISS-II WIMP search using a 4-kg array of cryogenic germanium detectors with interleaved electrodes. *Phys.Lett.*, B702:329–335, 2011.

[81] Z. Ahmed et al. Combined Limits on WIMPs from the CDMS and EDELWEISS Experiments. *Phys.Rev.*, D84:011102, 2011.

[82] J. Angle et al. A search for light dark matter in XENON10 data. *Phys.Rev.Lett.*, 107:051301, 2011.

[83] E. Aprile et al. Dark Matter Results from 100 Live Days of XENON100 Data. *Phys.Rev.Lett.*, 107:131302, 2011.

[84] Elena Aprile. The XENON1T Dark Matter Search Experiment. 2012.

[85] Paul L. Brink et al. Beyond the CDMS-II dark matter search: SuperCDMS. *eConf*, C041213:2529, 2004.

[86] H. Georgi and S.L. Glashow. Unity of All Elementary Particle Forces. *Phys.Rev.Lett.*, 32:438–441, 1974.

[87] Yoichiro Suzuki et al. Multimegaton water Cherenkov detector for a proton decay search: TITAND (former name TITANIC). pages 288–296, 2001.

[88] D.S. Akerib et al. Limits on spin-independent wimp-nucleon interactions from the two-tower run of the cryogenic dark matter search. *Phys.Rev.Lett.*, 96:011302, 2006.

[89] H. Georgi, Helen R. Quinn, and Steven Weinberg. Hierarchy of Interactions in Unified Gauge Theories. *Phys.Rev.Lett.*, 33:451–454, 1974.

[90] Georges Aad et al. Searches for heavy long-lived sleptons and R-Hadrons with the ATLAS detector in pp collisions at $\sqrt{s} = 7$ TeV. 2012.

[91] Serguei Chatrchyan et al. Search for heavy long-lived charged particles in pp collisions at $\sqrt{s} = 7$ TeV. *Phys.Lett.*, B713:408–433, 2012.

[92] Jens Erler and Paul Langacker. Precision Constraints on Extra Fermion Generations. *Phys.Rev.Lett.*, 105:031801, 2010.

[93] Otto Eberhardt, Alexander Lenz, and Jurgen Rohrwild. Less space for a new family of fermions. *Phys.Rev.*, D82:095006, 2010.

[94] K. Nakamura et al. Review of particle physics. *J.Phys.*, G37:075021, 2010.

[95] Jesse Thaler and Lian-Tao Wang. Strategies to Identify Boosted Tops. *JHEP*, 0807:092, 2008.

[96] David E. Kaplan, Keith Rehermann, Matthew D. Schwartz, and Brock Tweedie. Top Tagging: A Method for Identifying Boosted Hadronically Decaying Top Quarks. *Phys.Rev.Lett.*, 101:142001, 2008.

[97] Tilman Plehn, Michael Spannowsky, Michihisa Takeuchi, and Dirk Zerwas. Stop Reconstruction with Tagged Tops. *JHEP*, 1010:078, 2010.

[98] Keith Rehermann and Brock Tweedie. Efficient Identification of Boosted Semileptonic Top Quarks at the LHC. *JHEP*, 1103:059, 2011.

[99] D. Choudhury, Timothy M.P. Tait, and C.E.M. Wagner. Beautiful mirrors and precision electroweak data. *Phys.Rev.*, D65:053002, 2002.

[100] Kunal Kumar, William Shepherd, Tim M.P. Tait, and Roberto Vega-Morales. Beautiful Mirrors at the LHC. *JHEP*, 1008:052, 2010.

[101] Csaba Csaki, Adam Falkowski, and Andreas Weiler. The Flavor of the Composite Pseudo-Goldstone Higgs. *JHEP*, 0809:008, 2008.

[102] Gino Isidori, Yosef Nir, and Gilad Perez. Flavor Physics Constraints for Physics Beyond the Standard Model. *Ann.Rev.Nucl.Part.Sci.*, 60:355, 2010.

[103] G. D'Ambrosio, G.F. Giudice, G. Isidori, and A. Strumia. Minimal flavor violation: An Effective field theory approach. *Nucl.Phys.*, B645:155–187, 2002.

[104] Tobias Hurth, Gino Isidori, Jernej F. Kamenik, and Federico Mescia. Constraints on New Physics in MFV models: A Model-independent analysis of Δ F = 1 processes. *Nucl.Phys.*, B808:326–346, 2009.

[105] Riccardo Barbieri, Alex Pomarol, Riccardo Rattazzi, and Alessandro Strumia. Electroweak symmetry breaking after LEP-1 and LEP-2. *Nucl.Phys.*, B703:127–146, 2004.

[106] Savas Dimopoulos, Michael Dine, Stuart Raby, and Scott D. Thomas. Experimental signatures of low-energy gauge mediated supersymmetry breaking. *Phys.Rev.Lett.*, 76:3494–3497, 1996.

[107] Konstantin T. Matchev and Scott D. Thomas. Higgs and Z boson signatures of supersymmetry. *Phys.Rev.*, D62:077702, 2000.

[108] Stephen P. Martin. Collider signals from slow decays in supersymmetric models with an intermediate scale solution to the mu problem. *Phys.Rev.*, D62:095008, 2000.

[109] Z. Chacko, Christopher A. Krenke, and Takemichi Okui. Supersymmetry in Slow Motion. *JHEP*, 0901:050, 2009.

[110] Matthew J. Strassler and Kathryn M. Zurek. Echoes of a hidden valley at hadron colliders. *Phys.Lett.*, B651:374–379, 2007.

[111] Matthew J. Strassler and Kathryn M. Zurek. Discovering the Higgs through highly-displaced vertices. *Phys.Lett.*, B661:263–267, 2008.

[112] Jose E. Juknevich, Dmitry Melnikov, and Matthew J. Strassler. A Pure-Glue Hidden Valley I. States and Decays. *JHEP*, 0907:055, 2009.

[113] Junhai Kang and Markus A. Luty. Macroscopic Strings and 'Quirks' at Colliders. *JHEP*, 0911:065, 2009.

[114] Can Kilic, Takemichi Okui, and Raman Sundrum. Vectorlike Confinement at the LHC. *JHEP*, 1002:018, 2010.

[115] Can Kilic and Takemichi Okui. The LHC Phenomenology of Vectorlike Confinement. *JHEP*, 1004:128, 2010.

[116] Yang Bai and Richard J. Hill. Weakly Interacting Stable Pions. *Phys.Rev.*, D82:111701, 2010.

[117] G. Brooijmans et al. New Physics at the LHC. A Les Houches Report: Physics at TeV Colliders 2009 - New Physics Working Group. pages 191–380, 2010.

[118] A.C. Kraan, J.B. Hansen, and P. Nevski. Discovery potential of R-hadrons with the ATLAS detector. *Eur.Phys.J.*, C49:623–640, 2007.

[119] Aafke Christine Kraan. Interactions of heavy stable hadronizing particles. *Eur.Phys.J.*, C37:91–104, 2004.

[120] T. Aaltonen et al. Search for Long-Lived Massive Charged Particles in 1.96 TeV $\bar{p}p$ Collisions. *Phys.Rev.Lett.*, 103:021802, 2009.

[121] V.M. Abazov et al. Search for Long-Lived Charged Massive Particles with the D0 Detector. *Phys.Rev.Lett.*, 102:161802, 2009.

[122] A. Pukhov, E. Boos, M. Dubinin, V. Edneral, V. Ilyin, et al. CompHEP: A Package for evaluation of Feynman diagrams and integration over multiparticle phase space. 1999.

[123] J. Pumplin, D.R. Stump, J. Huston, H.L. Lai, Pavel M. Nadolsky, et al. New generation of parton distributions with uncertainties from global QCD analysis. *JHEP*, 0207:012, 2002.

[124] Victor Mukhamedovich Abazov et al. Measurement of the $WZ \to \ell\nu\ell\ell$ cross section and limits on anomalous triple gauge couplings in $p\bar{p}$ collisions at $\sqrt{s} = 1.96$ TeV. *Phys.Lett.*, B695:67–73, 2011.

[125] CDF Collaboration. CDF: Measurement of the WZ Production Cross Section in $p\bar{p}$ Collisions at $\sqrt{s} = 1.96$ TeV using 5.9 inv. fb of CDF Run II Data. CDF note 1076.

[126] V.M. Abazov et al. Measurement of the WW production cross section with dilepton final states in p anti-p collisions at s**(1/2) = 1.96-TeV and limits on anomalous trilinear gauge couplings. *Phys.Rev.Lett.*, 103:191801, 2009.

[127] T. Aaltonen et al. Measurement of the W+ W- Production Cross Section and Search for Anomalous WW gamma and WWZ Couplings in p p-bar Collisions at s**(1/2) = 1.96-TeV. *Phys.Rev.Lett.*, 104:201801, 2010.

[128] Johan Alwall, Pavel Demin, Simon de Visscher, Rikkert Frederix, Michel Herquet, et al. MadGraph/MadEvent v4: The New Web Generation. *JHEP*, 0709:028, 2007.

[129] Patrick Meade and Matthew Reece. BRIDGE: Branching ratio inquiry / decay generated events. 2007.

[130] Torbjorn Sjostrand, Stephen Mrenna, and Peter Z. Skands. PYTHIA 6.4 Physics and Manual. *JHEP*, 0605, 2006.

[131] J. *et al.* Conway. PGS 4: Pretty Good Simulation of high energy collisions. http://www.physics.ucdavis.edu/~conway/research/software/pgs/pgs4-general.htm, 2006.

[132] David B. Kaplan and Howard Georgi. SU(2) x U(1) Breaking by Vacuum Misalignment. *Phys.Lett.*, B136:183, 1984.

[133] J. Wess and B. Zumino. Supergauge Invariant Extension of Quantum Electrodynamics. *Nucl.Phys.*, B78:1, 1974.

[134] Pierre Fayet. Supersymmetry and Weak, Electromagnetic and Strong Interactions. *Phys.Lett.*, B64:159, 1976.

[135] Savas Dimopoulos and Howard Georgi. Softly Broken Supersymmetry and SU(5). *Nucl.Phys.*, B193:150, 1981.

[136] Steven Weinberg. Supersymmetry at Ordinary Energies. 1. Masses and Conservation Laws. *Phys.Rev.*, D26:287, 1982.

[137] N. Sakai and Tsutomu Yanagida. Proton Decay in a Class of Supersymmetric Grand Unified Models. *Nucl.Phys.*, B197:533, 1982.

[138] Savas Dimopoulos, Stuart Raby, and Frank Wilczek. Proton Decay in Supersymmetric Models. *Phys.Lett.*, B112:133, 1982.

[139] Savas Dimopoulos and David W. Sutter. The Supersymmetric flavor problem. *Nucl.Phys.*, B452:496–512, 1995.

[140] F. Gabbiani, E. Gabrielli, A. Masiero, and L. Silvestrini. A Complete analysis of FCNC and CP constraints in general SUSY extensions of the standard model. *Nucl.Phys.*, B477:321–352, 1996.

[141] Stephen P. Martin. Two loop effective potential for a general renormalizable theory and softly broken supersymmetry. *Phys.Rev.*, D65:116003, 2002.

[142] Stephen P. Martin. Two loop effective potential for the minimal supersymmetric standard model. *Phys.Rev.*, D66:096001, 2002.

[143] R. Barate et al. Search for the standard model Higgs boson at LEP. *Phys.Lett.*, B565:61–75, 2003.

[144] Marcela S. Carena, J.R. Espinosa, M. Quiros, and C.E.M. Wagner. Analytical expressions for radiatively corrected Higgs masses and couplings in the MSSM. *Phys.Lett.*, B355:209–221, 1995.

[145] Markus A. Luty. 2004 TASI lectures on supersymmetry breaking. pages 495–582, 2005.

[146] Ali H. Chamseddine, Richard L. Arnowitt, and Pran Nath. Locally Supersymmetric Grand Unification. *Phys.Rev.Lett.*, 49:970, 1982.

[147] E. Cremmer, S. Ferrara, L. Girardello, and Antoine Van Proeyen. Yang-Mills Theories with Local Supersymmetry: Lagrangian, Transformation Laws and SuperHiggs Effect. *Nucl.Phys.*, B212:413, 1983.

[148] Pierre Fayet. Mixing Between Gravitational and Weak Interactions Through the Massive Gravitino. *Phys.Lett.*, B70:461, 1977.

[149] Michael Dine, Ann E. Nelson, and Yuri Shirman. Low-energy dynamical supersymmetry breaking simplified. *Phys.Rev.*, D51:1362–1370, 1995.

[150] Graham D. Kribs, Takemichi Okui, and Tuhin S. Roy. Viable Gravity-Mediated Supersymmetry Breaking. *Phys.Rev.*, D82:115010, 2010.

[151] G.R. Dvali, G.F. Giudice, and A. Pomarol. The Mu problem in theories with gauge mediated supersymmetry breaking. *Nucl.Phys.*, B478:31–45, 1996.

[152] Gian F. Giudice, Markus A. Luty, Hitoshi Murayama, and Riccardo Rattazzi. Gaugino mass without singlets. *JHEP*, 9812:027, 1998.

[153] Lisa Randall and Raman Sundrum. Out of this world supersymmetry breaking. *Nucl.Phys.*, B557:79–118, 1999.

[154] Abdelhak Djouadi, Jean-Loic Kneur, and Gilbert Moultaka. SuSpect: A Fortran code for the supersymmetric and Higgs particle spectrum in the MSSM. *Comput.Phys.Commun.*, 176:426–455, 2007.

[155] Carola F. Berger, James S. Gainer, JoAnne L. Hewett, and Thomas G. Rizzo. Supersymmetry Without Prejudice. *JHEP*, 0902:023, 2009.

[156] R. Michael Barnett, Howard E. Haber, and Gordon L. Kane. Supersymmetry: Lost Or Found? *Nucl.Phys.*, B267:625, 1986.

[157] Howard Baer, Debra Karatas, and Xerxes Tata. ON THE SQUARK AND GLUINO MASS LIMITS FROM THE CERN p anti-p COLLIDER. *Phys.Lett.*, B183:220, 1987.

[158] Johan Alwall, Philip Schuster, and Natalia Toro. Simplified Models for a First Characterization of New Physics at the LHC. *Phys.Rev.*, D79:075020, 2009.

[159] Johan Alwall, My-Phuong Le, Mariangela Lisanti, and Jay G. Wacker. Model-Independent Jets plus Missing Energy Searches. *Phys.Rev.*, D79:015005, 2009.

[160] Abdus Salam and J.A. Strathdee. On Superfields and Fermi-Bose Symmetry. *Phys.Rev.*, D11:1521–1535, 1975.

[161] Marcus T. Grisaru, W. Siegel, and M. Rocek. Improved Methods for Supergraphs. *Nucl.Phys.*, B159:429, 1979.

[162] B.C. Allanach. SOFTSUSY: a program for calculating supersymmetric spectra. *Comput.Phys.Commun.*, 143:305–331, 2002.

[163] Werner Porod. SPheno, a program for calculating supersymmetric spectra, SUSY particle decays and SUSY particle production at e+ e- colliders. *Comput.Phys.Commun.*, 153:275–315, 2003.

[164] W. Porod and F. Staub. SPheno 3.1: Extensions including flavour, CP-phases and models beyond the MSSM. *Comput.Phys.Commun.*, 183:2458–2469, 2012.

[165] Joint LEP 2 Supersymmetry Working Group. Combined lep chargino results up to 208 gev. http://lepsusy.web.cern.ch/lepsusy/www/inos.moriond01/charginos.pub.html.

[166] S. Chatrchyan et al. The CMS experiment at the CERN LHC. *JINST*, 3:S08004, 2008.

[167] G. Aad et al. The ATLAS Experiment at the CERN Large Hadron Collider. *JINST*, 3:S08003, 2008.

[168] http://twiki.cern.ch/twiki/bin/view/CMSPublic/PhysicsResultsSUS. Also see the CMS TWiki pages.

[169] http://twiki.cern.ch/twiki/bin/view/AtlasPublic/SupersymmetryPublicResults. Also see the ATLAS TWiki pages.

[170] Paul de Jong. Supersymmetry searches at the LHC. 2012.

[171] Georges Aad et al. Search for squarks and gluinos with the ATLAS detector in final states with jets and missing transverse momentum using 4.7 inv. fb of $\sqrt{s} = 7$ TeV proton-proton collision data. 2012.

[172] S. Chatrchyan. Search for supersymmetry in hadronic final states using MT2 in pp collisions at $\sqrt{s} = 7$ TeV. *JHEP*, 1210:018, 2012.

[173] Search for supersymmetery in final states with missing transverse momentum and 0, 1, 2, or ≥ 3 b jets with CMS. 2012.

[174] Search for supersymmetry with the razor variables at CMS. 2012.

[175] Georges Aad et al. Search for light scalar top quark pair production in final states with two leptons with the ATLAS detector in $\sqrt{s} = 7$ TeV proton-proton collisions. *Eur.Phys.J.*, C72:2237, 2012.

[176] Georges Aad et al. Search for light top squark pair production in final states with leptons and b^- jets with the ATLAS detector in $\sqrt{s} = 7$ TeV proton-proton collisions. 2012.

[177] Georges Aad et al. Search for a heavy top-quark partner in final states with two leptons with the ATLAS detector at the LHC. *JHEP*, 1211:094, 2012.

[178] Georges Aad et al. Search for direct top squark pair production in final states with one isolated lepton, jets, and missing transverse momentum in $\sqrt{s} = 7$ TeV pp collisions using 4.7 fb^{-1} of ATLAS data. *Phys.Rev.Lett.*, 109:211803, 2012.

[179] Georges Aad et al. Search for a supersymmetric partner to the top quark in final states with jets and missing transverse momentum at $\sqrt{s} = 7$ TeV with the ATLAS detector. *Phys.Rev.Lett.*, 109:211802, 2012.

[180] Thomas J. LeCompte and Stephen P. Martin. Compressed supersymmetry after 1/fb at the Large Hadron Collider. *Phys.Rev.*, D85:035023, 2012.

[181] Herbi K. Dreiner, Michael Kramer, and Jamie Tattersall. How low can SUSY go? Matching, monojets and compressed spectra. *Europhys.Lett.*, 99:61001, 2012.

[182] Biplob Bhattacherjee and Kirtiman Ghosh. Degenerate SUSY search at the 8 TeV LHC. 2012.

[183] JiJi Fan, Matthew Reece, and Joshua T. Ruderman. Stealth Supersymmetry. *JHEP*, 1111:012, 2011.

[184] JiJi Fan, Matthew Reece, and Joshua T. Ruderman. A Stealth Supersymmetry Sampler. *JHEP*, 1207:196, 2012.

[185] Serguei Chatrchyan et al. Search for supersymmetry in events with photons and low missing transverse energy in pp collisions at $\sqrt{s} = 7$ TeV. *Phys. Lett. B.*, 2012.

[186] Serguei Chatrchyan. Search for anomalous production of multilepton events in pp collisions at $\sqrt{s} = 7$ TeV. *JHEP*, 1206:169, 2012.

[187] Serguei Chatrchyan et al. Search for three-jet resonances in pp collisions at $\sqrt{s} = 7$ TeV. *Phys.Lett.*, B718:329–347, 2012.

[188] Georges Aad et al. Search for lepton flavour violation in the emu continuum with the ATLAS detector in $\sqrt{s} = 7$ TeV pp collisions at the LHC. *Eur.Phys.J.*, C72:2040, 2012.

[189] Search for long-lived, heavy particles in final states with a muon and multi-track displaced vertex in proton-proton collisions at a centre-of-mass energy of 7 TeV with the ATLAS detector. 2012.

[190] R Aaij et al. First evidence for the decay $Bs \to \mu + \mu-$. *Phys.Rev.Lett.*, 110:021801, 2013.

[191] Wolfgang Altmannshofer, Marcela Carena, Nausheen Shah, and Felix Yu. Indirect Probes of the MSSM after the Higgs Discovery. *JHEP*, 1301:160, 2013.

[192] Howard Baer, Vernon Barger, Peisi Huang, and Xerxes Tata. Natural Supersymmetry: LHC, dark matter and ILC searches. *JHEP*, 1205:109, 2012.

[193] Riccardo Barbieri and G.F. Giudice. Upper Bounds on Supersymmetric Particle Masses. *Nucl.Phys.*, B306:63, 1988.

[194] Jonathan L. Feng and Konstantin T. Matchev. Focus point supersymmetry: Proton decay, flavor and CP violation, and the Higgs boson mass. *Phys.Rev.*, D63:095003, 2001.

[195] John R. Ellis, K. Enqvist, Dimitri V. Nanopoulos, and F. Zwirner. Observables in Low-Energy Superstring Models. *Mod.Phys.Lett.*, A1:57, 1986.

[196] Andrea Romanino and Alessandro Strumia. Are heavy scalars natural in minimal supergravity? *Phys.Lett.*, B487:165–170, 2000.

[197] Ryuichiro Kitano and Yasunori Nomura. Supersymmetry, naturalness, and signatures at the LHC. *Phys.Rev.*, D73:095004, 2006.

[198] Michele Papucci, Joshua T. Ruderman, and Andreas Weiler. Natural SUSY Endures. *JHEP*, 1209:035, 2012.

[199] Christopher Brust, Andrey Katz, Scott Lawrence, and Raman Sundrum. SUSY, the Third Generation and the LHC. *JHEP*, 1203:103, 2012.

[200] Yevgeny Kats, Patrick Meade, Matthew Reece, and David Shih. The Status of GMSB After 1/fb at the LHC. *JHEP*, 1202:115, 2012.

[201] Nathaniel Craig, Matthew McCullough, and Jesse Thaler. The New Flavor of Higgsed Gauge Mediation. *JHEP*, 1203:049, 2012.

[202] Nathaniel Craig, Matthew McCullough, and Jesse Thaler. Flavor Mediation Delivers Natural SUSY. *JHEP*, 1206:046, 2012.

[203] Howard Baer, Vernon Barger, Peisi Huang, Azar Mustafayev, and Xerxes Tata. Radiative natural SUSY with a 125 GeV Higgs boson. *Phys.Rev.Lett.*, 109:161802, 2012.

[204] Howard Baer, Vernon Barger, Peisi Huang, Dan Mickelson, Azar Mustafayev, et al. Radiative natural supersymmetry: Reconciling electroweak fine-tuning and the Higgs boson mass. 2012.

[205] Nima Arkani-Hamed, Arpit Gupta, David E. Kaplan, Neal Weiner, and Tom Zorawski. Simply Unnatural Supersymmetry. 2012.

[206] Biplob Bhattacherjee, Jason L. Evans, Masahiro Ibe, Shigeki Matsumoto, and Tsutomu T. Yanagida. Natural SUSY's Last Hope: R-parity Violation via UDD Operators. 2013.

[207] G.F. Giudice and R. Rattazzi. Living Dangerously with Low-Energy Supersymmetry. *Nucl.Phys.*, B757:19–46, 2006.

[208] Jonathan L. Feng, Konstantin T. Matchev, and Takeo Moroi. Multi - TeV scalars are natural in minimal supergravity. *Phys.Rev.Lett.*, 84:2322–2325, 2000.

[209] Jonathan L. Feng, Konstantin T. Matchev, and Takeo Moroi. Focus points and naturalness in supersymmetry. *Phys.Rev.*, D61:075005, 2000.

[210] Jonathan L. Feng, Konstantin T. Matchev, and Takeo Moroi. Naturalness reexamined: Implications for supersymmetry searches. pages 212–221, 1999.

[211] Jonathan L. Feng, Konstantin T. Matchev, and Frank Wilczek. Neutralino dark matter in focus point supersymmetry. *Phys.Lett.*, B482:388–399, 2000.

[212] Kaustubh Agashe. Can multi - TeV (top and other) squarks be natural in gauge mediation? *Phys.Rev.*, D61:115006, 2000.

[213] Stephen P. Martin. Generalized messengers of supersymmetry breaking and the sparticle mass spectrum. *Phys.Rev.*, D55:3177–3187, 1997.

[214] S. Dimopoulos and G.F. Giudice. Multimessenger theories of gauge mediated supersymmetry breaking. *Phys.Lett.*, B393:72–78, 1997.

[215] Savas Dimopoulos, Scott D. Thomas, and James D. Wells. Sparticle spectroscopy and electroweak symmetry breaking with gauge mediated supersymmetry breaking. *Nucl.Phys.*, B488:39–91, 1997.

[216] G. Anderson, C.H. Chen, J.F. Gunion, Joseph D. Lykken, T. Moroi, et al. Motivations for and implications of nonuniversal GUT scale boundary conditions for soft SUSY breaking parameters. *eConf*, C960625:SUP107, 1996.

[217] Gian F. Giudice, Hyung Do Kim, and Riccardo Rattazzi. Natural mu and B mu in gauge mediation. *Phys.Lett.*, B660:545–549, 2008.

[218] G.F. Giudice and R. Rattazzi. Extracting supersymmetry breaking effects from wave function renormalization. *Nucl.Phys.*, B511:25–44, 1998.

[219] Nima Arkani-Hamed, Gian F. Giudice, Markus A. Luty, and Riccardo Rattazzi. Supersymmetry breaking loops from analytic continuation into superspace. *Phys.Rev.*, D58:115005, 1998.

[220] Jonathan L. Feng and David Sanford. A Natural 125 GeV Higgs Boson in the MSSM from Focus Point Supersymmetry with A-Terms. *Phys.Rev.*, D86:055015, 2012.

[221] Howard Baer. Radiative natural supersymmetry with mixed axion/higgsino cold dark matter. 2012.

[222] Luis E. Ibanez and Graham G. Ross. Discrete gauge symmetries and the origin of baryon and lepton number conservation in supersymmetric versions of the standard model. *Nucl.Phys.*, B368:3–37, 1992.

[223] Diego J. Castano and Stephen P. Martin. Discrete symmetries and isosinglet quarks in low-energy supersymmetry. *Phys.Lett.*, B340:67–73, 1994.

[224] Kenzo Inoue, Akira Kakuto, and Hiroshi Takano. Higgs as (Pseudo)Goldstone Particles. *Prog.Theor.Phys.*, 75:664, 1986.

[225] A.A. Anselm and A.A. Johansen. SUSY GUT with Automatic Doublet - Triplet Hierarchy. *Phys.Lett.*, B200:331–334, 1988.

[226] Riccardo Barbieri, G.R. Dvali, and A. Strumia. Grand unified supersymmetric Higgs bosons as pseudoGoldstone particles. *Nucl.Phys.*, B391:487–500, 1993.

[227] Sidney R. Coleman, J. Wess, and Bruno Zumino. Structure of phenomenological Lagrangians. 1. *Phys.Rev.*, 177:2239–2247, 1969.

[228] Jr. Callan, Curtis G., Sidney R. Coleman, J. Wess, and Bruno Zumino. Structure of phenomenological Lagrangians. 2. *Phys.Rev.*, 177:2247–2250, 1969.

[229] M. Bando, T. Kugo, S. Uehara, K. Yamawaki, and T. Yanagida. Is rho Meson a Dynamical Gauge Boson of Hidden Local Symmetry? *Phys.Rev.Lett.*, 54:1215, 1985.

[230] Neal Weiner. Unification without unification. *Phys.Rev.Lett.*, 2001.

[231] Ofer Aharony, Steven S. Gubser, Juan Martin Maldacena, Hirosi Ooguri, and Yaron Oz. Large N field theories, string theory and gravity. *Phys.Rept.*, 323:183–386, 2000.

[232] Tony Gherghetta. Les Houches lectures on warped models and holography. pages 263–311, 2006.

[233] Yasunori Nomura, David Poland, and Brock Tweedie. Holographic grand unification. *JHEP*, 0612:002, 2006.

[234] Lisa Randall and Raman Sundrum. A Large mass hierarchy from a small extra dimension. *Phys.Rev.Lett.*, 83:3370–3373, 1999.

[235] Kaustubh Agashe and Geraldine Servant. Warped unification, proton stability and dark matter. *Phys.Rev.Lett.*, 93:231805, 2004.

[236] Kaustubh Agashe and Geraldine Servant. Baryon number in warped GUTs: Model building and (dark matter related) phenomenology. *JCAP*, 0502:002, 2005.

BIOGRAPHICAL SKETCH

KAROLINE KÖPP

Education

- Ph.D. in Physics, Florida State University, 2013
  - *Dissertation title:* Topics in Physics Beyond the Standard Model
  - *Committee:* Takemichi Okui (supervising professor), Ettore Aldrovandi, Laura Reina, Todd Adams, Christopher Gerardy
- Diplom (M.S. equivalent) in Physics, Julius-Maximilians-Universität Würzburg, 2009
  - *Diploma thesis title:* A Supersymmetric Higgsless Model of Electroweak Symmetry Breaking
  - *Supervising professor:* Thorsten Ohl

Publications

- Prerit Jaiswal, Karoline Köpp, Takemichi Okui: *Minimally tuned Gauge Mediation.* (in prep)
- Prerit Jaiswal, Karoline Köpp, Takemichi Okui: *Higgs Production Amidst the LHC Detector.* (to appear)
- Karoline Köpp, Takemichi Okui: *Effective Field Theory for a Heavy Majorana Particle.* Published in Phys.Rev. D84 (2011) 093007. arXiv: 1108.2702 [hep-ph]
- Can Kilic, Karoline Köpp, Takemichi Okui: *LHC Implications of the WIMP Miracle and Grand Unification.* Published in Phys.Rev. D83 (2011) 015006. arXiv:1008.2763 [hep-ph]

Honors, Awards & Fellowships

- 2012: Hagopian Family Endowment Award
- 2011: LHC Theory Initiative graduate scholarship

- 2009: Dean's Fellowship & Grace Moulton Fellowship
- 2005/06: Exchange Scholarship of the University of Würzburg for a year of study in Salamanca, Spain